
[All ETDs from UAB](#)

[UAB Theses & Dissertations](#)

2004

Differential signaling to SRC family kinases by specific isoforms of fibroblast growth factor receptor-1.

Jessica Samit Greendorfer
University of Alabama at Birmingham

Follow this and additional works at: <https://digitalcommons.library.uab.edu/etd-collection>

Recommended Citation

Greendorfer, Jessica Samit, "Differential signaling to SRC family kinases by specific isoforms of fibroblast growth factor receptor-1." (2004). *All ETDs from UAB*. 5193.
<https://digitalcommons.library.uab.edu/etd-collection/5193>

This content has been accepted for inclusion by an authorized administrator of the UAB Digital Commons, and is provided as a free open access item. All inquiries regarding this item or the UAB Digital Commons should be directed to the [UAB Libraries Office of Scholarly Communication](#).

NOTE TO USERS

Page(s) missing in number only; text follows. Page(s) were scanned as received.

26

This reproduction is the best copy available.

UMI[®]

DIFFERENTIAL SIGNALING TO SRC FAMILY KINASES BY SPECIFIC
ISOFORMS OF FIBROBLAST GROWTH FACTOR RECEPTOR-1

by

JESSICA SAMIT GREENDORFER

A DISSERTATION

Submitted to the graduate faculty of The University of Alabama at Birmingham,
in partial fulfillment of the requirements for the degree of
Doctor of Philosophy

BIRMINGHAM, ALABAMA

2004

UMI Number: 3132301

Copyright 2004 by
Greendorfer, Jessica Samit

All rights reserved.

INFORMATION TO USERS

The quality of this reproduction is dependent upon the quality of the copy submitted. Broken or indistinct print, colored or poor quality illustrations and photographs, print bleed-through, substandard margins, and improper alignment can adversely affect reproduction.

In the unlikely event that the author did not send a complete manuscript and there are missing pages, these will be noted. Also, if unauthorized copyright material had to be removed, a note will indicate the deletion.

UMI[®]

UMI Microform 3132301

Copyright 2004 by ProQuest Information and Learning Company.

All rights reserved. This microform edition is protected against unauthorized copying under Title 17, United States Code.

ProQuest Information and Learning Company
300 North Zeeb Road
P.O. Box 1346
Ann Arbor, MI 48106-1346

Copyright by
Jessica Samit Greendorfer
2004

ABSTRACT OF DISSERTATION
GRADUATE SCHOOL, UNIVERSITY OF ALABAMA AT BIRMINGHAM

Degree Ph.D. Program Biochemistry and Molecular Genetics

Name of Candidate Jessica Samit Greendorfer

Committee Chair John A. Thompson

Title Differential Signaling to Src Family Kinases by Specific Isoforms of
Fibroblast Growth Factor Receptor-1

Fibroblast growth factor receptor-1 (FGFR-1) and its ligand fibroblast growth factor-1 (FGF-1) are potent signaling molecules competent to modulate tumorigenesis, inflammation, and angiogenesis. These diverse effects may be mediated by the availability of specific FGFR-1 isoforms, FGFR-1 α and FGFR-1 β , that differ by the presence of three or two immunoglobulin-like (Ig-like) loops in the extracellular domain, respectively.

FGFR-1 α or FGFR-1 β can promote or reduce delayed cell death due to reactive nitrogen species (RNS). To establish the specific contribution of each FGFR-1 isoform in modulating the effects of RNS, FGFR negative resistance vessel endothelial cells (RVEC) were stably transfected with FGFR-1 α or FGFR-1 β . The RNS peroxynitrite (ONOO⁻) was used for in vitro studies to initiate a delayed cell death that was more characteristic of apoptosis than necrosis. This cytotoxicity was enhanced in cells expressing FGF-1-activated FGFR-1 α , but was dramatically inhibited in cells expressing FGF-1 activated FGFR-1 β . The protective effect of FGFR-1 β was due in part to signaling to Src family kinases (SFK).

The relationship between FGFR-1 β and SFK was further assessed in RVEC. FGF-1-activated FGFR-1 β , but not FGFR-1 α , directly associated with the SFK c-Yes.

This association was accompanied by an increase in c-Yes activity and an increase in cortactin tyrosine phosphorylation. Cells expressing FGFR-1 β , but not FGFR-1 α , demonstrated decreased contact-inhibition at high density in vitro and cord-like vascular structures both in vitro and in vivo.

Pancreatic adenocarcinoma, which predominantly expresses FGFR-1 β , is a devastating cancer due to its ability to grow, resist inflammatory insult, and metastasize. These studies demonstrate the presence of 3-nitrotyrosine, a marker of RNS, in human adenocarcinoma tissue. The tyrosine kinase c-Src, a FGFR-1 substrate, was identified as a target for tyrosine nitration in vivo and in cultured pancreatic adenocarcinoma cells treated with ONOO⁻. ONOO⁻-treated pancreatic cancer cells demonstrated enhanced c-Src activity that included the nitrated c-Src population, as well as enhanced signaling to the cytoskeletal substrate cortactin. Collectively, these results demonstrate the importance of the FGFR-1 β signaling pathway during the resolution of tumorigenesis, inflammation, and angiogenesis.

DEDICATION

To Andrew, for everything.

ACKNOWLEDGMENTS

I thank my family: my husband Andrew, my sister Leah, my parents, Royce and Alan, my grandmother Annette, and my in-laws, Estelle and Robert, for their encouragement during my graduate study. In particular, I thank my mom for her unwavering support, and my dad for giving a lab meeting. Andrew and Leah, thank you both for listening.

I thank Jing, Pei, Stacey, Kari, and the Thompson laboratory for their friendship and collaboration. I thank Lee Ann MacMillan-Crow and Selwyn Vickers for their assistance and guidance. I thank Joseph Beckman for his suggestions.

I acknowledge my committee: Drs. Louise Chow, Gerald Fuller, Richard Jope, and Charles Prince. Thank you for your encouragement, insight, and patience.

I thank my mentor, Tony Thompson. Thank you for your friendship, support, and guidance.

TABLE OF CONTENTS

	<u>Page</u>
ABSTRACT	iii
DEDICATION	v
ACKNOWLEDGMENTS	vi
LIST OF TABLES	viii
LIST OF FIGURES	ix
LIST OF ILLUSTRATIONS	xi
LIST OF ABBREVIATIONS	xii
INTRODUCTION	1
Pancreatic Adenocarcinoma	1
Fibroblast Growth Factors	3
Fibroblast Growth Factor Receptor-1	4
Src Family Kinases	8
Tumorigenesis	15
Inflammation and Reactive Nitrogen and Oxygen Species	16
Angiogenesis	22
Conclusions	23
ALTERNATIVELY SPLICED FGFR-1 ISOFORM SIGNALING DIFFERENTIALLY MODULATES ENDOTHELIAL CELL RESPONSES TO PEROXYNITRITE.....	25
DIFFERENTIAL SIGNALING TO THE SRC FAMILY KINASE c-YES BY FGFR-1 α AND FGFR-1 β IN ENDOTHELIAL CELLS	67
TYROSINE NITRATION OF c-SRC TYROSINE KINASE IN HUMAN PANCREATIC DUCTAL ADENOCARCINOMA	93
CONCLUSIONS	116
GENERAL LIST OF REFERENCES	127

LIST OF TABLES

<u>Table</u>		<u>Page</u>
	ALTERNATIVELY SPLICED FGFR-1 ISOFORM SIGNALING DIFFERENTIALLY MODULATES ENDOTHELIAL CELL RESPONSES TO PEROXYNITRITE	
1	High-Affinity Binding Constant (K_d) and Receptor Number Calculated from Scatchard Analysis of Individual Transfectants	41
	TYROSINE NITRATION OF c-Src TYROSINE KINASE IN HUMAN PANCREATIC DUCTAL ADENOCARCINOMA	
1	HPLC-EC Quantitative Measures of Tyrosine Modification in Human Pancreatic Tissue	102

LIST OF FIGURES

<u>Figure</u>	ALTERNATIVELY SPLICED FGFR-1 ISOFORM SIGNALING DIFFERENTIALLY MODULATES ENDOTHELIAL CELL RESPONSES TO PEROXYNITRITE	<u>Page</u>
1	Structure of the eukaryotic expression vectors and steady state levels of FGFR-1 mRNA in individual cell populations	30
2	Western analysis of individual RVEC transfectants	39
3	Scatchard analysis of FGF-1 binding to individual RVEC transfectants	42
4	In situ analysis and growth kinetics of individual RVEC transfectants	44
5	Oxidant-induced cell death in individual RVEC transfectants	45
6	Kinetic analysis of interval between FGF-1 pretreatment and ONOO ⁻ exposure	47
7	Effect of FGF-1 pretreatment on ONOO ⁻ -induced cytotoxicity in RVEC transfectants	49
8	Effect of FGFR-1 and Src-family kinase activities on FGF-1 modulation of ONOO ⁻ -induced cytotoxicity in RVEC transfectants	51
9	Effect of mitogen-activated protein kinase activity on FGF-1 modulation of ONOO ⁻ -induced cytotoxicity in RVEC transfectants	53
10	Western analysis of activated polypeptide substrates in individual RVEC transfectants	55
DIFFERENTIAL SIGNALING TO THE SRC FAMILY KINASE c-YES BY FGFR-1 α AND FGFR-1 β IN ENDOTHELIAL CELLS		
1	RT-PCR and Western analysis of RVEC	76
2	Kinetics of c-Yes activation	77
3	Phosphorylation of c-Yes tyrosines	79

LIST OF FIGURES (Continued)

<u>Figure</u>	<u>Page</u>
4 Association between FGFR-1 isoforms and c-Yes	80
5 c-Yes association and activation of cortactin	81
6 Differential cord formation in vitro	82
7 Differential cord formation in vivo.....	84
8 c-Yes-dependent cord formation in vitro	85

TYROSINE NITRATION OF c-Src TYROSINE KINASE IN
HUMAN PANCREATIC DUCTAL ADENOCARCINOMA

1 Western analysis of tyrosine nitration in human pancreatic tissue	101
2 Western analysis of modified tyrosine residues in c-Src associated with human pancreatic tissue	104
3 Western analysis of tyrosine modifications in ONOO ⁻ -treated human pancreatic adenocarcinoma cells	105
4 Western analysis of tyrosine modifications of c-Src following ONOO ⁻ treatment of human pancreatic adenocarcinoma cells	106
5 Analysis of c-Src activity in human pancreatic adenocarcinoma cells following ONOO ⁻ treatment	108
6 Schematic showing c-Src kinase (human) activation pathway	111

CONCLUSIONS

1 Viability of ONOO ⁻ -treated ARIP cells	118
2 Viability of irradiated ARIP	120

LIST OF ILLUSTRATIONS

<u>Illustration</u>	<u>Page</u>
INTRODUCTION	
1	Structure of the major FGFR-1 isoforms6
2	Structure of the non-receptor protein tyrosine kinase c-Src10
3	Major Src pathways11
4	Mechanisms of c-Src activation13
5	Generation and effects of ONOO ⁻18
DIFFERENTIAL SIGNALING TO THE SRC FAMILY KINASE c-YES BY FGFR-1 α AND FGFR-1 β IN ENDOTHELIAL CELLS	
1	Potential interactions between FGF-1-activated FGFR-1 β and SFK88
CONCLUSIONS	
1	Possible signaling pathways induced by FGFR-1 α or FGFR-1 β following FGF-1 stimulation121
2	Potential effects of tyrosine nitration within SFK domains123
3	Possible roles of FGFR-1 β and SFK during pancreatic tumorigenesis, inflammation, and angiogenesis126

LIST OF ABBREVIATIONS

ATA	Aurin tricarboxylic acid
ATP	Adenosine triphosphate
BCS	Bovine calf serum
β -Gal	Beta-Galactosidase
BrdU	Bromodeoxyuridine
c	Cellular
CA	Human pancreatic ductal adenocarcinoma tissue
CH	Human chronic pancreatitis tissue
Csk	C-terminal Src kinase
c-Src	c-Src tyrosine kinase
DMEM	Dulbecco's modified Eagle medium
DMSO	Dimethyl sulfoxide
E	Glutamate
Erk	Extracellular-regulated kinase
ESFM	Endothelial cell serum-free medium
FAK	Focal adhesion kinase
FBS	Fetal bovine serum
FDA	Fluorescein diacetate
FGF	Fibroblast growth factor
FGF-1	Fibroblast growth factor-1, acidic FGF

LIST OF ABBREVIATIONS (Continued)

FGFR	Fibroblast growth factor receptor
HLGAG	Heparin-like glycosaminoglycans
HPAC	Human pancreatic adenocarcinoma cells
HPLC-EC	High performance liquid chromatography-electrochemical detection
HSPG	Heparan sulfate proteoglycans
I	Isoleucine
i	Inducible
Ig-like	Immunoglobulin-like
JNK	c-Jun N-terminal kinase
kDa	kiloDalton
MAPK	Mitogen-activated protein kinase
MEK	Extracellular signal-regulated kinase kinase
MnSOD	Manganese superoxide dismutase
N	Normal human pancreatic tissue
NLS	Nuclear localization sequence
NO	Nitric oxide
NO ₂	Nitro
NOS	Nitric oxide synthase
O ₂ ⁻	Superoxide
ONOO ⁻	Peroxynitrite
P	Proline
p	Phospho

LIST OF ABBREVIATIONS (Continued)

PBS	Phosphate buffered saline
PCR	Polymerase chain reaction
PDGFR	Platelet-derived growth factor receptor
PLC γ	Phospholipase C gamma
PMSF	Phenyl methyl sulfonyl fluoride
PrI	Propidium iodide
PTK	Protein tyrosine kinase
PTP	Protein tyrosine phosphatase
pY	Phosphotyrosine
RNS	Reactive nitrogen species
RT-PCR	Reverse transcriptase-polymerase chain reaction
RVEC	Resistance vessel endothelial cells
SIN-1	3-Morpholinosydnonimine
SDS-PAGE	Sodium dodecyl sulfate-polyacrylamide gel electrophoresis
SFK	Src family kinases
SH	Src homology
SRC	Polyclonal anti-SRC2 antibody
TK	Tyrosine kinase
tyr	Tyrosine
^{99m}Tc	Technetium
v	Viral
VEGF	Vascular endothelial growth factor

LIST OF ABBREVIATIONS (Continued)

X	Any amino acid
Y	Tyrosine

INTRODUCTION

Pancreatic Adenocarcinoma

Pancreatic adenocarcinomas, malignant neoplasms of the ductal epithelium, are the 4th and 5th leading causes of death due to cancer in women and men, respectively [1]. The high mortality rate of approximately 28,000 patients per year is due in part to poor detection of treatable tumors [2]. This disease lacks consistent and specific symptoms. Symptoms usually do not occur until the cancer is well progressed. When a diagnosis is made >85% of patients have advanced tumors and distant metastases [1]. Pancreatic adenocarcinoma is an extremely resilient cancer. Median survival time following radical surgical resection is only 18-20 months, and survival time is not significantly improved by radiation or chemotherapy [3]. Less than 5% of patients survive for 5 years [1]. Understanding the factors that support the development and progression of pancreatic adenocarcinoma is crucial to developing diagnostic and therapeutic intervention strategies.

In normal physiology, pancreatic ductal epithelial cells produce bicarbonate, ionic fluid, and mucus [4] and form drainage channels leading into the duodenum [5]. These drainage networks allow the secretion of digestive enzymes produced by pancreatic epithelial acinar cells and are necessary for the breakdown of dietary proteins, fats, and carbohydrates [6]. This exocrine function of the pancreas should be distinguished from its endocrine function, the ductless secretion of metabolic-regulatory hormones, including insulin, somatostatin, and glucagon, by the islets of Langerhans [7]. Pancreatic ductal

adenocarcinoma, which comprises more than 95% of cases, is the most common pancreatic exocrine cancer [2].

While the etiology of pancreatic adenocarcinoma is not well understood, chronic inflammation [2] and inappropriate angiogenesis [8] are hallmarks of all pancreatic adenocarcinomas. These three processes, tumorigenesis, inflammation, and angiogenesis, act in concert and can result in the promotion of tumor growth, survival, and metastasis. Inflammation occurs when the developing tumor outgrows its vascular capacity (1-2 mm) [9] and cannot maintain a supply of oxygen and nutrients [10]. Tumors release cytokines and trophic factors that recruit circulating inflammatory cells, including macrophages and neutrophils [10]. Macrophages, stimulated by the hypoxic environment, release additional cytokines, reactive nitrogen and oxygen species, and angiogenic growth factors, including fibroblast growth factors (FGF) [11,12]. Angiogenesis not only supports the tumor, but provides an avenue for chronic inflammation by allowing further infiltration of inflammatory cells [11] and metastasis of migrating tumor cells. The degree of new blood vessel growth correlates with enhanced tumor growth and metastasis [13].

Fibroblast growth factor receptor-1 (FGFR-1) and its FGF ligands are important mediators of cell growth, survival, and migration. The appearance of FGFR-1 and FGF family member FGF-1 are observed in a number of inflammatory and angiogenic pathologies, including rheumatoid arthritis [14], chronic renal allograft rejection [15,16], atherosclerosis [17], and tumorigenesis [18]. Pancreatic adenocarcinomas overexpress FGF and FGFR-1 [19] and demonstrate enhanced activity of the FGFR-1 substrate c-Src [20]. Overexpression of FGFR-1 is accompanied by alternative splicing to produce

FGFR-1 β , an isoform that is structurally different than the normal FGFR-1 α isoform [21]. Studies presented in this manuscript examine differential signaling by FGFR-1 α and FGFR-1 β and identify a specific pathway between FGFR-1 β and Src family kinases (SFK) during pancreatic tumorigenesis, inflammation, and angiogenesis.

Fibroblast Growth Factors

The FGF family is composed of at least 23 members [22]. The majority contain a leader sequence for secretion through the endoplasmic reticulum-Golgi complex, while the prototypical members FGF-1 (acidic FGF) and FGF-2 (basic FGF), as well as FGF-9 and FGF-11 through -14, lack this secretion signal [23]. Secretion of FGF-1 can be induced by injury [24], heat shock [25], oxidative stress [26], hypoxia [27], and serum deprivation [28], and occurs through non-classical pathways that involve aggregation with phospholipid-binding proteins synaptotagmin-1 and S100A13 [29]. The limited release of FGF-1 suggests that its in vivo availability may be limited to prevent inopportune consequences during normal biology [30].

FGF initiates intracellular cascades by binding to their cognate receptors on the cell surface. FGF binds to FGFR with high affinity and to heparin/heparan sulfate proteoglycans (HSPG)/heparin-like glycosaminoglycans (HLGAG) with lower affinity [23]. FGF heparin/HSPG/HLGAG complexes protect FGF from thermal degradation and proteolysis and localize secreted FGF to the extracellular matrix [31]. In addition, heparin stabilizes the interaction between FGF-1 and FGFR-1 and allows maximal induction of FGFR-1 signaling [32]. FGF-1 contains a nuclear localization sequence (NLS) that may target FGF-1 trafficking to the nucleus and may also stabilize the binding

interaction between FGF-1 and FGFR-1 [33]. Indeed, FGF-1 demonstrates high affinity for FGFR-1 and is the only FGF family member capable of activating all four FGFRs [34]. FGF-1, a potent mitogen and pro-angiogenic factor, was used in these studies to dissect isoform-specific FGFR-1 signaling.

Fibroblast Growth Factor Receptor-1

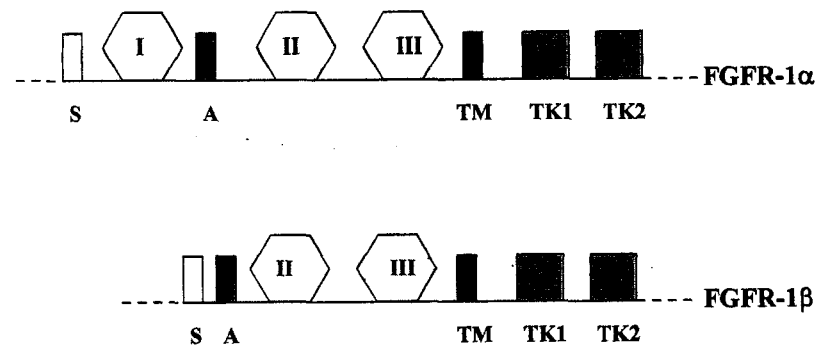
The FGFR family of receptor tyrosine kinases, FGFR-1, FGFR-2, FGFR-3, and FGFR-4, are encoded by four separate gene products and are widely expressed in a variety of cells and tissues [35]. FGFR-1 stimulates diverse physiological processes, including mitogenesis, chemotaxis, neurite outgrowth, wound repair, and embryogenesis, and is capable of mediating tumorigenesis, inflammation, and angiogenesis [36].

Productive FGF-1 binding to FGFR-1 and heparin/HSPG/HLGAG induces receptor dimerization, trans- and autophosphorylation at intracellular tyrosine residues, and subsequent recruitment and phosphorylation of substrates [23]. Phosphorylation is a transient modification that affects protein conformation, activity, and intermolecular interactions [37]. Tyrosine can accept a phosphate from a protein tyrosine kinase (PTK) or donate a phosphate to a protein tyrosine phosphatase (PTP) and is therefore an important mediator of signaling cascades [37].

The general extracellular structure of FGFR-1 includes three immunoglobulin-like (Ig-like) disulfide loops, an acidic box containing eight adjacent acidic amino acids between the first and second Ig-like loops, and a putative NLS that may permit perinuclear trafficking of the receptor-ligand complex and regulation of gene transcription [38,39]. Glycosylation of FGFR-1 in the extracellular region increases the

apparent molecular mass and is a requirement for maturation to a receptor capable of tyrosine phosphorylation [40]. An exon at the end of the third Ig-like loop allows three variants of FGFR-1. FGFR-1(IIIc) is a full transmembrane-spanning receptor capable of initiating intracellular signals, while FGFR-1(IIIa) is a secreted receptor that lacks an intracellular domain and is not involved in signal transduction [34]. FGFR-1(IIIb) has only recently been isolated *in vivo* and appears to be expressed predominantly in the skin and brain [41]. The intracellular features of FGFR-1 include a large juxtamembrane domain, a split tyrosine kinase domain in which the ATP binding site and catalytic region are separated by fifteen amino acids, and seven tyrosines that serve as autophosphorylation sites [38]. Once a mature FGFR-1 complexes with FGF and heparin/HSPG/HLGAG, autophosphorylation at two conserved tyrosines (Y653 and Y654 in full-length FGFR-1) induces kinase activity, while the five additional phosphorylation sites (Y463, Y583, Y585, Y730, and Y766 in full-length FGFR-1) can serve as docking sites for proteins containing src homology 2 (SH2) domains [42].

Alternative splicing of the mRNA transcript encoding the first Ig-like loop results in two major FGFR-1(IIIc) isoforms containing Ig-like loops I, II, and III (FGFR-1 α) or Ig-like loops II and III only (FGFR-1 β) [43] (Ill. 1). Pancreatic adenocarcinoma cells express FGFR-1 and its isoforms as the IIIc variant [44], and the ratio of FGFR-1 α to FGFR-1 β mRNA favors the expression of FGFR-1 β [21]. FGFR-1 α and FGFR-1 β exhibit different ligand affinities and activities. The second and third Ig-like loops are both required and sufficient for ligand binding, while the first Ig-like loop in FGFR-1 α may conformationally restrict the ligand binding site and reduce the affinity of FGFR-1 α for FGF-1 and heparin [43,45]. FGFR-1 α , which has an eight-fold lower affinity for



Ill. 1: Structure of the major FGFR-1 isoforms. Domains: S = signal sequence. A = acidic box. I, II, III = Ig-like disulfide loops. TM = transmembrane sequence. TK1, TK2 = tyrosine kinase sequences separated by a 15 amino acid split.

FGF-1 and heparin than FGFR-1 β , completely loses its ability to bind FGF-1 in the absence of heparin [46]. FGFR-1 may be situated near focal adhesions and the cytoskeleton [47]; however, only ligand-activated FGFR-1 α translocates to a perinuclear location [40]. Differences in FGFR-1 isoform structure and compartmentalization may contribute to different signaling pathways.

Although the physiological effects of activated FGFR-1 are well characterized, established substrates remain largely unknown. This is due in part to the complexity involved in FGFR-1 signaling, including the existence of multiple FGFR-1 isoforms, differential glycosylation of mature and immature FGFR-1 proteins [40], and the ability of FGFR family members to homo- and heterodimerize [46]. In addition, time of exposure to ligand may affect the signaling pathways of FGFR-1. Zhan et al. (1993) found that while tyrosine phosphorylation cascades occurred with immediate to early activation (10-30 min) of FGFR-1 by FGF-1/heparin, initiation of DNA synthesis required the presence of ligand for the complete G₀ to G₁ cell cycle period (12+ h) [48]. Despite these challenges, SFK [23], the mitogenic proteins phospholipase C γ (PLC γ) and mitogen activated protein kinase [49], the Shc adaptor Crk [50], the F-actin binding protein cortactin [51], the adaptor Grb14 [52], and the Grb2 adaptor SNT-1/FRS2 [53] have been identified as potential substrates. A direct association has been verified between FGFR-1 and PLC γ (via FGFR-1 pY766) [23], Crk (via FGFR-2 pY463) [50], Grb14 (dependent on activated FGFR-1) [52], and FRS2 (via FGFR-1 juxtamembrane residues 407-433) [53].

The signaling interaction between FGFR-1 and SFK remains controversial. Treatment of Swiss 3T3 and Balb/c 3T3 cells with FGF-1 [30] and human melanocytes

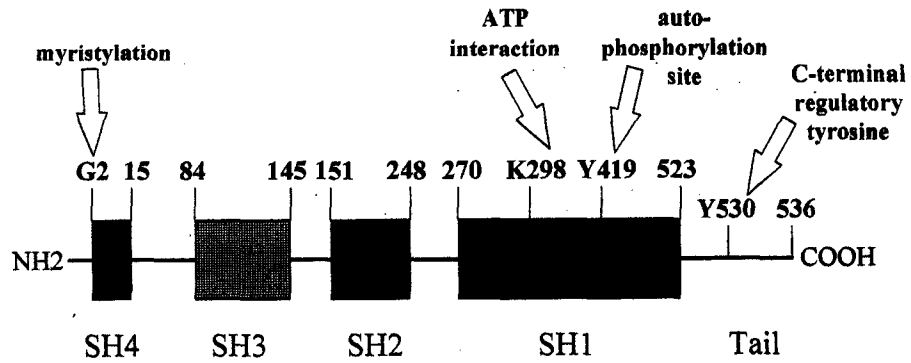
with FGF-2 [54] results in increased c-Src kinase activity. Activation of c-Src by FGFR-1 leads to endothelial cell differentiation, tube formation in collagen, and neurite outgrowth, processes that can be prevented with SFK inhibitors [55] or neutralizing antibodies [56]. However, while Zhan et al. (1994) [57] reported a SH2-dependent association between FGFR-1 and c-Src following FGF-1 treatment of NIH 3T3 cells, Landgren et al. (1995) [58] reported no association between FGFR-1 and SFK in FGF-2-treated porcine aortic endothelial cells, lung endothelial cells, human fibroblasts, and chinese hamster fibroblasts. In fact, while increased c-Src activity was observed in FGF-2-treated lung endothelial cells, NIH 3T3 cells, and human fibroblasts, a FGFR-1 Y766-dependent decrease in c-Src autophosphorylation was observed in porcine aortic endothelial cells [58]. Studies indicate that c-Src can promote separate functions when activated by individual platelet-derived growth factor receptor (PDGFR) isoforms α and β [59]. Clarifying the interaction between FGFR-1 isoforms and SFK is particularly important due to the role of SFK as protooncogenic tyrosine kinases. Results presented here provide the first evidence that SFK may signal specifically through FGFR-1 β .

Src Family Kinases

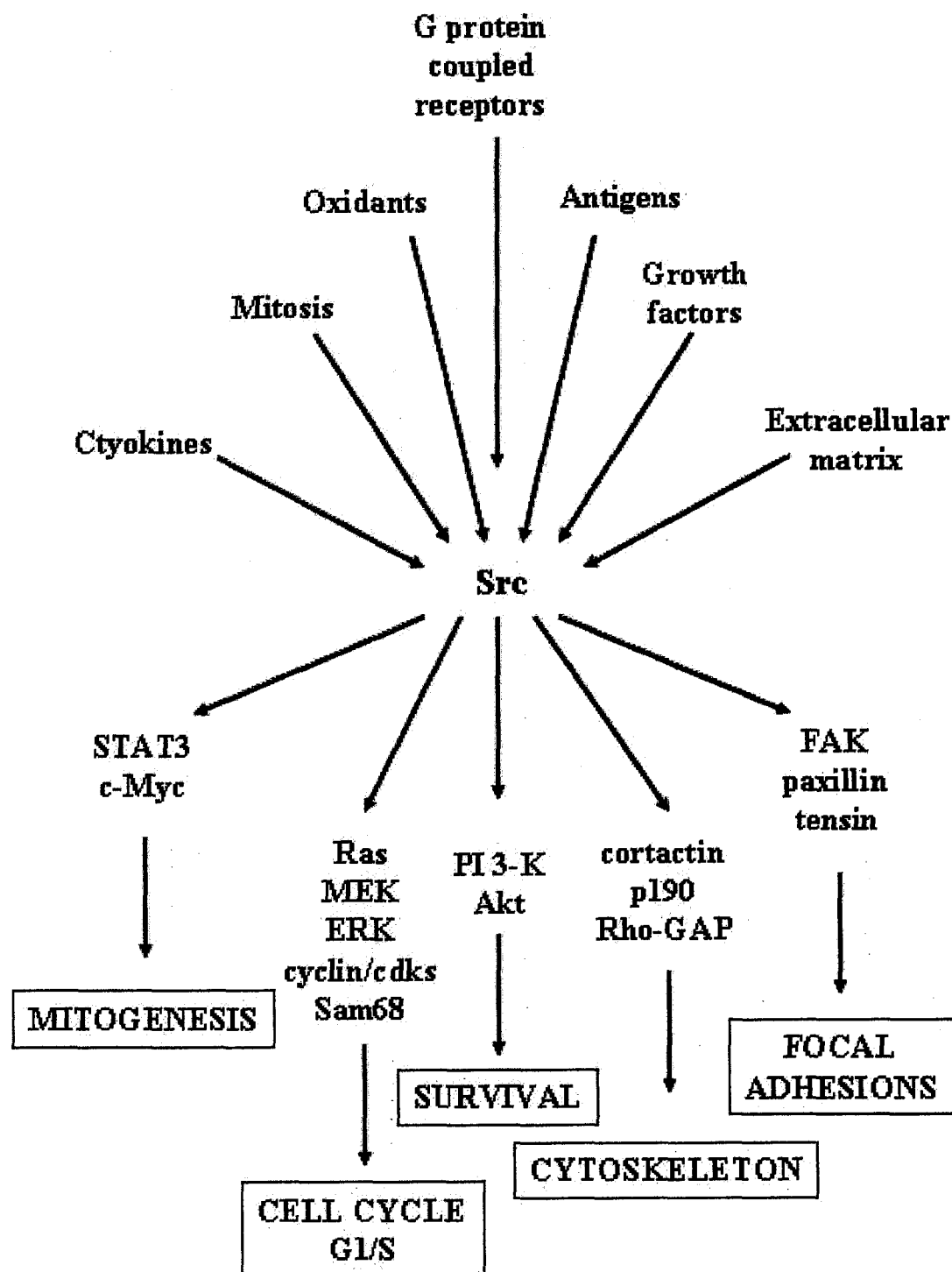
The Src family of non-receptor tyrosine kinases includes nine members (Blk, c-Fgr, Fyn, Hck, Lck, Lyn, c-Src, c-Yes, and Yrk) [60]. The c- designates particular SFK as cellular forms that have a corresponding oncogenic viral (v-) form [61]. c-Src, Fyn, and c-Yes are ubiquitously expressed, while the expression of the remaining family members is restricted to cells of hematopoietic lineage [62]. The structure of SFK generally includes a non-conserved N-terminal unique domain and conserved src

homology 3 (SH3), SH2, catalytic tyrosine kinase (SH1), and negative regulatory tail domains [63] (Ill. 2). SFK associate with cellular membranes through myristoylation sites on a N-terminal glycine residue and, with the exception of c-Src and Blk, additional N-terminal palmitoylation sites (SH4 domain) [61]. Knockout studies of single SFK in mice demonstrate minimal changes in phenotype, suggesting that SFK have redundancy in many functions [64]. However, disruption of multiple SFK, including the most closely homologous members c-Src and c-Yes, imparts a neonatal lethal phenotype [65]. Studies suggest that both c-Src and c-Yes play prominent roles in tumorigenesis [66-68].

As the prototypical member of the Src family, c-Src structure and function have been well characterized. c-Src can be activated by a number of stimuli, including ligand-activated growth factor receptors, integrins, G-protein-coupled receptors [62], and oxidants [69], and can subsequently phosphorylate a variety of substrates, including focal adhesion and cytoskeletal proteins, G-protein-related proteins, and RNA binding proteins [63] (Ill. 3). The activity and substrate specificity of c-Src are regulated by tyrosine modifications within a number of domains conserved across the Src protein family. Phosphorylation of a negative regulatory tyrosine (Y530) by the C-terminal src kinase (Csk) causes the c-Src tail domain to bind to the SH2 domain, a protein binding domain that recognizes phosphotyrosyl (pY) sequences [70]. This closed conformation inhibits c-Src kinase activity [71]. Mutation of this tyrosine to phenylalanine results in constitutive kinase activity and is sufficient to induce transformation of NIH 3T3 cells [72]. v-Src, an oncogenic form of c-Src encoded by the Rous sarcoma virus and avian sarcoma viruses, lacks the regulatory tail and is constitutively active [73].

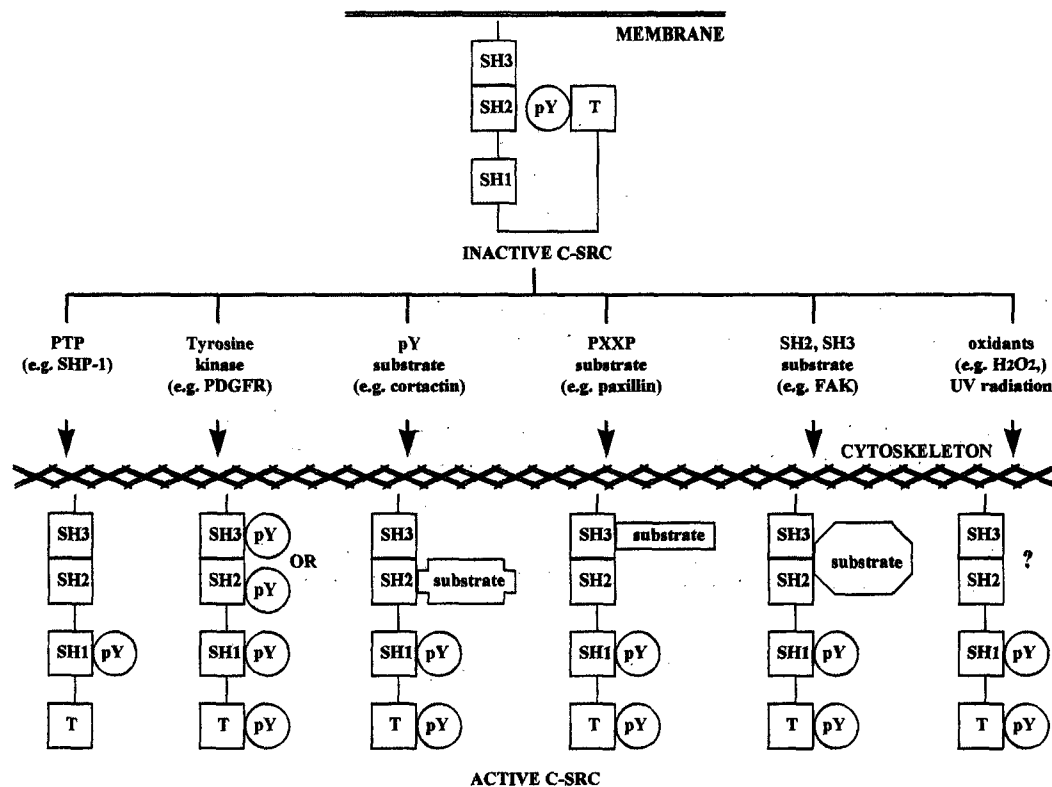


Ill. 2: Structure of the non-receptor protein tyrosine kinase c-Src. SH4 domain: directs membrane localization. SH3 domain: recognizes proline-rich sequences. SH2 domain: recognizes phosphotyrosyl sequences. SH1 domain: kinase catalytic region. Tail domain: negative regulation. A unique region separates the SH4 and SH3 domains.



III. 3: Major Src pathways.

Activation of c-Src requires opening of the closed conformation, either through direct removal of the phosphate group from pY530 by a PTP or via displacement of the tail by protein-protein interactions [71] (Ill. 4). The PTP SHP-1 [74] and PTP α [75] have been shown to dephosphorylate pY530 in vitro. Protein-protein interactions are mediated by the SH2 and SH3 protein-binding domains. The SH2 domain recognizes specific sequences that contain a phosphotyrosine and a hydrophobic residue at position Y+3 [76]. The local sequence around the phosphotyrosine may determine substrate availability; pYEEI has optimal binding affinity for the c-Src SH2 domain but is not accessible to the SH2 domain of the SFK Hck [77]. The SH3 domain recognizes sequences containing multiple proline residues, with a minimal recognition motif of PXXP [78]. A substrate with an appropriate binding motif can bind to the appropriate SH domain and displace the regulatory tail from the SH2 domain. Proteins with a pY sequence, including PDGFR [79] and cortactin [80], can displace the tail via competition for the SH2 domain. Proline-rich substrates, such as Sam68 [81], paxillin [82], and YAP65 [83], displace the tail through interaction with the SH3 domain while some substrates, including focal adhesion kinase (FAK) [84], AFAP-110 [85], and p85 PI3K [79], contain both binding motifs and interact with SFK through both the SH2 and SH3 domains. In some SFK, substrate binding to the SH3 domain may induce activation independently of SH2 domain-tail displacement [86]. c-Src activity can also be regulated by phosphorylation within its protein binding domains. PDGFR has been shown to phosphorylate c-Src within the SH2 domain at Y213 (avian c-Src, corresponding to human c-Src Y216) [87] in vivo or within the SH3 domain at Y138 (murine c-Src, corresponding to human c-Src Y139) [88] in vitro. Phosphorylation of Y213 activates



Ill. 4: Mechanisms of c-Src activation. Activation alters the phosphotyrosine pattern, requires opening of the closed conformation, and is followed by auto-phosphorylation within the SH1 kinase domain.

c-Src because the addition of the negatively charged phosphate group electrostatically repels the tail from the SH2 domain [87]. Phosphorylation of Y138 may help displace the tail, but appears to interfere with binding of proline-rich substrates to this domain [88]. Phosphorylated sequences within SFK potentially can serve as docking sites for other proteins containing SH2 domains, including the tyrosine kinases Csk and Btk [79]. In addition, during mitosis, phosphorylation of c-Src serine and threonine residues by Cdc2 kinase can help displace the SH2 domain, leaving the tail susceptible to dephosphorylation and subsequent c-Src activation [89].

Once c-Src is activated, it phosphorylates in cis at a conserved tyrosine (Y419) within the catalytic domain [90]. Auto-phosphorylation prevents inactivation by the regulatory tail, and dephosphorylation of pY419 by PTP-1B is required before pY530 inactivation can occur [90]. Phosphorylation of Y419 is essential for physiological kinase activity and mutation of this residue (Y416F in avian c-Src, corresponding to human c-Src Y419F) inhibits transformation in activated c-Src mutants (e.g., Y416F-Y527F in avian c-Src, corresponding to human c-Src Y419F-Y530F) or in the constitutively active v-Src [72]. Once the open conformation is established, c-Src is activated. The conformation change causes c-Src to translocate from the plasma membrane to focal adhesion sites in a manner dependent on N-terminal residues and the phosphorylation status of Y530, but independent of kinase activity [91]. While docked at the cytoskeleton, active c-Src can phosphorylate a variety of target substrates, including FAK and tensin, and regulate organization of focal adhesions [92].

Despite sharing a greater than 80% homology in their amino acid sequences, c-Src and c-Yes appear to differ in their regulation [93]. Like c-Src, c-Yes can be activated

by autophosphorylation at a tyrosine within its kinase domain (murine c-Yes Y424, analogous to human c-Src Y419) [94]. However, inactivation of c-Yes appears dependent on intracellular calcium levels and independent of phosphorylation of the regulatory tail tyrosine (human c-Yes Y535) [93]. Zhao et al. (1993) found that, while calcium treatment results in three- to five-fold increases in c-Src activity via PTP-induced dephosphorylation of the tail domain, c-Yes is inactivated in a manner dependent on binding to 110-kDa and 220-kDa inhibitory proteins [93]. c-Src and c-Yes also differ in their affinity for some substrates in kinase assays in vitro [95]. c-Yes, but not c-Src, targets the Pyk2 tyrosine kinase [96] and membrane protein occludin [97] in rat pulmonary vein endothelial cells and kidney epithelial cells, respectively. Both the SH2 and SH3 domains of c-Src and c-Yes direct their preference for specific substrates [98]. In addition, the c-Yes sequence contains a unique autophosphorylation site (Y32) in the N-terminus, the function of which is unknown [94].

Tumorigenesis

Several lines of evidence suggest that the expression of FGFR-1 α or FGFR-1 β can differentially modulate tumorigenesis. FGFR-1 β has been identified as the major FGFR-1 isoform in malignant astrocytomas [99], prostate carcinomas, and breast carcinomas [100]. Overexpression of FGFR-1 in pancreatic adenocarcinomas is associated with malignancy and poor prognostic outcome [101]. In the normal pancreas, FGFR-1 α is the predominant isoform, while over 90% of pancreatic adenocarcinomas overexpress FGFR-1 as the β isoform [21]. In addition, approximately 60% of pancreatic adenocarcinomas overexpress both FGF-1 mRNA and protein, suggesting that continuous

FGFR-1 β signal transduction may occur in most pancreatic tumors [102]. FGF-2, FGF-5, and FGF-7 [103] also demonstrate enhanced expression in pancreatic adenocarcinoma, and the presence of FGF-2 is also associated with poor outcome [102]. Transfection of cDNA encoding a dominant negative, truncated FGFR-1 attenuates cell growth and tumorigenesis in cultured pancreatic adenocarcinoma cells [104]. Systemic delivery of FGF-1 to the pancreatic ductal epithelial cell line ARIP, which predominantly expresses FGFR-1 β , induces tumor formation in nude mice [105].

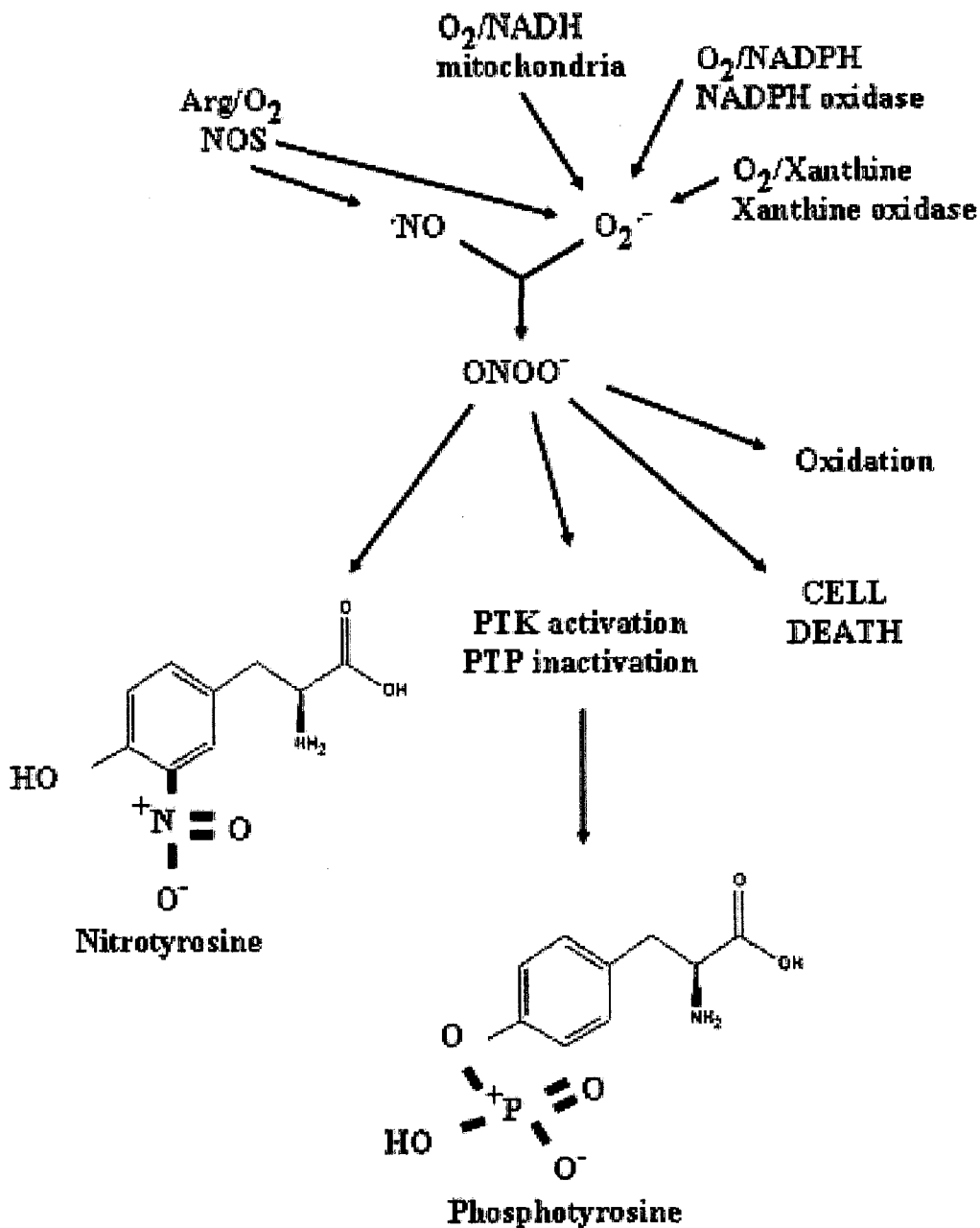
Both c-Src and c-Yes have been implicated in tumorigenesis. SFK activity is increased in cancers of the breast, colon, pancreas, lung, brain, esophagus, and stomach as well as in melanoma, Kaposi's sarcoma, and leukemia [106]. In particular, both c-Src and c-Yes have increased activity in breast cancer cells [107]. In colon cancer, enhanced c-Yes expression is associated with shorter survival time [67]. c-Src activity is increased in pancreatic adenocarcinoma tissue, and in vitro growth of cultured pancreatic cell lines is inhibited with SFK inhibitors [20]. Increases in c-Src and c-Yes specific activity have been shown to be independent of increased mRNA, protein levels, regulatory factors such as Csk [20], or genetic mutations [108], indicating that posttranslational modifications may be responsible for this enhancement. Results presented in this dissertation examine modifications of active c-Src, including tyrosine nitration, a marker of reactive nitrogen species, in pancreatic adenocarcinoma tissue and cultured cell lines.

Inflammation and Reactive Nitrogen and Oxygen Species

Inflammatory events serve as sources of reactive nitrogen species (RNS), including peroxynitrite (ONOO⁻), nitric oxide (NO), and nitrogen dioxide, and reactive

oxygen species, including superoxide (O_2^-), hydrogen peroxide, and hypochlorous acid [109]. Neuronal, inducible (i), and endothelial nitric oxide synthases (NOS) produce NO through the conversion of L-arginine to L-citrulline, while sources of O_2^- include NOS, oxidase enzymes, and electron transport in the mitochondria [110]. During inflammation and angiogenesis, active macrophages produce FGF, RNS [11], and reactive oxygen species [12]. In pancreatic tumors, reactive nitrogen and oxygen species may also be generated due to enzyme dysfunction within the ductal cancer cells themselves. Vickers et al. (1999) reported that pancreatic adenocarcinoma tumors have upregulated expression of iNOS [111]. Preliminary studies also suggest that pancreatic adenocarcinomas have decreased manganese superoxide dismutase (MnSOD) activity, resulting in increased O_2^- (L. A. MacMillan-Crow, personal communication). Immunohistochemistry has demonstrated the co-appearance of FGFR-1 and FGF-1 with nitrotyrosine, a marker of RNS, in human pancreatic adenocarcinomas [111]. Studies presented here utilize the RNS ONOO⁻ as an experimental reagent in vitro. ONOO⁻, formed in a diffusion-limited reaction ($k = 6.7 \times 10^9 M^{-1} s^{-1}$) [112] between NO and superoxide O_2^- , can react with tyrosine residues to produce 3-nitrotyrosine via the addition of a nitro (NO_2) group to the tyrosyl phenolic ring [113].

ONOO⁻ affects signal transduction in several ways (Ill. 5). Proteins identified as targets for tyrosine nitration in vivo show alterations in activity and include MnSOD (inactivation), neurofilament L (aggregation), and prostaglandin H synthase (activation) [114]. Nitration of tyrosine prevents subsequent phosphorylation at that residue [115] and may interfere with protein function [116,117]. Conversely, by providing an area of similar density and charge, nitration may mimic phosphorylation [118,119]. Mallozzi et



Ill. 5: Generation and effects of ONOO^- . ONOO^- is generated from a reaction between NO and O_2^- and can induce multiple cellular effects.

al. (2001) reported that activation of lyn kinase could be equally stimulated by a peptide containing nitrotyrosine substituted for phosphotyrosine [120]. ONOO⁻ treatment can also result in increased tyrosine phosphorylation via activation of PTK [121,122] or inactivation of PTP [123]. The degree of ONOO⁻-induced tyrosine nitration and phosphorylation is dependent upon ONOO⁻ dose, time, trophic environment, cell type, and protein target [121,124,125]. ONOO⁻ can also decrease tyrosine phosphorylation and inhibit signaling pathways [124]. Tyrosine nitration appears to be a stable modification in vitro that is resistant to chemical reducing agents (ascorbate, dithiothreitol, glutathione, sodium borohydrate) [126], but may be transient in vivo [125]. However, while an enzymatic activity for removing the NO₂ group from nitrotyrosine has been alluded to in some tissues, a specific enzyme has not been identified [127]. Nitration may target proteins for proteosomal degradation, resulting in the removal of critical proteins from signaling pathways [128]. ONOO⁻ can therefore modulate signaling pathways by altering posttranslational protein modifications, by promoting or attenuating protein activity, or by changing the regulation of signaling pathways.

ONOO⁻ induces activation of specific SFK in specific cell types, including c-Src in red blood cells and c-Src, Fyn, and Lyn in synaptosomes [129]. Methods of activation may be specific to each SFK. Di Stasi et al. (1999) found that increased c-Src activity in ONOO⁻-treated synaptosomes was independent of dephosphorylation of pY530 [130]. However, ONOO⁻-induced activation of Hck is reversible and dependent on cysteine modifications, while Lyn activation is irreversible and cysteine-independent [131]. These findings are similar to the actions of other reactive species on SFK. NO [132] and oxidative stress induced by ultraviolet radiation [133] and heavy metal ions [69] activate

SFK in a manner that appears independent of dephosphorylation of pY530 but is dependent on sulfhydryl formation. In addition, substrates containing nitrotyrosine may induce displacement of the SFK regulatory tail from the SH2 domain in a mechanism comparable to substrates containing phosphotyrosine, thereby resulting in activation [120]. Activation of SFK by ONOO⁻ can initiate signal transduction cascades, including signaling to the Src substrate p120 [124] and mitogenic proteins p38 and ERK1/2 [121]. The results presented in this dissertation identify c-Src as a target for tyrosine nitration in pancreatic cancer and suggest mechanisms for activation.

In addition to altering the function of biomolecules, ONOO⁻ can induce both necrotic and apoptotic cell death in vitro in a variety of cell lines [134-136]. Necrosis and apoptosis are differentiated by several features. Necrosis occurs within minutes to hours following traumatic cell injury (such as large doses of ONOO⁻), includes surrounding cells, and invokes an inflammatory response [137]. Apoptosis, which involves single cells and does not induce inflammation, is a delayed cell death: induction occurs hours after cytotoxic insult and requires intracellular signaling cascades [138], de novo protein synthesis, and ATP [137]. Initiation of apoptosis by ONOO⁻ involves activation of the cysteine proteases caspase-2, -3, -8, and -9 [136]. Removal of growth factors or serum deprivation can also induce apoptosis through ONOO⁻-mediated mechanisms [139]. ONOO⁻-induced apoptosis can be modulated by antioxidants, trophic factors, factors that stimulate antioxidant production, or the endonuclease inhibitor aurin tricarboxylic acid (ATA) [140]. Morphological features of apoptosis include shrunken cytoplasm, membrane blebbing, condensed chromatin, and DNA fragmentation [138].

FGF-1 treatment can have opposing actions on ONOO⁻-induced effects. In PC12 cells [135] and primary murine fibroblasts [140], FGF-1 enhances ONOO⁻-induced apoptosis, while FGF-1 pretreatment protects osteoblasts, osteoblast precursor cells [141], and ARIP cells [105]. FGF-1-enhanced apoptosis is dependent on p21 ras in PC12 cells and can be inhibited by overexpression of the antiapoptotic protein Bcl-2 [142]. In addition to modulating apoptosis, FGF-1 treatment increases ONOO⁻-induced tyrosine nitration and phosphorylation in primary murine fibroblasts and ARIP cells [140,105]. These differential effects induced by FGF-1 may be dependent on cellular expression of FGFR-1 α or FGFR-1 β . Pancreatic adenocarcinoma cells, ARIP cells, osteoblasts, and osteoblast progenitor cells, which demonstrate resistance to ONOO⁻, express FGFR-1 β as the major isoform, while ONOO⁻-sensitive cells, including PC12 cells and primary murine fibroblasts, express FGFR-1 α (J. A. Thompson, personal communication). Immunohistochemistry has demonstrated the co-appearance of FGFR-1, FGF-1, and nitrotyrosine in human pancreatic adenocarcinomas, suggesting the involvement of ONOO⁻ in pancreatic tumors [111]. While the factors regulating these opposing actions are unclear, these findings suggest that FGFR-1 α and FGFR-1 β signaling may differentially target tyrosine phosphorylation cascades and allow differential regulation of cell growth and death. This dissertation presents evidence that specific signaling between FGFR-1 β and SFK protects resistance vessel endothelial cells from ONOO⁻-induced death.

Angiogenesis

Angiogenesis is a multistage process incorporating endothelial cell activation, proliferation, migration, remodeling, and maturation of new vessels [9]. Formation of the tubule structure of the vessel requires alterations in morphology and adherence [143], processes governed by the cytoskeleton and focal adhesion complexes [144]. In the adult, the majority of endothelial cells are quiescent and are only activated during regulated processes such as wound healing [143]. During pathophysiology, there is a loss of regulation, and both tumor cells and infiltrating inflammatory cells stimulate angiogenesis from the surrounding microvasculature, resulting in abnormal vessels with altered vascular permeability [10].

FGFR-1 signaling is also an important mediator of angiogenesis. Activation of FGFR-1 by FGF-1 or FGF-2 stimulates endothelial cell proliferation, differentiation, and formation of tubule structures on a collagen matrix *in vitro* [145]. *In vivo*, blood vessel formation [146] and maturation of the vasculature [147] can be prevented by expression of a dominant-negative FGFR-1 and this effect is due in part to endothelial cell apoptosis and impaired cell migration [148]. Of all the FGF family members, FGF-1 and FGF-2 play prevalent roles in initiating angiogenesis both in normal physiology and in the vascular support of specific tumors [149]. In pancreatic cancer tissue, tumor cell and endothelial cell activation occur in conjunction with the appearance of FGF-2 [150]. FGF-1 and FGF-2 stimulate angiogenesis in xenografts of bladder carcinoma cells expressing FGFR-1, but only FGF-1 promotes tumorigenesis as well [151]. Expression of antisense FGFR-1 [152] and soluble FGFR-1 [153] (a dominant negative lacking a tyrosine kinase) stops tumor growth due to inhibition of angiogenesis. Due to the

prominent role of FGFR-1 and its ligands in tumor angiogenesis, several antiangiogenic drugs that target FGFR-1 signaling are in clinical trials. These include phase I trials of SU6668 (an inhibitor of FGFR, vascular endothelial growth factor receptor, and platelet-derived growth factor receptor (PDGFR)), phase II trials with Thalidomide (an inhibitor of FGF-2 initiated angiogenesis), phase II/III trials with Interferon- α (an inhibitor of FGF-2 synthesis), and trials with platelet factor 4 (an inhibitor of heparin-FGF-2 binding) [154].

SFK play important roles in angiogenesis in vitro and in vivo by regulating endothelial cell chemotaxis [155], vascular permeability [156], and cord-formation [157]. Integrin inhibitors block FGF-2 mediated chemotaxis by attenuating c-Src activity and translocation into focal adhesion sites [155]. Both FGF-2 and vascular endothelial growth factor (VEGF) activate c-Src during angiogenesis, but only VEGF effects, including vascular permeability, are completely dependent on c-Src or c-Yes [156]. c-Src's role in cord-formation includes modifying the actin cytoskeleton [158]. Findings presented in this dissertation provide the first evidence that activation of FGFR-1 β , but not FGFR-1 α , by FGF-1/heparin results in enhanced cord-formation in vivo and SFK dependent cord-formation in vitro.

Conclusions

Pancreatic adenocarcinoma is a lethal cancer due to its propensity to form advanced and metastatic tumors that are resistant to surgical resection, radiation, and chemotherapy. Understanding this persistent resilience requires elucidation of the molecular mechanisms that regulate cell survival and progression during neoplasia.

This review has argued that signal transduction pathways initiated by FGF-1 activated FGFR-1 appear capable of mediating these effects.

The subsequent papers are designed to test the hypothesis that specific FGFR-1 isoforms FGFR-1 α and FGFR-1 β differentially signal to SFK and initiate pathways regulating cell growth, survival, and invasiveness, processes essential to tumorigenesis, inflammation, and angiogenesis.

ALTERNATIVELY SPLICED FGFR-1 ISOFORM SIGNALING DIFFERENTIALLY
MODULATES ENDOTHELIAL CELL RESPONSES TO PEROXYNITRITE

by

JING JIAO, JESSICA S. GREENDORFER, PEI ZHANG, KURT R. ZINN,
CLEMENT A. DIGLIO, AND JOHN A. THOMPSON

Archives of Biochemistry and Biophysics 410:187-200

Copyright

2002

by

Academic Press

Used by permission

Format adapted for dissertation

INTRODUCTION

In adult humans, trauma injury is typically followed by the infiltration of active inflammatory cells. Despite the fact that local production of cytotoxic agents, such as cytokines, chemokines, and reactive nitrogen species (RNS) [1], are produced by active inflammation, this process is typically accompanied by angiogenesis. Within this proinflammatory environment, normally quiescent endothelial cells proliferate, migrate, and form new vascular structures. Inflammation promotes excess production of RNS, including peroxynitrite (ONOO^-), the product of a diffusion-limited reaction between superoxide and nitric oxide. At physiologic pH, protonated ONOO^- (peroxynitrous acid) decomposes to form a strong oxidant with the reactivity of hydroxyl radical plus nitrogen dioxide [1,2]. As a potent oxidant, ONOO^- attacks many macromolecules [3-9], including its reaction with specific tyrosine residues in target proteins that results in the formation of nitrotyrosine [8,10]. The increased appearance of nitrotyrosine has been detected during atherosclerosis, arthritis, chronically rejecting renal allografts, and pancreatic adenocarcinoma, pathophysiologic conditions also demonstrating enhanced expression of acidic fibroblast growth factor (FGF-1) and its high affinity FGF receptors [11-19]. These observations have predicted the in vivo coexistence of both FGF-1- and ONOO^- -induced signaling pathways that may modulate cellular growth and death responses in relevant pathophysiologic situations.

In vitro studies have demonstrated that addition of ONOO^- induced a dose-dependent, delayed cell death that was more characteristic of apoptosis than necrosis [20-24]. Mounting experimental evidence has suggested further that the trophic environment of cells in culture is an important determinant of their vulnerability to reactive oxidants

such as ONOO⁻. For instance, pretreatment of PC12 cells [20] and primary fibroblasts [21] with FGF-1 significantly enhanced apoptosis mediated by ONOO⁻. However, additional efforts have demonstrated that FGF-1 pretreatment in vitro renders some cell populations [22-24] resistant to the cytotoxic effects of ONOO⁻. Whereas the biological mechanism responsible for this differential FGF-1 effect is not known, we have predicted the interaction between ONOO⁻ and FGF-1-induced signaling pathways [21,22].

FGF-1 is 1 of 23 members of the human FGF gene family of polypeptides, which share a high degree of sequence similarity at both the nucleotide and the amino acid levels and have in common several structural motifs [25-28]. Numerous studies have established that the biological activity of the FGF ligands involves productive HSPG-dependent cell surface interactions with the FGFRs followed by activation of the intrinsic tyrosine kinase and responding signal transduction cascades [28-31]. To date, four similar high affinity FGF receptor genes (FGFR-1, FGFR-2, FGFR-3, and FGFR-4) have been identified and generally contain an extracellular immunoglobulin (Ig)-like domain(s), a transmembrane region, and an intracellular tyrosine kinase. Structural variants of these FGFRs are generated by alternative splicing, resulting in receptor isoforms containing different ligand-binding specificities and affinities [31-33]. The major FGFR-1 splice variants give rise to receptors with either three (FGFR-1 α) or two (FGFR-1 β) Ig-like domains in the extracellular region. The differential expression of these FGFR-1 isoforms may be biologically significant since normal pancreatic ductal epithelium and brain tissue express FGFR-1 α primarily, whereas malignant pancreatic adenocarcinoma and astrocytoma overexpress FGFR-1 primarily as the β isoform [29,34,35].

To examine whether ligand activation of alternatively spliced FGFR-1 modulates cellular responses to ONOO⁻ in vitro, we have stably transfected FGFR-negative rat endothelial cells with human cDNA sequences encoding either FGFR-1 α or FGFR-1 β . Several lines of evidence provide the first indication that ligand activation of alternatively spliced FGFR-1 isoforms differentially modulates cellular responses to ONOO⁻ in a signaling-dependent manner. These observations provide mechanistic insight relevant not only to regulation of FGF biology but also to processes controlling cellular growth and death during the resolution of inflammation and repair.

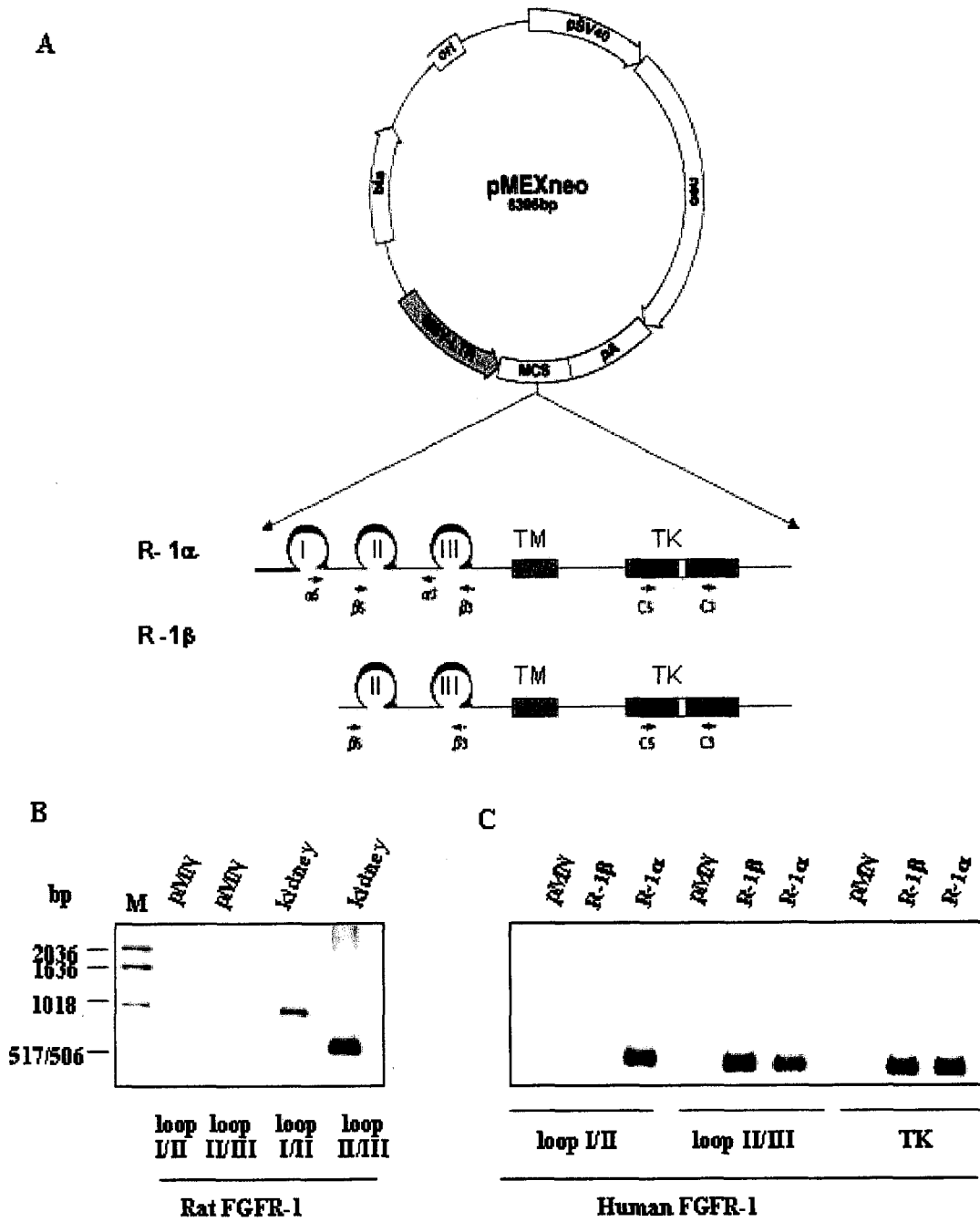
MATERIALS AND METHODS

Recombinant plasmids

Plasmids (Fig. 1A) pXZ106 and pXZ85 contained the complete human cDNA coding sequences for FGFR-1 α or FGFR-1 β , respectively, which were subcloned 3' of the murine sarcoma virus LTR promoter and 5' of the SV40 polyadenylation signal in the eukaryotic expression vector pMEXneo [36]. The pMEXneo plasmid (pMN) includes the neomycin phosphotransferase gene under control of the early SV40 promoter and served as a transfection control.

Tissue culture and transfections

Resistant vessel endothelial cells (RVEC) were isolated from rat cerebrocortical tissue [37] and established in culture using DMEM supplemented with 10% (v/v) heat-inactivated fetal bovine serum (FBS) and 100 U/100 μ g penicillin/streptomycin. Routine passage of isolated cells was performed at confluence following 0.25% (w/v) trypsin, 0.5



mM EDTA treatment, and replating (1×10^4 cells/cm²). Cells were transfected with 10 μ g of either pMN, pXZ106, or pXZ85 using calcium phosphate-mediated precipitation followed by selection (21 days) in 800 μ g/ml active Geneticin. Stably transfected RVEC(pMN), RVEC(R-1 α), and RVEC(R-1 β) were maintained in culture under normal culture conditions.

Growth Analysis

Stably transfected cells (3×10^3 /cm²) were seeded in six-well plates and allowed to attach (16 h) under normal culture conditions. Cells were washed (PBS) and fed every 2 days with fresh endothelial cell serum-free medium (ESFM; Invitrogen) containing FGF-1 (10 ng/ml) complexed with heparin (10 U/ml). Viable cells (trypan exclusion) for each transfectant were counted by hemacytometer at 2-day intervals, in duplicate, using five separate measurements/well. To measure the proliferation index of each transfectant, cells (3×10^3 /cm²) were seeded and allowed to attach (16 h) under normal culture conditions. Cells were washed (PBS) and maintained (48 h) in ESFM. Following washing (PBS), cells were incubated (24 h) with ESFM containing FGF-1 (10 ng/ml) complexed with heparin (10 U/ml) and labeled with bromodeoxyuridine (BrdU; Sigma; 10 μ M) during the final 4 h. Cells were harvested, fixed, and analyzed in situ using monoclonal mouse anti-BrdU (1:100; Dako) as described [38].

RNA Analysis

Total RNA (1.0 μg) was converted to cDNA using reverse transcriptase (RT) and the reverse transcribed cDNA product was amplified by the polymerase chain reaction (PCR) using previously described conditions [38]. RT-PCR products were analyzed by 2% (w/v) agarose gel electrophoresis using PCR amplification of specific expression vectors (Fig. 1) as positive controls. Accuracy of amplification was confirmed further by restriction endonuclease mapping of the PCR products. Non-transfected cellular RNA served as a negative control. RT-PCR performed in the absence of RT was used to determine the potential of contaminating genomic DNA in total RNA preparations. Following electrophoresis, PCR products were stained with ethidium bromide and visualized with UV light. Photographs of gels were digitized using a Xerox 7650 scanner. Comparative analysis of specific RT-PCR products from separate cell populations was achieved following standardization to levels of amplified GAPDH from identical samples evaluated within the same gel [39]. Synthetic DNA amplimers for the neomycin phosphotransferase gene were identical to those previously described [38]. The synthetic DNA sense amplimer sequence specifically recognizing rat FGFR-1 α cDNA was CTG ACT CTG GCC TCT ACG CTT GTG TG. The synthetic DNA sense amplimer sequence specifically recognizing both FGFR-1 α and FGFR-1 β rat cDNA was ACG GCA AGG AAT TCA AAC CTG ACC ACC. The common synthetic DNA antisense amplimer specifically recognizing both FGFR-1 α and FGFR-1 β rat cDNA was TGA GGT CAT CAC GGC TGG TCT CTC TTC CA. Synthetic DNA amplimers for human FGFR-1 α cDNA were sense, CTC TAT GCT TGC GTA ACC AGC and antisense, ATG AAC TCC ACG TTG CTA CCC. Synthetic DNA amplimers for both

human FGFR-1 α and FGFR-1 β cDNA were sense, GAC AGT GAA GTT CAA ATG CCC and antisense, GAT AGA GTT ACC CGC CAA GC. Synthetic DNA amplimers for the cytoplasmic domain encoding the split tyrosine kinase for both human FGFR-1 α and FGFR-1 β cDNA were sense, AAG GAC AAA CCC AAC CGT GTG ACC and antisense, GCC AAA GTC TGC TAT CTT CAT CAC.

Scatchard Analysis

Recombinant human FGF-1 (amino acids 21-154) was purified [40], modified with succinimidyl 6-hydrazinonicotinate, and radiolabeled with ^{99m}Tc as described [41]. Cells were grown under normal conditions (70-80% confluent), harvested with 1mM EDTA, and resuspended in DMEM containing 0.1% (w/v) BSA and 20 mM Hepes (pH 7.2). Cells (1×10^6 /assay) were incubated (2 h, 4°C) with five or six different concentrations of ^{99m}Tc -FGF-1 (0.9 MBq/ μg) complexed to 10 U/ml heparin. Cell-bound ^{99m}Tc -FGF-1 was determined after washing two times with PBS (4°C) and gamma counting. Scatchard plots of specific binding of ^{99m}Tc -FGF-1 to RVEC transfectants were analyzed using the Ligand program [42].

Peroxyinitrite treatment

RVEC transfectants were seeded ($3 \times 10^3/\text{cm}^2$) onto fibronectin-coated ($1 \mu\text{g}/\text{cm}^2$) glass coverslips (4.8 cm^2) in six-well plates and allowed to attach (16 h) under normal culture conditions. Where indicated, FGF-1 (50 ng/ml) complexed with heparin (50 U/ml) was added for 2 h prior to oxidant treatment. PD166866 ($1 \mu\text{M}$; 60 min; Warner-

Lambert), PP2 (20 μM ; 20 min; Calbiochem), PD98059 (37 μM ; 30 min; Calbiochem), SB203580 (25 μM ; 30 min; Calbiochem), and SB202190 (25 μM ; 30 min; Calbiochem) were added for indicated times prior to FGF-1/heparin treatment. Aurin tricarboxylic acid (ATA; 25 μM ; Sigma) was added to the culture medium subsequent to oxidant treatment.

Prepared RVEC transfectants were washed twice with PBS and each well received 1.0 ml Buffer A, containing 50 mM Na_2HPO_4 , 90 mM NaCl, 5 mM KCl, 0.8 mM MgCl_2 , and 1 mM CaCl_2 . ONOO^- was synthesized from sodium nitrite and acidified H_2O_2 and quantified as described [21]. RVEC transfectants were treated with aliquots of a 50 mM stock solution, which was added as a single bolus against one side of the wall while rapidly agitating (5-10 s). Control treatments consisted of either 0.1 M NaOH vehicle alone or decomposed ONOO^- obtained by adding ONOO^- to Buffer A prior (20 min) to cell exposure (reverse order of addition). Following ONOO^- treatment (5 min), the Buffer A was removed and replaced with fresh ESFM. Stock solutions (100 mM) of SIN-1 were added to RVEC transfectants at a final concentration of 1 mM, which generates production of ONOO^- (10 $\mu\text{M}/\text{min}$). Following incubation (37°C; 1.5 h), the SIN-1-containing Buffer A was removed and replaced with ESFM.

Following (20 h) oxidant treatment, washed (PBS) cells were incubated (15 min, 22°C) with a mixture of fluorescein diacetate (FDA; 15 $\mu\text{g}/\text{ml}$; Sigma) and propidium iodide (PrI; 5 $\mu\text{g}/\text{ml}$; Sigma) as described [21] and immediately observed by epifluorescence microscopy. The percentage of non-viable cells was calculated by assessing the ratio of red-staining (PrI) cells to the total of red and green (FDA) cells in at least five representative fields per coverslip. Quantitative analysis of FDA and PrI

staining was enumerated on duplicate wells with at least five separate samples per well. Each experiment was performed at least three times. Data are reported as the mean \pm standard error and statistical significance was performed with one-way ANOVA or Student's *t* test, as appropriate. A difference of $p < 0.05$ was considered significant.

Western Analysis

RVEC transfectants ($1 \times 10^4/\text{cm}^2$) were seeded and allowed to attach and grow to approximately 80% confluency under normal growth conditions. Cultures were washed (PBS) and fed DMEM, supplemented with 0.3% (v/v) FBS for 16 h. Quiescent cells were treated (10 min) with either FGF-1 (50 ng/ml) alone or FGF-1 (50 ng/ml) complexed with heparin (50 U/ml). Cells were washed and scrape-harvested with PBS (4°C), containing 1 mM sodium orthovanadate, and recovered by centrifugation. For analysis of MAP kinases, cells were lysed with 20 mM Tris-HCl (pH 7.4), 150 mM NaCl, 1 mM EDTA, 1 mM EGTA, 1% (v/v) Triton X-100, 2.5 mM sodium pyrophosphate, and 1 mM β -glycerolphosphate (lysis buffer). For analysis of FGFR-1 isoforms, SFK, and cortactin, cells were lysed with 1% (v/v) Triton X-100, 0.1% (w/v) SDS, 1% (v/v) sodium deoxycholate, 50 mM Hepes (pH 7.4), 150 mM NaCl, and 1 mM EGTA (RIPA buffer). Both the lysis and RIPA buffers contained 1 mM sodium orthovanadate, 1 mM PMSF, 10 μM leupeptin, and 10 $\mu\text{g}/\text{ml}$ aprotinin. Detergent-insoluble material was removed by centrifugation (14,000 rpm; 4°C) and detergent-soluble protein concentrations were determined using the Bradford assay (Pierce). For removal of carbohydrate residues, recovered extracts (70 μg total protein) were denatured and incubated (37°C, 1 h) with 2000 U *N*-Glycosidase F using buffers and conditions

provided by the manufacturer (New England Biolabs). To examine FGFR-1 and cortactin phosphorylation, total extracted proteins (500 μg) were incubated with monoclonal antiphosphotyrosine antibody (4 $\mu\text{g}/\text{ml}$; Transduction Laboratories) for 16 h (4°C) followed by precipitation (2 h; 4°C) with a 50 μl suspension of protein A-coupled Sepharose (Pharmacia Biotech Inc.). The Sepharose beads were washed and transferred to a new tube using RIPA buffer, resuspended in Laemmli buffer, and boiled (5 min). Recovered phosphoproteins, total extracted proteins (70 μg), and deglycosylated proteins (70 μg) were fractionated by reducing SDS-PAGE and Western analyzed using antibodies against FGFR-1 (C-15; Santa Cruz), cortactin (Upstate Biotechnology), total and phospho-p38 MAPK (Cell Signaling), total and phospho-JNK (Cell Signaling), or total and phospho-Erk 1/2 (Cell Signaling). Western analyses of the SFK included total SFK (SRC 2; Santa Cruz) or phospho-SFK (Tyr 416; Cell Signaling), antibodies recognizing multiple family members, including c-Src, YES, Hck, and Fyn. Immunoreactive bands were identified by the enhanced chemiluminescence system (Kirkegaard & Perry) as described [38].

RESULTS

Early passages of RVECs were transfected independently with expression vectors (Fig. 1A), selected in Geneticin, and expanded for biochemical analyses. Each individual transfection was repeated at least three times, all of which resulted in similar results. No attempt was made to subclone specific cell populations relative to expression levels of either the selectable marker (neomycin phosphotransferase) or the modulatory transgenes (FGFR-1 α or FGFR-1 β). A characteristic RT-PCR product (790 bp) was identified for

the neomycin phosphotransferase gene in pMN-, R-1 α - and R-1 β - transfected cells, which was consistent with the ability of these cells to maintain growth in Geneticin. Expression of FGFR-1 α and FGFR-1 β mRNA in total RNA extracted from rat kidneys was demonstrated by the appearance (Fig. 1B) of the predicted 834- and 535-bp, respectively, RT-PCR products using rat-specific amplicon sequences. In contrast, non-transfected RVEC, RVEC(pMN), RVEC(R-1 α), and RVEC(R-1 β) cells failed to exhibit expression of rat FGFR-1 α or FGFR-1 β mRNA as determined by RT-PCR analysis using rat-specific amplicon sequences (Fig. 1B). Both non-transfected RVEC and RVEC(pMN) cells failed to exhibit expression of human FGFR-1 α and FGFR-1 β mRNA following RT-PCR analysis (Fig. 1C) using human-specific amplicon sequences encoding either the extracellular Ig-like loops I/II (Fig 1A; amplicon pair $\alpha 5/\alpha 3$), the Ig-like loops II/III (Fig. 1A; amplicon pair $\beta 5/\beta 3$), or the intracellular split tyrosine kinase (Fig. 1A; amplicon pair C5/C3). Expression of human FGFR-1 α mRNA was restricted to RVEC(R-1 α) cells as evidenced by the appearance of a predicted 530-bp amplicon following RT-PCR analysis using human-specific amplicon sequences encoding the extracellular Ig-like loops I and II (Fig. 1C). Both RVEC(R-1 α) and RVEC(R-1 β) cells expressed mRNA sequences encoding the extracellular Ig-like loops II and III of human FGFR-1 that was demonstrated by the appearance of a predicted 526-bp RT-PCR product (Fig. 1C). In addition both RVEC(R-1 α) and RVEC(R-1 β) cells expressed human FGFR-1 mRNA sequences encoding the intracellular split tyrosine kinase as determined by the appearance of a predicted 437-bp RT-PCR product (Fig. 1C).

Translation of human FGFR-1 mRNA was investigated by Western analysis (Fig. 2), wherein cellular extracts from individual transfectants were examined. Total cellular

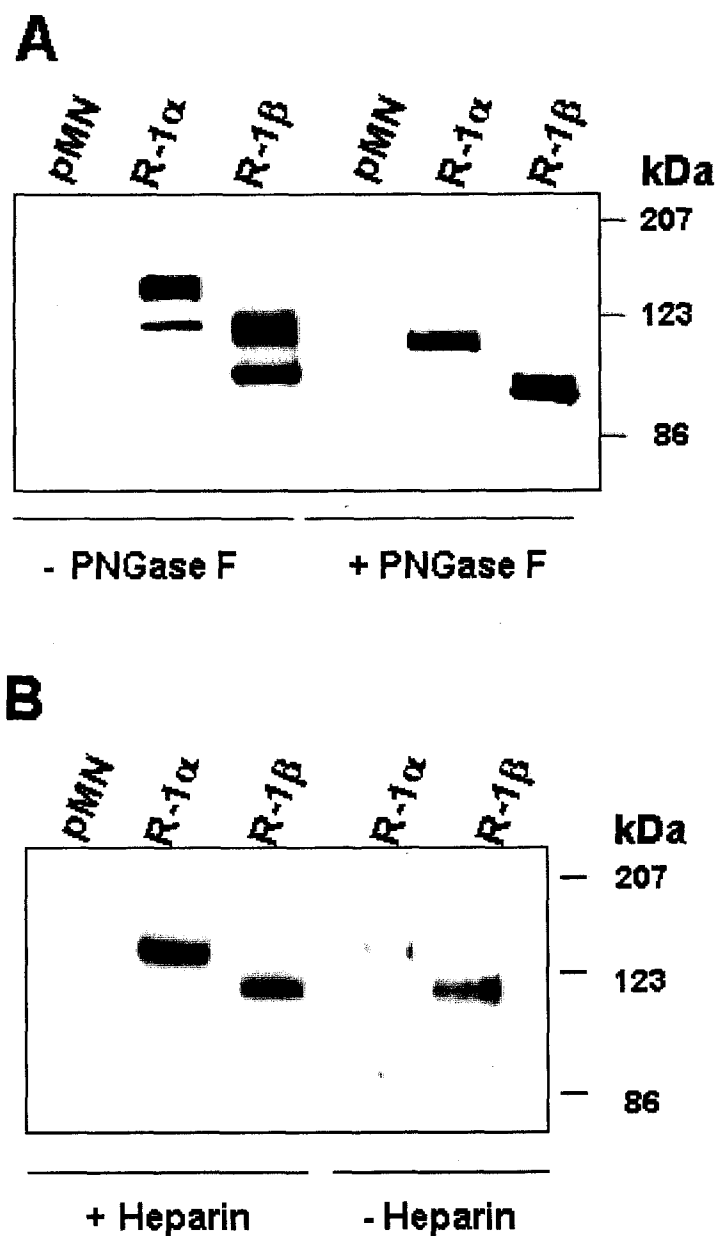


Fig. 2. Western analysis of individual RVEC transfectants. (A) Total cellular proteins (70 μ g), harvested from either RVEC(pMN), RVEC(R-1 α), or RVEC(R-1 β) cells, exposed (10 min) to extracellular FGF-1 (50 ng/ml) complexed with heparin (50 U/ml), were treated in the presence (+) or absence (-) of *N*-Glycosidase F (PNGase F), fractionated by 7.5% (w/v) reducing SDS-PAGE, and Western analyzed with a polyclonal antibody against the carboxyl termini of FGFR-1 (C-15). (B) Total cellular proteins (700 μ g), harvested from either RVEC (pMN), RVEC-1 α or RVEC-1 β cells subsequent (10 min) to treatment with FGF-1 (50 ng/ml) either alone (-) or complexed (+) with heparin (50 U/ml) were immunoprecipitated with anti-phosphotyrosine, fractionated by 7.5% (w/v) reducing SDS-PAGE, and Western analyzed with anti-FGFR-1 (C-15). Approximate sizes of immunoreactive bands were estimated using prestained molecular mass (kDa) standards.

extracts from both non- and control (pMN)-transfected RVECs failed to demonstrate the appearance of immunoreactive FGFR-1 protein, either in the presence or in the absence of treatment with N-Glycosidase F (Fig. 2A). RVEC(R-1 α) cells readily demonstrated two resolved bands of immunoreactive FGFR-1, migrating with apparent molecular masses of approximately 145 and 120 KDa. RVEC(R-1 β) cells also demonstrated two resolved bands of immunoreactive FGFR-1, migrating with apparent molecular masses of approximately 118 and 105 KDa. Deglycosylation of total cellular proteins prior to reducing SDS-PAGE resulted in the appearance of a single band of immunoreactive FGFR-1, migrating as a single band with apparent molecular masses of 115 KDa and 90 KDa, respectively, in RVEC(R-1 α) and RVEC(R-1 β) cells. The fully glycosylated transgenes were reduced by similar amounts (30 KDa), suggesting that the individual FGFR-1 isoforms were posttranslationally modified in a similar manner by RVECs. Following (10 min) treatment of RVEC transfectants with FGF-1 (50 ng/ml) complexed to heparin (50 U/ml), total cellular proteins were immunoprecipitated with polyclonal antibodies against phosphotyrosine and Western analyzed with antibodies against FGFR-1 (Fig. 2B). Immunoprecipitated extracts from control-transfected RVEC(pMN) cells failed to demonstrate the immunoappearance of tyrosine phosphorylated FGFR-1. In RVEC(R-1 α) and RVEC(R-1 β) transfected cells, FGF-1-induced tyrosine phosphorylation of FGFR-1 was restricted to the higher-molecular-mass structures of glycosylated FGFR-1 (145 KDa and 115 KDa, respectively). In the absence of heparin, FGF-1 (50 ng/ml) treatment (10 min) induced similar levels of tyrosine phosphorylated FGFR-1 in RVEC(R-1 β) cells and significantly lower levels of this posttranslational modification in RVEC(R-1 α) cells.

In the presence or absence of heparin, no binding of ^{99m}Tc -labeled FGF-1 (Fig. 3) was observed with control-transfected RVEC cells (pMN). Scatchard analysis demonstrated specific binding of ^{99m}Tc FGF-1 (complexed with heparin) to both RVEC(R-1 α) and RVEC(R-1 β) cells. The calculated binding constant (Table 1) for RVEC(R-1 β) cells ($K_d = 383$ pM) was approximately three times higher than that determined for RVEC(R-1 α) cells ($K_d = 950$ pM). In the absence of heparin, RVEC(R-1 β) cells retained high affinity ($K_d=890\text{pM}$) ^{99m}Tc -FGF-1 binding; however, RVEC(R-1 α) failed to demonstrate high-affinity binding interactions (data not shown). Binding of ^{99m}Tc -FGF-1 was specific since it was completely inhibited by the addition of 100-fold excess of unlabeled FGF-1. Non-specific binding accounted for less than 5% of the total cellular binding. Calculations of receptor number from the Scatchard analysis (Table 1) of the individual RVEC transfectants revealed that both RVEC(R-1 α) and RVEC(R-1 β) cells contained approximately 3×10^4 FGFR-1 per cell.

Table 1
High-affinity Binding Constant (K_d) and Receptor Number Calculated
From Scatchard Analysis of Individual Transfectants

	K_d^a	Receptor number/cell ^b
PMN	Not detectable	Not detectable
R-1 α	950pM	3.0×10^4
R-1 β	383pM	3.1×10^4

^a $K_d = -1/\text{slope}$.

^bReceptor number/cell = $\frac{([\text{X-intercept}][10^{-9}][10^{-3}][6.02 \times 10^{23}]})}{\text{Total cell number}}$.

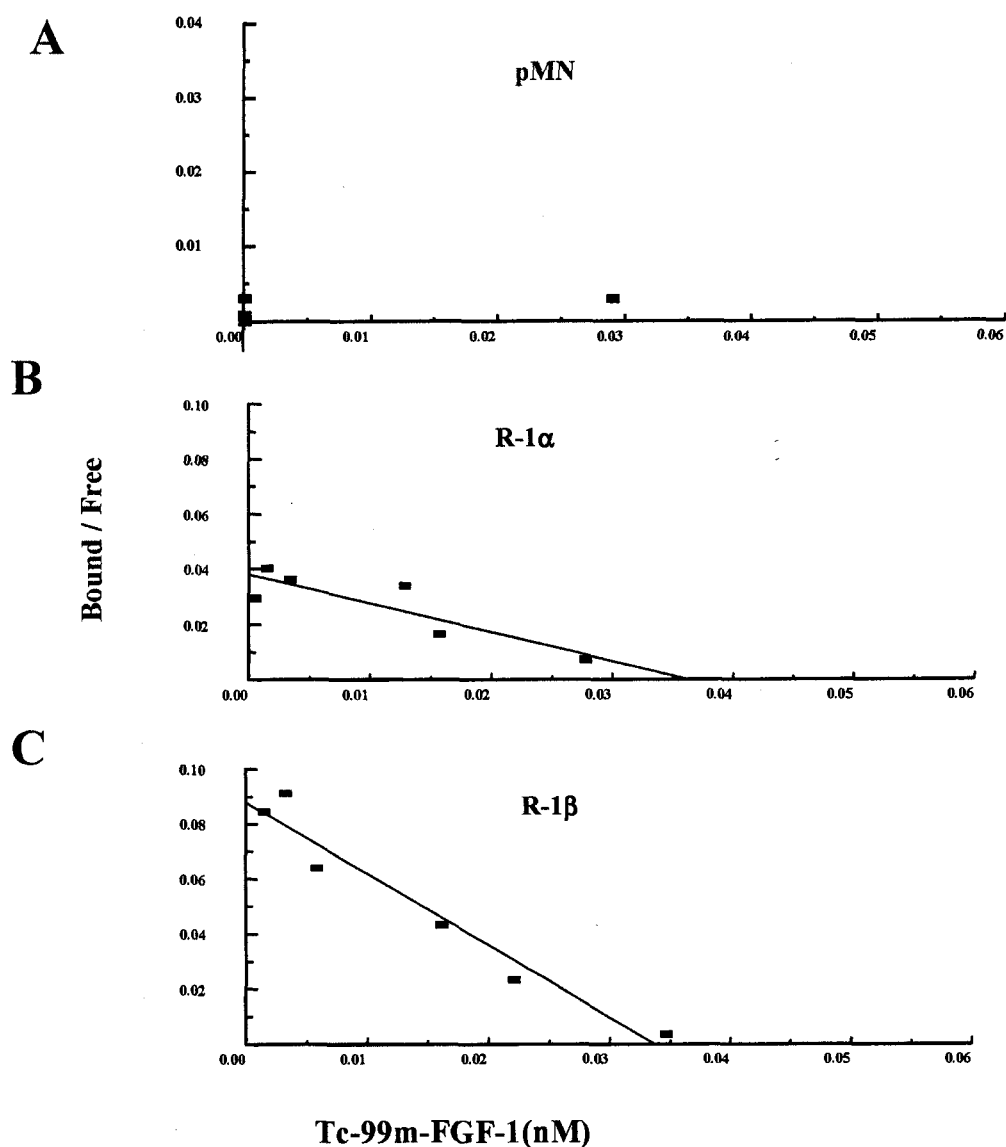


Fig. 3. Scatchard analysis of FGF-1 binding to individual RVEC transfectants. Recombinant human FGF-1 was radiolabeled with ^{99m}Tc . Cell binding analyses were determined by incubating different concentrations of ^{99m}Tc -FGF-1 (0.9 MBq/ μg) complexed with 10 U/ml heparin to RVEC(pMN) (A), RVEC(R-1 α) (B), or RVEC(R-1 β) (C) cells (1×10^6 /assay). Cell-bound ^{99m}Tc -FGF-1 was determined by gamma counting to generate individual Scatchard plots.

The morphological differences between individual populations of transfected cells were compared microscopically (Figs. 4A-C). Non-transfected control, RVEC(pMN), and RVEC(R-1 α) cells displayed a typical cobblestone phenotype following treatment (24 h) with ESFM containing FGF-1(10 ng/ml) complexed with heparin (10 U/ml). In contrast, treatment (24 h) of RVEC(R-1 β) cells with FGF-1/heparin resulted in the induction of an altered phenotype, characterized by a spindle-like morphology (Fig. 4C). This morphological response was dependent on constant presentation of FGF-1/heparin since its elimination resulted in reversion to a more normal cobblestone phenotype.

Compared to non- and control (pMN)-transfected RVEC cells, both RVEC(R-1 α) and RVEC(R-1 β) cells demonstrated a significantly increased growth advantage (Fig. 4D) when maintained in the constant presence of FGF-1(10 ng/ml) complexed with heparin (10 U/ml). For more detailed analytical measurements, growth potential (Fig. 4E) was evaluated by determining the proliferation index (BrdU incorporation) of individual populations of RVEC transfectants maintained (24 h) in the presence of FGF-1 (10 ng/ml) complexed with heparin (10 U/ml). The percentages of non- and control(pMN)-transfected cells labeled under these conditions was very similar (20%). In contrast, both RVEC(R-1 α) and RVEC(R-1 β) cells exhibited a significantly ($p < 0.01$) higher proliferation index (35 and 42%, respectively).

To determine the sensitivity of RVEC transfectants to ONOO⁻, cells were exposed to increasing concentrations of the strong oxidant and analyzed for cell death 20 h after treatment (Fig. 5). Quantitative FDA/PrI staining demonstrated that in the absence of FGF-1/heparin, ONOO⁻ toxicity for each of the RVEC transfectants was dose-dependent with a similar EC₅₀ of approximately 1.35 mM (Fig. 5A). Immediately following

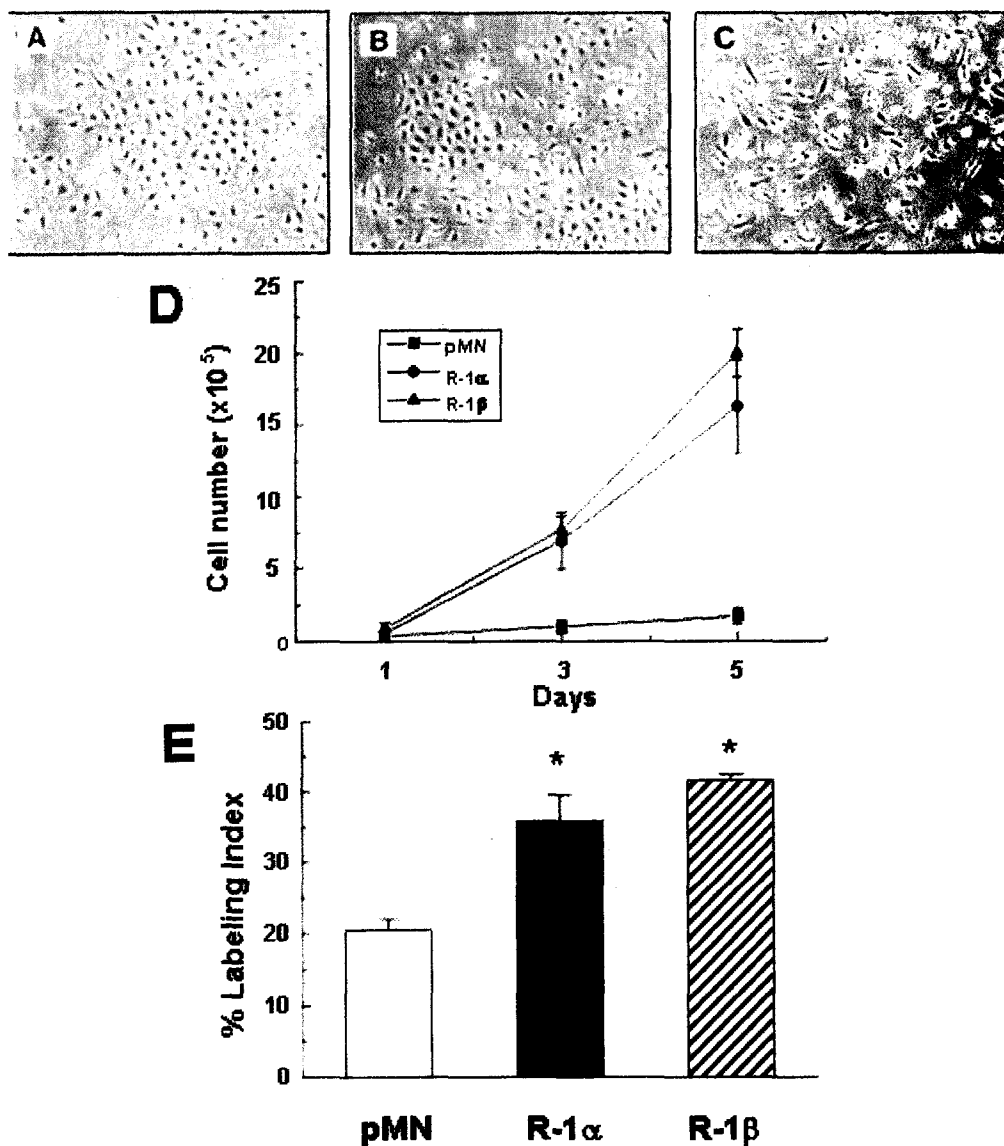


Fig. 4. In situ analysis and growth kinetics of individual RVEC transfectants. The phenotypes of RVEC(pMN) (A), RVEC(R-1 α) (B), RVEC(R-1 β) (C) transfectants were examined by phase-contrast microscopy following treatment (24 h) with FGF-1 (10 ng/ml) complexed with heparin (10 U/ml). (D) Number of viable (trypan exclusion) RVEC(pMN), RVEC(R-1 α), and RVEC(R-1 β) cells maintained in serum-free media containing FGF-1 (10 ng/ml) complexed with heparin (10 U/ml) were determined at 2-day intervals. (E) Proliferation indexes of RVEC(pMN), RVEC(R-1 α), and RVEC(R-1 β) cells maintained (24 h) in serum-free media containing FGF-1 (10 ng/ml) complexed with heparin (10 U/ml) were determined following labeling with BrdU during the final 4 h. The labeling index was determined in situ by calculating the percentage of nuclei staining positive with anti-BrdU. * Differential significance of $p < 0.01$ compared to control-transfected RVEC(pMN) cells.

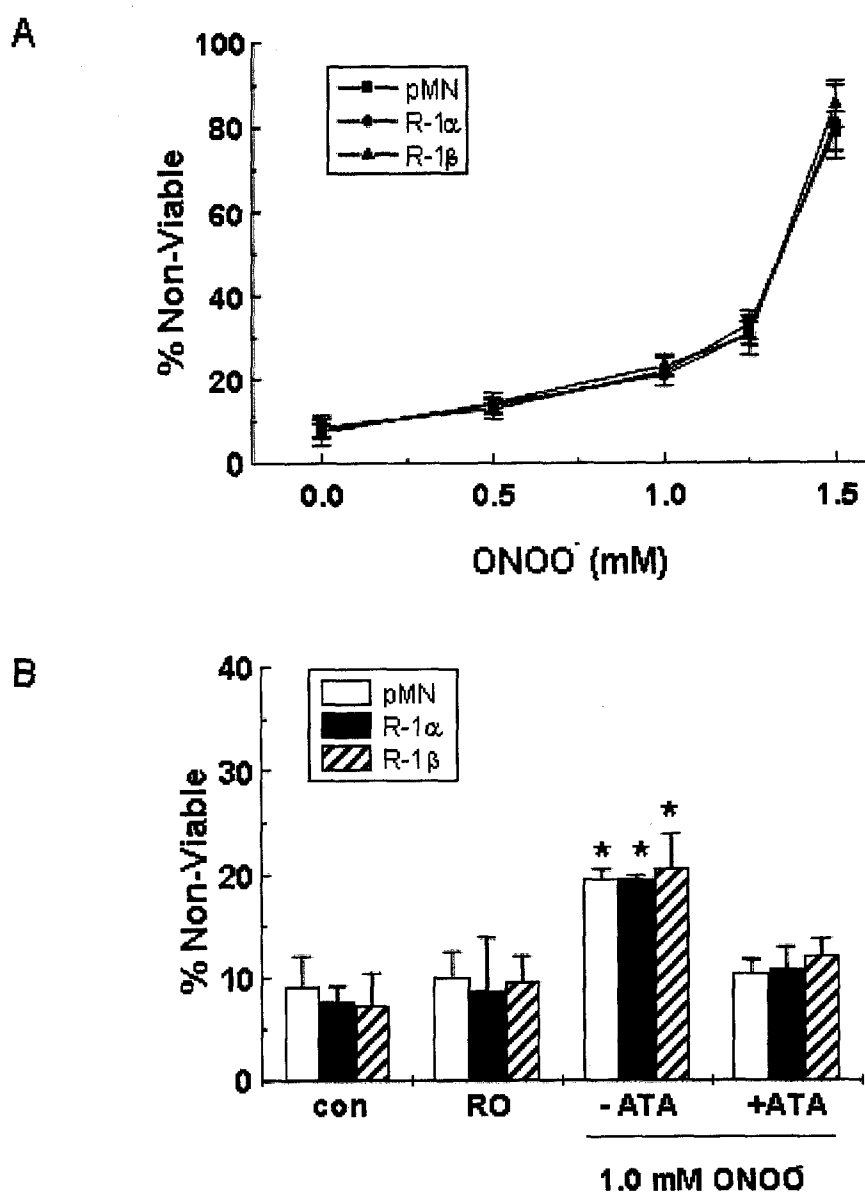


Fig. 5. Oxidant-induced cell death in individual RVEC transfectants. (A) Cell death (% non-viable) was assessed by quantitative viability staining (FDA/PrI) of RVEC(pMN), RVEC(R-1 α), and RVEC(R-1 β) cells following (20 h) exposure to the indicated concentrations of ONOO⁻. (B) Cell death (% non-viable) was determined (FDA/PrI) in RVEC(pMN), RVEC(R-1 α), and RVEC(R-1 β) cells following (20 h) exposure to 1.0 mM ONOO⁻. Controls included either no treatment (con) or exposure to decomposed ONOO⁻, reverse order (RO) of addition. Subsequent to ONOO⁻ exposure, cells were maintained in the absence (-) or presence (+) of the nuclease inhibitor, ATA. * Differential significance of $p < 0.01$ compared to controls and ATA treatment.

ONOO⁻ exposure and up to 2 hours following oxidant treatment, minimal changes in cell death were observed at all concentrations of ONOO⁻ examined. By 6 h and at all subsequent time points after oxidant exposure, increasing numbers of non-viable cells were evident. From 6 to 20 h after exposure to 1 mM ONOO⁻, cell death correlated with membrane blebbing, cytoplasmic shrinkage, nuclear condensation, and increased DNA fragmentation as evidenced by increased TUNEL staining (data not shown). By 20 h following ONOO⁻ exposure, maximal levels of cell death were observed. Each of the RVEC transfectants similarly demonstrated these time-dependent features. Quantitative FDA/PrI staining detected baseline death (< 10%) in untreated cells and those exposed to decomposed ONOO⁻ (reverse order of addition) with no significant differences between individual transfectants (Fig. 5B). In addition, non-oxidant treated RVEC transfectants exhibited no change in cell death following exposure (2 h) to FGF-1 (50 ng/ml) complexed with heparin (50 U/ml). In the absence of FGF-1/heparin, RVEC transfectants treated with 1 mM ONOO⁻ exhibited a significant ($p < 0.01$) 2-fold increase in cell death (approximately 20%) with no significant differences between individual transfectants (Fig. 5B). Addition of the endonuclease inhibitor ATA to media immediately after oxidant exposure significantly ($p < 0.01$) abrogated the ONOO⁻-induced toxicity of each of the RVEC transfectants.

A detailed kinetic analysis of the time interval between FGF-1/heparin pretreatment and exposure to ONOO⁻ was performed on each of the RVEC transfectants (Fig. 6). Compared to non-treated controls and those treated with decomposed ONOO⁻, RVEC(pMN) cells demonstrated a consistent 2-fold increase in oxidant-induced death regardless of the time of FGF-1 pretreatment. FGF-1 pretreatment of RVEC(R-1 α)

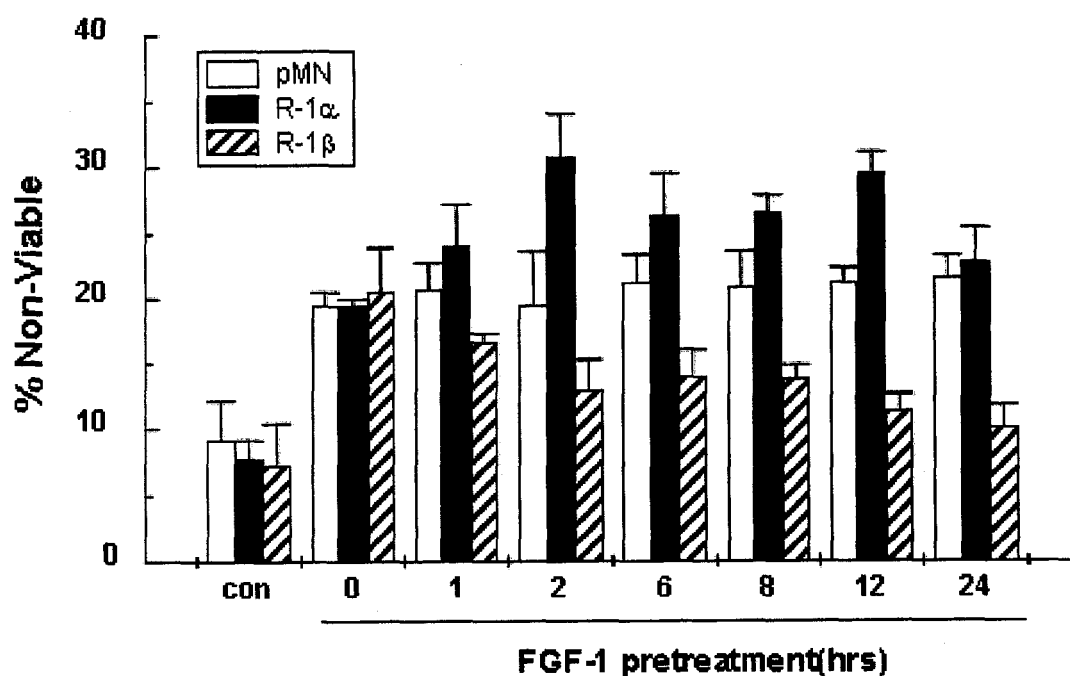


Fig. 6. Kinetic analysis of interval between FGF-1 pretreatment and ONOO⁻ exposure. Cell death (% non-viable) was assessed by quantitative viability staining (FDA/PrI) of RVEC(pMN), RVEC(R-1 α), and RVEC(R-1 β) cells following (20 h) pretreatment for the indicated times with FGF-1 (50 ng/ml) complexed with heparin (50 U/ml) and subsequent exposure to 1.0 mM ONOO⁻. Controls included no oxidant treatment (con).

transfectants for 1, 2, 6, 8, and 12 h prior to oxidant exposure consistently enhance the cytotoxic effects of ONOO⁻. FGF-1/heparin pretreatment of RVEC(R-1 α) transfectants for 24 h prior to oxidant exposure had no significant effect on ONOO⁻-induced cell death. In contrast, FGF-1 pretreatment of RVEC(R-1 β) transfectants for 1, 2, 6, 8, 12, and 24 h prior to oxidant exposure consistently protected cells from the cytotoxic effects of ONOO⁻.

In the absence of FGF-1 pretreatment, exposure of RVEC transfectants to 1.0 and 1.25 mM ONOO⁻, and to 1.0 mM SIN-1, which produces ONOO⁻ by simultaneously generating superoxide and nitric oxide, resulted in a significant ($p < 0.01$) 2-3-fold increase in cell death with no significant differences between individual transfectants (Fig. 7). FGF-1 pretreatment (2 h) of RVEC(pMN) cells had no effect on cell death induced by increasing levels of ONOO⁻ or SIN-1 when compared to oxidant-treated RVEC(pMN) cells in the absence of growth factor pretreatment. In contrast, pretreatment (2 h) with FGF-1 (50 ng/ml) complexed with heparin (50 U/ml) significantly ($p < 0.01$) enhanced the cytotoxic effects of 1.0 mM ONOO⁻, 1.25 mM ONOO⁻, and 1.0 mM SIN-1 in RVEC(R-1 α) transfectants by 58.2%, 46.4%, and 50.8%, respectively. Furthermore, FGF-1/heparin pretreatment (2 h) of RVEC(R-1 β) transfectants significantly ($p < 0.01$) reduced the cytotoxic effects of 1.0 mM ONOO⁻, 1.25 mM ONOO⁻, and 1.0 mM SIN-1 by 33.8%, 43.2%, and 32.6%, respectively. Pretreatment of RVEC(pMN), RVEC(R-1 α), or RVEC(R-1 β) transfectant with heparin (50 U/ml) alone had no modulatory effect on ONOO⁻-induced cell death (data not shown).

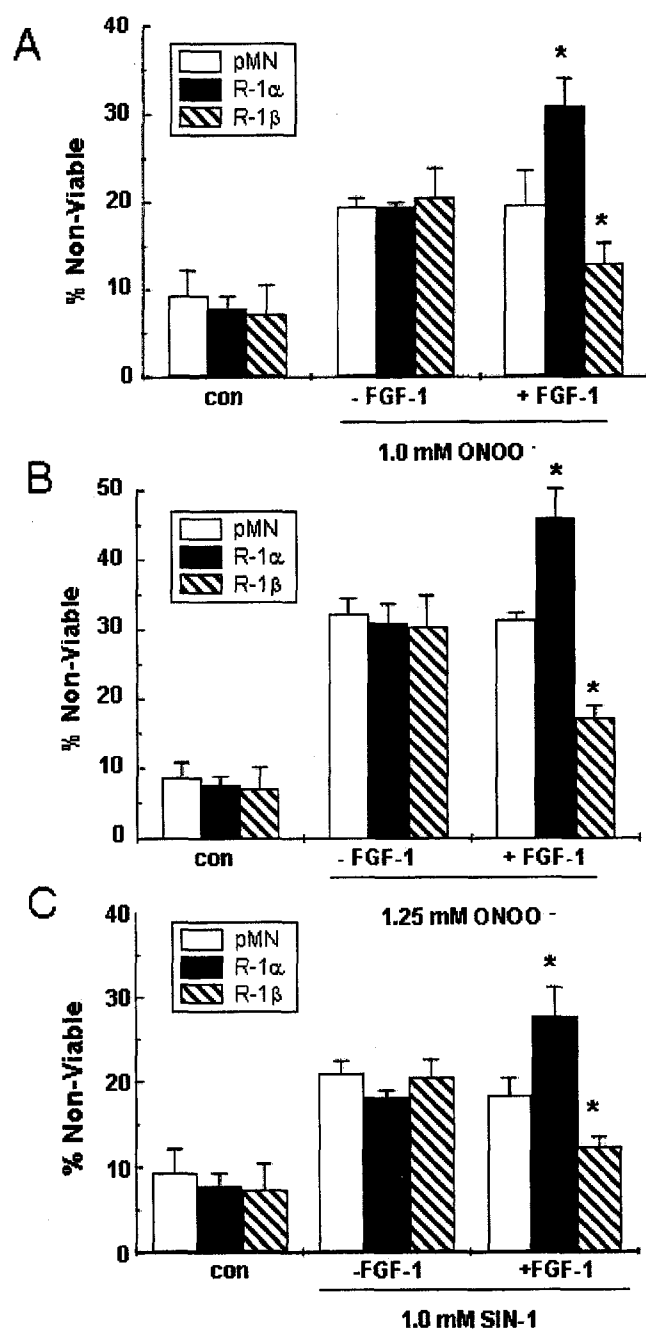


Fig. 7. Effect of FGF-1 pretreatment on ONOO⁻-induced cytotoxicity in RVEC transfectants. Cell death (% non-viable) was assessed by quantitative viability staining (FDA/PrI) of RVEC(pMN), RVEC(R-1 α), and RVEC(R-1 β) transfectants following (20 h) pretreatment (2 h) in the absence (-) or presence (+) of FGF-1 (50 ng/ml) complexed with heparin (50 U/ml) and subsequent exposure to either 1.0 mM ONOO⁻ (A), 1.25 mM ONOO⁻ (B), or 1.0 mM SIN-1 (C). Controls included no oxidant treatment (con). *Differential significance of $p < 0.01$ when compared to oxidant-treated transfectants in the absence of FGF-1 pretreatment.

To further confirm the FGFR-1 dependence of FGF-1 modulation of ONOO⁻-induced cytotoxicity, RVEC transfectants were exposed to 1 μ M PD166866, a highly selective and potent inhibitor of FGFR-1 tyrosine kinase, for 1 h. Cells were then pretreated (2 h) with FGF-1 (50 ng/ml) complexed with heparin (50 U/ml), treated with 1.25 mM ONOO⁻, and evaluated for cell death (PrI/FDA) 20 h following oxidant exposure. In the absence of FGF-1/heparin treatment, exposure of each individual RVEC transfectant population to PD166866 had no effect on cellular death either in the absence or presence of ONOO⁻ treatment (Fig. 8A). FGF-1/heparin pretreatment of PD166866-exposed RVEC(pMN) transfectants had no effect on cell death induced by ONOO⁻. In contrast, PD166866 exposure effectively inhibited the ability of FGF-1/heparin to modulate the cytotoxic effect of ONOO⁻ in both RVEC(R-1 α) and RVEC(R-1 β) transfectants. These observations further confirm that differential FGF-1 modulation of ONOO⁻-induced cell death in vitro is mediated through activation of FGFR-1 tyrosine kinase in both RVEC(R-1 α) and RVEC(R-1 β) transfectants.

To elucidate other potential downstream signaling pathways involved in differential FGF-1 modulation of ONOO⁻-induced cell death, individual RVEC transfectants were exposed to other specific tyrosine kinase inhibitors prior to FGF-1/heparin pretreatment and subsequent ONOO⁻ treatment. Preexposure (20 min) of each individual RVEC transfectant population to 20 μ M PP2, a selective inhibitor of SFK activity, had no effect on cellular death either in the absence or in the presence of ONOO⁻ treatment (Fig. 8B). FGF-1/heparin pretreatment of PP2-exposed RVEC(pMN) cells had no effect on cell death induced by ONOO⁻. FGF-1/heparin pretreatment of PP2-exposed RVEC(R-1 α) cells had no effect on the ability of the growth factor to enhance the

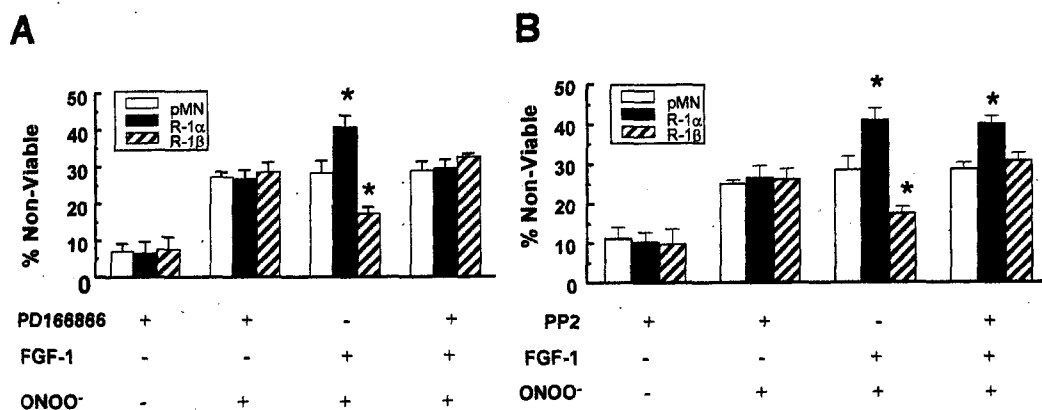


Fig. 8. Effect of FGFR-1 and Src-family kinase activities on FGF-1 modulation of ONOO⁻-induced cytotoxicity in RVEC transfectants. RVEC(pMN), RVEC(R-1 α) and RVEC(R-1 β) cells were incubated in the presence (+) or absence (-) of kinase inhibitors PD166866 (A) or PP2 (B) prior to pretreatment (2 h) in the absence (-) or presence (+) of FGF-1 (50 ng/ml) complexed with heparin (50 U/ml). Cell death (% non-viable) was assessed (FDA/PrI) 20 h following exposure to 1.25 mM ONOO⁻. Differential significance of $p < 0.01$ when compared to inhibitor- and oxidant-treated transfectants in the absence of FGF-1 pretreatment.

sensitivity of these cells to the cytotoxic effect of ONOO^- . In contrast, preexposure of RVEC(R-1 β) transfectants to PP2 effectively inhibited the ability of FGF-1/heparin pretreatment to protect these cells from ONOO^- -induced death. Preexposure (30 min) of each individual RVEC transfectant population to 37 μM PD98059, a selective inhibitor of the MEK/Erk 1/2 kinase, had no effect on cellular death either in the absence or presence of ONOO^- treatment (Fig. 9A). FGF-1/heparin pretreatment of PD98059-exposed RVEC(pMN) cells had no effect on cell death induced by ONOO^- . However, preexposure to PD98059 effectively inhibited the ability of FGF-1/heparin both to enhance ONOO^- -induced death in RVEC(R-1 α) cells and to prevent ONOO^- -induced death in RVEC(R-1 β) cells. Preexposure (30 min) of each individual RVEC transfectant population to 25 μM of either SB202190 or SB203580, potent inhibitors of the p38 MAPK and/or JNK kinases, had no effect on cellular death either in the absence or in the presence of ONOO^- treatment (Fig. 9B and C). FGF-1/heparin pretreatment of SB202190- or SB203580-exposed RVEC(pMN) cells had no effect on cell death induced by ONOO^- . Preexposure to SB202190 or SB203580 effectively inhibited the ability of FGF-1/heparin to enhance the cytotoxic effects of ONOO^- in RVEC(R-1 α) cells. However, preexposure to the p38 MAPK and JNK kinase inhibitors had no effect on the ability of FGF-1/heparin pretreatment to protect RVEC(R-1 β) cells from ONOO^- -induced death.

Following FGF-1/heparin treatment of individual RVEC transfectants for defined periods (0-2 h), total extracted cellular proteins were subjected to reducing SDS-PAGE and Western analyzed with antibodies specific for total p38 MAPK, activated phosphor-p38 MAPK, total JNK, activated phosphor-JNK, total Erk 1/2, active phosphor-Erk 1/2,

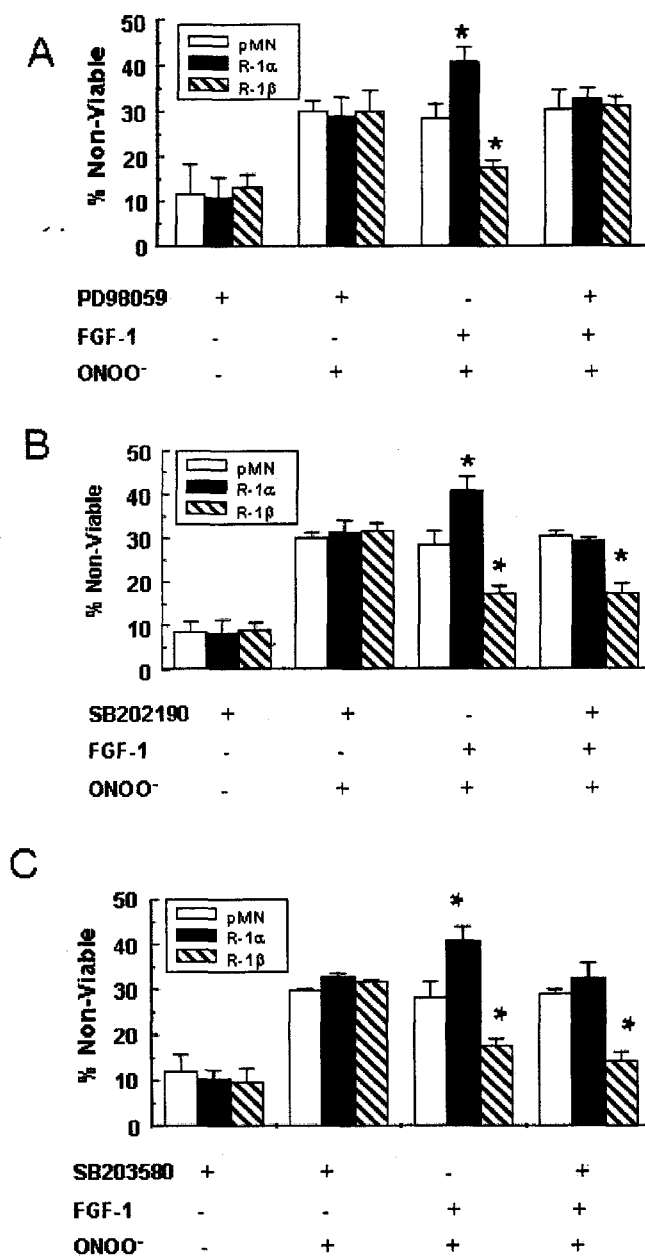


Fig. 9. Effect of mitogen-activated protein kinase activity on FGF-1 modulation of ONOO⁻-induced cytotoxicity in RVEC transfectants. RVEC(pMN), RVEC(R-1 α), and RVEC(R-1 β) cells were incubated in the presence (+) or absence (-) of kinase inhibitors PD98059 (A), SB202190 (B), or SB203580 (C) prior to pretreatment (2 h) in the absence (-) or presence (+) of FGF-1 (50 ng/ml) complexed with heparin (50 U/ml). Cell death (% non-viable) was assessed (FDA/PrI) 20 h following exposure to 1.25 mM ONOO⁻. * Differential significance of $p < 0.01$ when compared to inhibitor- and oxidant-treated transfectants in the absence of FGF-1 pretreatment.

total SFK, active phosphor(pY⁴¹⁶)-SFK, total cortactin, and active phosphorylated cortactin (Fig. 10). In all FGF-1/heparin-treated RVEC transfectants, total levels of p38 MAPK, SFK, cortactin, and Erk 1/2 did not change over the 2-h period of analysis (data not shown). Phosphorylation of p38 MAPK and JNK was restricted to RVEC(R-1 α) cells, and activation of these MAPKs transiently peaked at 10 min postFGF-1 treatment and returned to baseline levels within 30 min. Phosphorylation of SFK and its substrate cortactin was restricted to RVEC(R-1 β) cells, and activation of these focal adhesion proteins transiently peaked at 10 min postFGF-1 treatment and returned to baseline levels within 30 min. Phosphorylation of Erk 1/2 was observed in both RVEC(R-1 α) and RVEC(R-1 β) transfectants and not in RVEC(pMN) cells, and activation of this MAPK peaked within 10 min postFGF-1 treatment and persisted throughout the 2 h of study. In the absence of FGF-1/heparin treatment (or treatment with heparin alone), increased levels of phosphorylated p38 MAPK, JNK, Erk 1/2, and cortactin were not observed in RVEC(R-1 α) and RVEC(R-1 β) cells (data not shown). Instead, low to undetectable intrinsic levels of these phosphorylated substrates were similar to those observed (Fig. 10) for FGF receptor-negative, control-transfected RVEC(pMN) cells treated with FGF-1/heparin.

DISCUSSION

High-affinity FGF receptors are members of a multigene family containing multiple structural variants with different ligand-binding specificities and affinities [30,32]. Consequently, characterizing specific signal transduction pathways responding to the FGF ligands has been complex, particularly since a wide variety of established cell

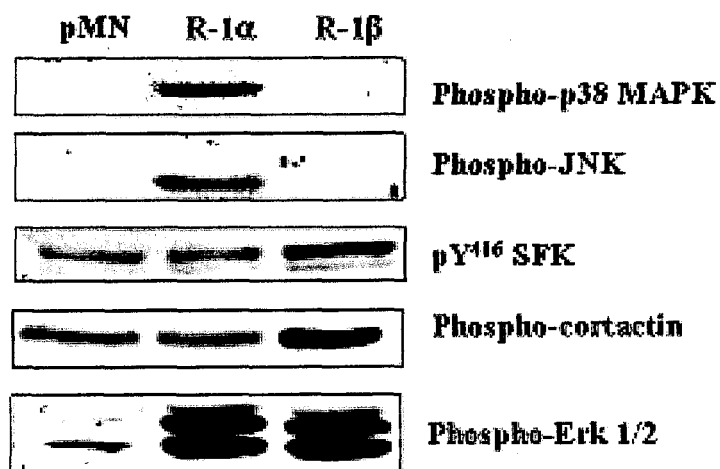


Fig. 10. Western analysis of activated polypeptide substrates in individual RVEC transfectants. Total cellular proteins recovered from either RVEC (pMN), RVEC (R-1 α), and RVEC (R-1 β) cells, exposed (10 min) to extracellular FGF-1 (50 ng/ml) complexed with heparin (50 U/ml), were fractionated by reducing SDS-PAGE and Western analyzed with the identified specific antibodies according to procedures described under Materials and methods.

lines and diploid cell strains express more than one type of FGF receptor. This issue is complicated further by the observation that binding of the FGF ligand to FGFR induces receptor dimerization, including formation of homo- and heterodimers between different structural isoforms [31,43]. Previous efforts to examine the properties of a specific FGFR isoform have utilized L6 myoblasts, which have been classified as an FGFR-deficient cell line [44]. However, we and others [45,46] routinely have observed low, detectable levels of FGFR-1 and a minimal FGF-1-dependent growth response in L6 myoblasts. In studies reported here with non- and control (pMN)-transfected RVECs, RT-PCR and Western analyses failed to detect intrinsic rat FGFR-1 mRNA or protein, the extracellular addition of FGF-1 failed to induce either a growth or mitogenic response, and Scatchard analysis failed to detect high-affinity binding of ^{99m}Tc -labeled FGF-1. Collectively, these results confirmed that RVECs lack intrinsic expression of functional high-affinity FGF receptors (including FGFR-1) and predicted the utility of transfection experiments to examine functional properties of different human FGFR-1 structural isoforms. Indeed, results from RT-PCR and Western analyses were consistent with the engineered transgene constructs and confirmed delivery of the transfected plasmids, stable integration of the nucleic acids, and the ability of RVECs to coordinate transcriptional and translational responses from these templates.

Several lines of evidence from the experimental models described here are consistent with previously published results supporting the posttranslational modification and biological functionality of human FGFR-1 α and FGFR-1 β expressed in RVECs: (i) variable molecular mass structures of FGFR-1 α and FGFR-1 β were posttranslationally modified by N-glycosylation and derived from a single precursor [45,47]; (ii) Scatchard

analysis revealed that both RVEC(R-1 α) and RVEC(R-1 β) transfectants exhibited heparin-dependent binding of FGF-1 with affinities similar to that previously reported [30,48]; (iii) following high-affinity ligand binding, autophosphorylation of both FGFR-1 isoforms was observed and limited to the high-molecular-mass, fully glycosylated structure [45]; and (iv) in the case of FGFR-1 α transfectants, both high-affinity FGF-1 binding and tyrosine phosphorylation of the receptor were heparin dependent [32,48]; (v) compared with controls, both RVEC(R-1 α) and RVEC(R-1 β) transfectants exhibited a high-proliferation index and enhanced growth potential following treatment with FGF-1; and (vi) ligand-activation of cells expressing FGFR-1 α maintained a more normal, flattened monolayer phenotype, whereas, cells expressing RVEC(R-1 β) acquired a characteristic FGF-1-dependent transformed phenotype [45].

Whereas these collective results established the ability of RVECs to coordinate characteristic posttranslational modifications of the human FGFR-1 transgenes and confirmed their biological functionality, several results from these experimental models provided insight into the physiologic consequences of alternative FGFR-1 splicing beyond that reported previously. Here we demonstrated that ligand activation of the alternatively spliced FGFR-1 isoforms differentially modulated endothelial cell responses to ONOO⁻. The extracellular addition of ONOO⁻ induced a dose- and time-dependent, delayed cell death in RVECs that was more characteristic of apoptosis than necrosis and morphologically equivalent to apoptosis induced by this reactive nitrogen species in PC12 cells [20], primary murine fibroblast [21], rat pancreatic ductal epithelial cells [22], murine osteoblasts [23], and both human and rat osteoblast progenitors [23,24].

Whereas millimolar bolus addition of synthetic ONOO⁻ may seem considerable, the net

exposure was significantly lower due to the short (< 1 s) half-life of this strong oxidant at physiological pH [49]. Consequently, the vast majority of ONOO^- decomposed before it ever contacted RVECs. Previous studies have demonstrated that a 1 mM bolus addition of ONOO^- is equivalent to generating submicromolar concentrations of this oxidant [21]. Compared on the basis of concentration multiplied by time, exposure to 1 mM SIN-1 for 1 h should be equivalent to a bolus addition of $650 \mu\text{M ONOO}^-$ [50]. During ischemia, nitric oxide synthase can produce 2-4 μM levels of nitric oxide concentrations [51], which are sufficient to compete effectively with superoxide dismutase for superoxide and promote formation of ONOO^- [52]. Furthermore, submicromolar concentrations of ONOO^- are generated readily by alveolar macrophages [50]. Collectively, these efforts argue that the levels of ONOO^- used in these studies were consistent with those determined in vivo, particularly under pathophysiologic conditions.

The ability of FGF-1 to modulate ONOO^- -induced cell death in both FGFR-1 α and FGFR-1 β transfectants was equally effective between 1 and 12 h of pretreatment. The exogenous FGF-1 signaling pathway has been demonstrated in vitro [53] to require continuous cellular exposure to the growth factor during the G_0 to G_1 cell cycle transition. During this time, receptor-mediated internalization of FGF-1 is accompanied by autophosphorylation and activation of the FGFR-1 intrinsic tyrosine kinase. Consequently, it was reasoned that the ability of FGF-1 to modulate cellular responses to ONOO^- was directly dependent on preactivation of early FGFR-1 signaling events rather than mitogenic responses to the growth factor. Indeed, treatment of both RVEC(R-1 α) and RVEC(R-1 β) transfectants with PD166866, a selective inhibitor of the intrinsic

FGFR-1 tyrosine kinase [54], prior to FGF-1 exposure prevented the ability of the growth factor to modulate the cytotoxic effects of ONOO⁻.

FGF-1-induced signaling rendered FGFR-1 α transfectants more sensitive to ONOO⁻ and FGFR-1 β transfectants resistant to ONOO⁻, observations which were consistent with our previous studies. RT-PCR analysis of PC12 cells [20] and primary fibroblasts [21], which exhibited enhanced sensitivity to the cytotoxic effect of ONOO⁻ following FGF-1 treatment, exhibited a ratio of FGFR-1 α to FGFR-1 β mRNA favoring the expression of FGFR-1 α . RT-PCR analysis of pancreatic ductal epithelial cells [22], MC3T3 cells [23], and osteoblast progenitors [23,24], which exhibited resistance to ONOO⁻-mediated death following FGF-1 treatment, predominantly expressed FGFR-1 β mRNA (J. A. Thompson, unpublished observations). FGFR-1 and ONOO⁻ appear to signal cellular responses through similar intracellular substrates, including SFK, p38 MAPK, JNK, and Erk 1/2 [29,55-61]. However, since alternatively spliced FGFR-1 isoforms exhibit differential trafficking [45], we anticipated that FGFR-1 isoform-specific signaling to different intracellular substrates may ultimately determine RVEC responses to ONOO⁻. Consequently, cell death was determined in RVEC transfectants following selective inhibition of various catalytic activities using either PP2, an SFK inhibitor [62], PD98059, a MEK/Erk 1/2 kinase inhibitor [63], SB203580, a specific p38 MAP kinase inhibitor [64], or SB202190, which demonstrates inhibition of both JNK and p38 MAP kinase activities [64].

These specific inhibitor studies demonstrated that the ability of FGF-1 pretreatment to both enhance and inhibit ONOO⁻-induced death of RVECs was associated with preactivation of MEK/Erk 1/2. This initial effort predicted that the

MEK/Erk 1/2 pathway is common to both FGFR-1 α and FGFR-1 β signaling. Indeed, FGF-1 activation of both FGFR-1 α and FGFR-1 β induced sustained phosphorylation (activation) of Erk 1/2. However, since Erk activation has been demonstrated to exert either a proapoptotic or an antiapoptotic influence on cells [63,65,66], additional efforts will be required to examine the regulatory mechanisms whereby MEK/Erk 1/2 preactivation modulates growth and death responses to ONOO $^-$.

The other two major subtypes of the MAPK family include JNK and p38 MAPK, whose activation processes generally are associated with apoptosis. Specific inhibitor studies suggested that the ability of FGF-1 pretreatment to enhance the cytotoxic effects of ONOO $^-$ was associated with activation of p38 MAPK. Since this observation was limited to RVEC(R-1 α) transfectants and since activation of the p38 MAPK pathway was also restricted to RVEC(R-1 α) cells, we have concluded that preactivation of this prodeath pathway rendered cells more sensitive to the cytotoxic effects of ONOO $^-$. This prediction would be consistent with the observations that: (i) NGF prevented apoptosis induced by factor-starved lymphocytes following inactivation of p38 MAPK [76], (ii) NGF pretreatment of PC12 cells protected against ONOO $^-$ -induced apoptosis[20], and (iii) pretreatment with FGF-1 or FGF-2 significantly enhanced ONOO $^-$ -induced apoptosis in PC12 cells, which predominantly express FGFR-1 α mRNA [20].

Specific inhibitor studies further suggested that the ability of FGF-1 pretreatment to significantly inhibit ONOO $^-$ -induced cell death was associated with preactivation of the SFK pathway. Since this observation was limited to RVEC(R-1 β) transfectants and since activation of the SFK pathway was also restricted to RVEC(R-1 β) cells, we have concluded that preactivation of this survival pathway rendered cells resistant to the

cytotoxic effects of ONOO^- . This premise is consistent with previous observations, including (i) levels of total nitrotyrosine (footprint marker of RNS), FGF ligands, and FGFR-1, primarily as the FGFR-1 β isoform, are elevated in pancreatic adenocarcinoma [19], (ii) SFK activity is increased in pancreatic adenocarcinoma [58], and (iii) FGF-1 signaling inhibited ONOO^- -induced death of pancreatic epithelial cells, which predominantly express FGFR-1 β mRNA [22].

These studies have provided compelling evidence that ligand activation of FGFR-1 modulated endothelial cell responses to ONOO^- -mediated death in a manner consistent with distinct signal transduction cascades induced by alternatively spliced FGFR-1 isoforms. The ability of FGFR-1 α signaling to render RVECs more sensitive to ONOO^- -mediated death was dependent on FGFR-1 tyrosine kinase, MEK/Erk 1/2 kinase, and p38 MAPK activities and independent of SFK activity. The ability of FGFR-1 β signaling to render RVECs resistant to the cytotoxic effects of ONOO^- was dependent on FGFR-1 tyrosine kinase, MEK/Erk 1/2, and SFK activities and independent of p38 MAPK activity. Collectively, these studies provide a first indication that FGFR-1 α and FGFR-1 β induce differential signal transduction cascades, particularly those involving SFK and p38 MAPK. Molecular mechanisms whereby early alternative FGFR-1 isoform signaling differentially modulates cellular responses to oxidative stress are unclear but may relate to previous studies demonstrating a paradoxical effect for FGF ligands functioning as inducers of either cell survival [68-71] or cell death [72-76]. Ongoing rigorous experimentation will be required to realize this potential.

ACKNOWLEDGMENTS

Synthesis of oligonucleotide amplimers was supported by NCI grant CA13148 to the University of Alabama at Birmingham Comprehensive Cancer Center. The authors thank Xi Zhan, American Red Cross, for generously providing eukaryotic expression vectors, pXZ106 and pXZ85, containing FGFR-1 α and FGFR-1 β , respectively. We also thank Q. Li for excellent technical assistance.

REFERENCES

- [1] J.P. Crow, C. Spruell, J. Chen, C. Gunn, H. Ischiropoulos, M. Tsai, C.D. Smith, R. Radi, W.H. Koppenol, J.S. Beckman, *Free Radicals Biol. Med.* 16 (1994) 331-338.
- [2] W.H. Koppenol, J.J. Moreno, W.A. Pryor, H. Ischiropoulos, J.S. Beckman, *Chem. Res. Toxicol.* 5 (1992) 834-842.
- [3] R. Radi, J. S. Beckman, K.M. Bush, B.A. Freeman, *J. Biol. Chem.* 266 (1991) 4244-4250.
- [4] J.J. Moreno, W.A. Pryor, *Chem. Res. Toxicol.* 5 (1992) 425-431.
- [5] L. Castro, M. Rodriguez, R. Radi, *J. Biol. Chem.* 269 (1994) 29409-29415.
- [6] A. Hausladen, I. Fridovich, *J. Biol. Chem.* 269 (1994) 29405-29408.
- [7] W.A. Pryor, G. L. Squadrito, *Am. J. Physiol* 268 (1995) L699-L722.
- [8] J.S. Beckman, W.H. Koppenol, *Am. J. Physiol* 271 (1996) C1424-C1437.
- [9] H. Ischiropoulos, A.B. al Mehdi, *FEBS Lett.* 364 (1995) 279-282.
- [10] S.A. Greenacre, H. Ischiropoulos, *Free Radicals Res.* 34 (2001) 541-581.
- [11] J.S. Beckman, Y.Z. Ye, P. Anderson, J. Chen, M.A. Accavetti, M.M. Tarpey, C.R. White, *Biol. Chem. Hoppe-Seyler* 375 (1994) 81-88.
- [12] L.A. MacMillan-Crow, J.P. Crow, J.D. Kerby, J.S. Beckman, J.A. Thompson, *Proc. Natl. Acad. Sci. USA* 93 (1996) 11853-11858.
- [13] H. Kaur, B. Halliwell, *FEBS Lett.* 350 (1994) 9-12.

- [14] E. Brogi, J.A. Winkles, R. Underwood, S.K. Clinton, G.F. Alberts, P. Libby, J. Clin. Invest 92 (1993) 2408-2418.
- [15] H. Sano, R. Forough, J.A. Maier, J.P. Case, A. Jackson, K. Engleka, T. Maciag, R.L. Wilder, J. Cell Biol. 110 (1990) 1417-1426.
- [16] J.D. Kerby, D.J. Verran, K.L. Luo, Q. Ding, Y. Tagouri, G.A. Herrera, A.G. Diethelm, J.A. Thompson, Transplantation 62 (1996) 467-475.
- [17] J.D. Kerby, D.J. Verran, K.L. Luo, Q. Ding, Y. Tagouri, G.A. Herrera, A.G. Diethelm, J.A. Thompson, Transplantation 62 (1996) 190-200.
- [18] J.D. Kerby, K.L. Luo, Q. Ding, Y. Tagouri, G.A. Herrera, A.G. Diethelm, J.A. Thompson, Transplantation 63 (1997) 988-995.
- [19] S.M. Vickers, L.A. MacMillan-Crow, M. Green, C. Ellis, J.A. Thompson, Arch. Surg. 134 (1999) 245-251.
- [20] A.G. Estevez, R. Radi, L. Barbeito, J.T. Shin, J.A. Thompson, J.S. Beckman, J. Neurochem. 65 (1995) 1543-1550.
- [21] J.T. Shin, L. Barbeito, L.A. MacMillan-Crow, J.S. Beckman, J.A. Thompson, Arch. Biochem. Biophys. 335 (1996) 32-41.
- [22] S.M. Vickers, L. MacMillan-Crow, Z. Huang, J.A. Thompson, Free Radicals Biol. Med. 30 (2001) 957-966.
- [23] S.S. Kelpke, D. Reiff, C.W. Prince, J.A. Thompson, J. Bone Miner. Res. 16 (2001) 1917-1925.
- [24] D.A. Reiff, S. Kelpke, L. Rue III, J.A. Thompson, J. Trauma 50 (2001) 433-438.
- [25] D.M. Ornitz, N. Itoh, Genome Biol. 2 (2001) REVIEWS3005-.
- [26] T. Shimada, S. Mizutani, T. Muto, T., Yoneya, R. Hino, S. Takeda, Y. Takeuchi, T. Fujita, S. Fukumoto, T. Yamashita, Proc. Natl. Acad. Sci. USA 98 (2001) 6500-6505.
- [27] W.L. McKeehan, F. Wang, M. Kan, Prog. Nucleic Acid Res. Mol. Biol. 59 (1998) 135-176.
- [28] C.J. Powers, S.W. McLeskey, A. Wellstein, Endocr. Relat. Cancer 7 (2000) 165-197.
- [29] R.E. Friesel, T. Maciag, FASEB J. 9 (1995) 919-925.

- [30] D.E. Johnson, L.T. Williams, *Adv. Cancer Res.* 60 (1993) 1-41.
- [31] M. Jaye, J. Schlessinger, C.A. Dionne, *Biochim. Biophys. Acta* 1135 (1992) 185-199.
- [32] S. Werner, D.S. Duan, C. de Vries, K.G. Peters, D.E. Johnson, L.T. Williams, *Mol. Cell Biol.* 12 (1992) 82-88.
- [33] D.M. Ornitz, J. Xu, J.S. Colvin, D.G. McEwen, C.A. MacArthur, F. Coulier, G. Gao, M. Goldfarb, *J. Biol. Chem.* 271 (1996) 15292-15297.
- [34] H. Friess, Y. Yamanaka, M. Buchler, H.G. Beger, D.A. Do, M.S. Kobrin, M. Korc, *Am. J. Pathol.* 144 (1994) 117-128.
- [35] M.S. Kobrin, Y. Yamanaka, H. Friess, M.E. Lopez, M. Korc, *Cancer Res.* 53 (1993) 4741-4744.
- [36] D. Martin-Zanca, R. Oskam, G. Mitra, T. Copeland, M. Barbacid, *Mol. Cell Biol.* 9 (1989) 24-33.
- [37] C.A. Diglio, W. Liu, P. Grammas, F. Giacomelli, J. Wiener, *Tissue Cell* 25 (1993) 833-846.
- [38] S.R. Opalenik, J.T. Shin, J.N. Wehby, V.K. Mahesh, J.A. Thompson, *J. Biol. Chem.* 270 (1995) 17457-17467.
- [39] G. Li, Y.F. Chen, S.S. Kelpke, S. Oparil, J.A. Thompson, *Circulation* 101 (2000) 2949-2955.
- [40] R. Forough, K. Engleka, J.A. Thompson, A. Jackson, T. Imamura, T. Maciag, *Biochim. Biophys. Acta* 1090 (1991) 293-298.
- [41] K.R. Zinn, S. Kelpke, T.R. Chaudhuri, T. Sugg, J.M. Mountz, J.A. Thompson, *Nucl. Med. Biol.* 27 (2000) 407-414.
- [42] P.J. Munson, D. Rodbard, *Anal. Biochem.* 107 (1980) 220-239.
- [43] E. Shi, M. Kan, J. Xu, F. Wang, J. Hou, W.L. McKeehan, *Mol. Cell Biol.* 13 (1993) 3907-3918.
- [44] B.B. Olwin, S.D. Hauschka, *J. Cell Biochem.* 39 (1989) 443-454.
- [45] I.A. Prudovsky, N. Savion, T.M. LaVallee, T. Maciag, *J. Biol. Chem.* 271 (1996) 14198-14205.
- [46] J.R. Hawker Jr., H.J. Granger, *In Vitro Cell Dev. Biol. Anim* 30A (1994) 653-663.

- [47] J.J. Feige, A. Baird, *J. Biol. Chem.* 263 (1988) 14023-14029.
- [48] F. Wang, M. Kan, G. Yan, J. Xu, W.L. McKeehan, *J. Biol. Chem.* 270 (1995) 10231-10235.
- [49] L. Zhu, C. Gunn, J.S. Beckman, *Arch. Biochem. Biophys.* 298 (1992) 452-457.
- [50] L. Brunelli, J.P. Crow, J.S. Beckman, *Arch. Biochem. Biophys.* 316 (1995) 327-334.
- [51] T. Malinski, F. Bailey, Z.G. Zhang, M. Chopp, *J. Cereb. Blood Flow Metab* 13 (1993) 355-358.
- [52] J.S. Beckman, J.H.M. Tsai, *Biochemist* 16 (1994) 8-10.
- [53] X. Zhan, X. Hu, R. Friesel, T. Maciag, *J. Biol. Chem.* 268 (1993) 9611-9620.
- [54] R.L. Panek, G.H. Lu, T.K. Dahring, B.L. Batley, C. Connolly, J.M. Hamby, K.J. Brown, *J. Pharmacol. Exp. Ther.* 286 (1998) 569-577.
- [55] P. Klint, L. Claesson-Welsh, *Front Biosci.* 4 (1999) D165-D177.
- [56] G. Szebenyi, J.F. Fallon, *Int. Rev. Cytol.* 185 (1999) 45-106.
- [57] C. Mallozzi, A.M. Di Stasi, M. Minetti, *FEBS Lett.* 456 (1999) 201-206.
- [58] L.A. MacMillan-Crow, J.S. Greendorfer, S.M. Vickers, J.A. Thompson, *Arch. Biochem. Biophys.* 377 (2000) 350-356.
- [59] X. Li, P. De Sarno, L. Song, J.S. Beckman, R.S. Jope, *Biochem. J.* 331 (Pt 2) (1998) 599-606.
- [60] R.S. Jope, L. Zhang, L. Song, *Arch. Biochem. Biophys.* 376 (2000) 365-370.
- [61] Y.M. Go, R.P. Patel, M.C. Maland, H. Park, J.S. Beckman, V.M. Darley-Usmar, H. Jo, *Am. J. Physiol* 277 (1999) H1647-H1653.
- [62] J.H. Hanke, J.P. Gardner, R.L. Dow, P.S. Changelian, W.H. Brissette, E.J. Weringer, B.A. Pollok, P. A. Connelly, *J. Biol. Chem.* 271 (1996) 695-701.
- [63] S. Mohr, T.S. McCormick, E.G. Lapetina, *Proc. Natl. Acad. Sci. USA.* 95 (1998) 5045-5050.
- [64] J. Okano, A.K. Rustgi, *J. Biol. Chem.* 276 (2001) 19555-19564.

- [65] M.H. Son, K.W. Kang, C.H. Lee, S.G. Kim, *Biochem. Pharmacol.* 62 (2001) 1379-1390.
- [66] N.R. Bhat, P. Zhang, *J. Neurochem.* 72 (1999) 112-119.
- [67] M. Torcia, G. De Chiara, L. Nencioni, S. Ammendola, D. Labardi, M. Lucibello, P. Rosini, L.N. Marlier, P. Bonini, S.P. Dello, A.T. Palamara, N. Zambrano, T. Russo, E. Garaci, F. Cozzolino, *J. Biol. Chem.* 276 (2001) 39027-39036.
- [68] M. Bryckaert, X. Guillonneau, C. Hecquet, Y. Courtois, F. Mascarelli, *Oncogene* 18 (1999) 7584-7593.
- [69] M. Tamatani, S. Ogawa, G. Nunez, M. Tohyama, *Cell Death. Differ.* 5 (1998) 911-919.
- [70] Y. Miho, Y. Kouroku, E. Fujita, T. Mukasa, K. Urase, T. Kasahara, A. Isoai, M.Y. Momoi, T. Momoi, *Cell Death. Differ.* 6 (1999) 463-470.
- [71] S.H. Lee, D.J. Schloss, J.L. Swain, *J. Biol. Chem.* 275 (2000) 33679-33687.
- [72] G. Westwood, B.C. Dibling, D. Cuthbert-Heavens, S.A. Burchill, *Oncogene* 21 (2002) 809-824.
- [73] Y. Yokoyama, S. Ozawa, Y. Seyama, H. Namiki, Y. Hayashi, K. Kaji, K. Shirama, M. Shioda, K. Kano, *J. Neurochem.* 68 (1997) 2212-2215.
- [74] D.A. Muir, D.A. Compston, *J. Neurosci. Res.* 44 (1996) 1-11.
- [75] U.K. Messmer, V.A. Briner, J. Pfeilschifter, *J. Am. Soc. Nephrol.* 11 (2000) 2199-2211.
- [76] N. Funato, K. Moriyama, H. Shimokawa, T. Kuroda, *Biochem. Biophys. Res. Commun.* 240 (1997) 21-26.

DIFFERENTIAL SIGNALING TO THE SRC FAMILY KINASE C-YES
BY FGFR-1 α AND FGFR-1 β IN ENDOTHELIAL CELLS

by

JESSICA S. GREENDORFER, JING JIAO, PEI ZHANG,
AND JOHN.A. THOMPSON

In preparation for *Archives of Biochemistry and Biophysics*

Format adapted for dissertation

ABSTRACT

Activation of fibroblast growth factor receptor-1 (FGFR-1) by its FGF ligands stimulates diverse cellular processes associated with growth and migratory behavior. The predominant FGFR-1 isoform (FGFR-1 α) contains three immunoglobulin-like (Ig-like) loops in the extracellular domain and is routinely associated with normal cell populations, including pancreatic ductal epithelial cells and astrocytes. However, in pancreatic adenocarcinoma and malignant astrocytoma, FGFR-1 α is alternatively spliced to FGFR-1 β , an isoform containing only two of the Ig-like loops. These observations suggest that ligand activation of these FGFR-1 isoforms may induce different signal transduction cascades associated with normally differentiated and transformed cells. To examine this potential further, we have examined early signal transduction cascades in receptor-negative microvascular endothelial cells that have been stably transfected with cDNA encoding either FGFR-1 α or FGFR-1 β . Co-immunoprecipitation studies indicated that c-Yes, a Src family kinase, directly associated with FGFR-1 β , but not FGFR-1 α , following stimulation with FGF-1 (50 ng/ml, 10 min). Western analysis with phospho-specific antibodies revealed increased Yes tyrosine phosphorylation in the kinase domain in activated R-1 β . Activation of Yes was accompanied by its direct docking with the actin-binding protein cortactin as well as increased cortactin tyrosine phosphorylation. R-1 β exhibited decreased contact inhibition at high density in vitro. Cord-formation on Matrigel was dramatically increased in R-1 β in a manner dependent on Yes activity. In vivo formation of angiogenic-like structures was restricted to cells expressing activated FGFR-1 β . These findings suggest that FGFR-1 α and FGFR-1 β stimulate different signal transduction cascades to focal adhesion sites. The relevancy of these responses to cell

growth, migration, and survival predict pivotal roles for alternative splicing of FGFR-1 as regulators of cellular responses during tumorigenesis and angiogenesis.

INTRODUCTION

The fibroblast growth factor (FGF) family, composed of at least 23 members [1], binds to high affinity FGF receptors (FGFR) and low affinity heparan sulfate proteoglycans (HSPG) to stimulate intracellular signaling cascades [2]. The prototypical members of the FGF family, FGF-1 (acidic FGF) and FGF-2 (basic FGF) are proangiogenic signaling proteins during normal physiology, such as wound healing, and pathophysiology, such as neoplasia [3].

The high-affinity FGFR-1 generally contains three extracellular immunoglobulin-like (Ig-like) disulfide loops, an acidic box that includes eight adjacent acidic amino acids, a putative nuclear localization sequence (NLS), and an intracellular split tyrosine kinase domain [4]. Seven intracellular tyrosines serve as autophosphorylation sites to stimulate kinase activity and recruit substrates [5]. Alternative splicing of FGFR-1 mRNA produces two major isoforms, FGFR-1 α and FGFR-1 β , that contain loops I, II, and III or only II and III, respectively [6]. FGFR-1 α and FGFR-1 β differ in their affinity for FGF-1 [6], their requirement for heparin/HSPG [7], and their translocation to the nucleus following ligand stimulation [8]. Endothelial cells and keratinocytes undergoing wound repair [9], pancreatic adenocarcinomas [10], and malignant astrocytomas [11] express FGFR-1 β as the predominant FGFR-1 isoform.

The Src family of nonreceptor tyrosine kinases (SFK) also play important signaling roles during angiogenesis, including regulating endothelial cell chemotaxis

[12], vascular permeability [13], and cord formation [14]. SFK activity is upregulated in multiple cancers, including pancreatic adenocarcinoma [15]. SFK have been reported to be FGFR-1 substrates, but the association between FGFR-1 and SFK has been controversial. While Zhan et al. (1994) found an association between FGFR-1 and c-Src in FGF-1 stimulated cells, Landgren et al. (1995) found no association in FGF-2-treated cells and actually observed a decrease in Src activity [16,17].

We have recently characterized a FGFR-negative resistance vessel endothelial cell (RVEC) and RVEC in which we have stably transfected FGFR-1 α or FGFR-1 β [18]. Using this model, we have explored the relationship between specific FGFR-1 isoforms and the SFK c-Yes. In this report, we demonstrate a specific association between FGFR-1 β and c-Yes that is accompanied by c-Yes activation and signaling to the actin binding protein cortactin. In addition, the ability of FGFR-1 β to stimulate angiogenic cord structures in vivo and c-Yes-dependent cords in vitro was assessed. These findings have important implications for FGFR-1 β signaling during angiogenesis and tumorigenesis.

MATERIALS AND METHODS

Tissue culture and transfection

RVEC were harvested from Sprague-Dawley rat cerebral tissue as previously described [19]. The absence of endogenous fibroblast growth factor receptors in RVEC was assessed by RT-PCR analysis using primers specific to rat FGFR-1 cDNA and by Scatchard analysis of FGF-1 binding using technetium-labeled FGF-1 as previously described [18]. To create cell lines expressing FGFR-1 α (R-1 α) or FGFR-1 β (R-1 β), RVEC cells were transfected with the eukaryotic expression vector pMEXneo encoding

the neomycin phosphotransferase gene under control of the early SV40 promoter (pMN, transfection control), and the complete human cDNA for FGFR-1 α (pXZ106) or FGFR-1 β (pXZ85) subcloned 5' of the SV40 polyadenylation signal and 3' of the murine virus LTR promoter [20]. Subconfluent cells were transfected with 10 μ g pMEXneo, pXZ106, or pXZ85 using calcium phosphate (Promega) and selected with 800 μ g/ml Geneticin (Life Technologies). Stably transfected cells expressing FGFR-1 α (R-1 α), FGFR-1 β (R-1 β), or control (pMN) were maintained in Dulbecco's modified Eagle medium (DMEM; Life Technologies) supplemented with 10% (v/v) heat-inactivated, defined, bovine calf serum (BCS; Hyclone) and 1 U/ μ g penicillin/streptomycin (Life Technologies) and passaged at confluence with 0.25% trypsin and 0.5 mM EDTA.

Characterization of Src Family Kinases

Src family kinases (SFK) c-src, fyn, and c-yes were characterized in RVEC by RT-PCR. Isolated mRNA was converted to cDNA using RT and the cDNA product was amplified by the polymerase chain reaction as previously described [21]. RT-PCR products were analyzed by 2% (w/v) agarose gel electrophoresis, stained with ethidium bromide, and visualized with UV light. Gel photographs were digitized with a Xerox 7650 scanner. c-src, fyn, and c-yes were identified with primers specific to non-homologous regions in the rat sequence (c-src forward: ACG GAC AGA GAC TGA CCT GTC C, c-src reverse: AAG TAC CAC TCC TCA GCC TGG, fyn forward: AGC CTG AAC CAG AGC TCT GG, fyn reverse: CAG GGT CCC GGT GTG AGA GG, c-yes forward: CCT CAT TCT CAG TGG TGC C, c-yes reverse: GCC TGA ATG GAA TCT GCA GGC G) [22]. RT-PCR products from pMN, R-1 α , and R-1 β cells were

standardized to levels of GAPDH from identical samples within the same gel, as previously described [23].

Western Analysis

pMN, R-1 α , and R-1 β cells were plated (1×10^6 cells/100 mm plate) and grown to 80% confluency under normal growth conditions. Cells were washed in Dulbecco's phosphate buffered saline (D-PBS; Life Technologies), cultured in DMEM supplemented with 0.3% (v/v) BCS and 1 U/ μ g penicillin/streptomycin for 24 h, and treated with a complex of 50 ng/ml FGF-1 and 50 U/ml heparin (Sigma) for 10 min at 37°C. Cells were washed in D-PBS, placed on ice, and scrape-harvested with lysis buffer (50 mM HEPES (pH 7.4), 150 mM NaCl, 1% (v/v) Triton X-100, 10% (v/v) glycerol, 1 mM EGTA, 1 mM sodium orthovanadate, 1 mM PMSF, 10 μ g/ml leupeptin, 10 μ g/ml aprotinin). Cell lysates were clarified by centrifugation (14,000 rpm, 10 min, 4°C). Protein concentrations were determined by Bradford assay (Pierce). For immunoprecipitation, cell lysates were normalized to equal protein levels (1 mg/ml) and incubated at 4°C for 24 h with appropriate antibodies (5 μ g) recognizing FGFR-1 (C-15; Santa Cruz), SFK (SRC2; Santa Cruz), c-Yes (Transduction), or phosphotyrosine (PY20; Transduction). Immune complexes were incubated with fast flow recombinant protein A-agarose (Upstate Biotechnologies) at 4°C for 1.5 h, precipitated by centrifugation (10,000 rpm, 4°C, 15 sec), and washed with lysis buffer. Immune complexes or whole cell extracts (50 μ g) were suspended in 4X Laemmli sample buffer (200 mM Tris (pH 6.8), 8% (w/v) SDS, 40% (v/v) glycerol, 0.004% (w/v) bromophenol blue, 5% (v/v) 2-mercaptoethanol), resolved by 7.5% (w/v) SDS-PAGE (100 V), and transferred to PVDF membrane (100 V,

4°C, 1 h). For Western analysis, membranes were blocked at room temperature for 30 min in 5% (w/v) BSA (used with primary antibodies recognizing phosphotyrosine) or 5% (w/v) nonfat dry milk (used with all other primary antibodies) dissolved in Tris-buffered saline containing 0.05% Tween-20 (TBS-T). Membranes were incubated at room temperature for 1.5 h in blocking buffer containing antibodies recognizing c-Yes (1:5000; Transduction), c-Src (clone327, 1:100; Oncogene), Fyn (Fyn(15), 1:500; Santa Cruz), active SFK (SRC2, 1:1000; Santa Cruz), active phospho-SFK (pY⁴¹⁶, 1:500; Cell Signaling), phospho-SFK (pY⁵²⁹, 1:500; Biosource), FGFR-1 (C15, 1:1000; Santa Cruz), cortactin (1:3000; UBI). Membranes were washed in TBS-T three times at room temperature for 10 min. Membranes were incubated in appropriate horseradish peroxidase-conjugated secondary antibody (goat anti-mouse-HRP or goat anti-rabbit-HRP, 1:20000; KPL) in TBS-T at room temperature for 1 h. Membranes were washed in TBS-T three times at room temperature for 10 min. Immunoreactivity was assessed by enhanced chemiluminescence (Lumiglo; KPL). Signaling experiments were performed in triplicate.

Cord Formation Assay

pMN, R-1 α , and R-1 β cells were grown to confluency and incubated in reduced serum medium as described above. Cells were treated with 20 μ M Src family kinase inhibitor PP2 (Oncogene) or DMSO (vehicle control) for 30 min prior to treatment with 50 ng/ml FGF-1 and 50 U/ml heparin for 2 h. Twenty-four well cell culture plates were coated with 250 μ l of 10 mg/ml Matrigel and allowed to polymerize for 30 min at 37°C. Treated pMN, R-1 α , and R-1 β cells (2.5×10^5 cells/well) were plated onto coated plates in

DMEM supplemented with 0.3% (v/v) BCS and 1% (v/v) penicillin/streptomycin. Cord formation was assessed at 24 h, photographed at 40X magnification, and quantified by counting intersection points +/- SD as previously described [24].

In Vivo Angiogenesis

To produce a continuous delivery of FGF-1, pMN, R-1 α , and R-1 β cells were incubated in conditioned medium containing retroviral particles encoding a secreted form of FGF-1 as previously described [21]. Briefly, the helper-free packaging cell line GP+envAm12 [25] was cotransfected with pCV108, containing the neomycin phosphotransferase gene, and (hst/KS) FGF-1, containing the β -galactosidase gene and the FGF-1 gene subcloned with the signal peptide sequence (KS) from FGF-4. Transduced pMN, R-1 α , and R-1 β cells expressing β -Galactosidase and secreted FGF-1 were trypsinized (0.25% trypsin, 0.5 mM EDTA), suspended at 10^8 cells/ml in staining medium (10 mM HEPES, 4% (v/v) BCS, PBS), incubated at 37°C for 1 min with 0.2 mM fluorescein digalactoside (Molecular Probes), and collected by FACS. Transduced cells were expanded under normal culture conditions. Expression of β -Galactosidase and secreted FGF-1 was routinely assessed by fixation (2% (v/v) formaldehyde, 0.2% glutaraldehyde, PBS) at room temperature for 15 min followed by staining (5 mM potassium ferricyanide, 5 mM potassium ferrocyanide, 2 mM MgCl₂, PBS, 1/10 volume of 20 mg Bluo-Gal (Sigma)/ml N,N-dimethyl-formamide) at 37°C for 24 h. Transduced pMN, R-1 α , and R-1 β cells (20×10^6) were pelleted, resuspended in 100 μ l of 10 mg/ml Matrigel (BD Biosciences), and allowed to polymerize for 15 min at 37°C. Male, 8 week-old Balb/c nude mice were anesthetized with isoflurane and implanted

subcutaneously with matrigel plugs containing transduced pMN, R-1 α , or R-1 β cells. Matrigel implants were harvested after 10 days [26] and fixed and stained for β -Galactosidase activity as described above.

RESULTS

Transfected RVEC expressing FGFR-1 α (R-1 α), FGFR-1 β (R-1 β), or control vector (pMN) were examined for expression of the Src family kinases c-Src, c-Yes, and Fyn by RT-PCR and Western analysis (Fig. 1). Expression of c-yes in total RNA extracted from pMN, R-1 α , and R-1 β was demonstrated by the appearance of a predicted 237-bp RT-PCR product using rat-specific amplifier sequences within the unique Src family domain (Fig. 1A). In contrast, pMN, R-1 α , and R-1 β cells demonstrated minimal expression of c-src (169 bp) and failed to demonstrate expression of fyn (fyn data not shown). Translation of c-yes mRNA was investigated by Western analysis (Fig. 1B). Total cellular extracts from pMN, R-1 α , and R-1 β failed to demonstrate immunoreactivity to monoclonal antibodies recognizing c-Src or Fyn, but readily demonstrated a band of immunoreactive c-Yes migrating at an apparent molecular mass of approximately 62 kDa. These results indicated that c-Yes is the predominant Src family kinase in RVEC cells.

Exposure of pMN, R-1 α , and R-1 β cells to FGF-1 (50 ng/ml) complexed with heparin (50 U/ml) (2 to 30 min) resulted in increased c-Yes activity at 5 min and 10 min as assessed by antibodies recognizing active Src family kinases (Fig. 2). Total c-Yes levels did not change following FGF-1/heparin treatment (data not shown). To further evaluate c-Yes activation, pMN, R-1 α , and R-1 β cells were treated with FGF-1 (50

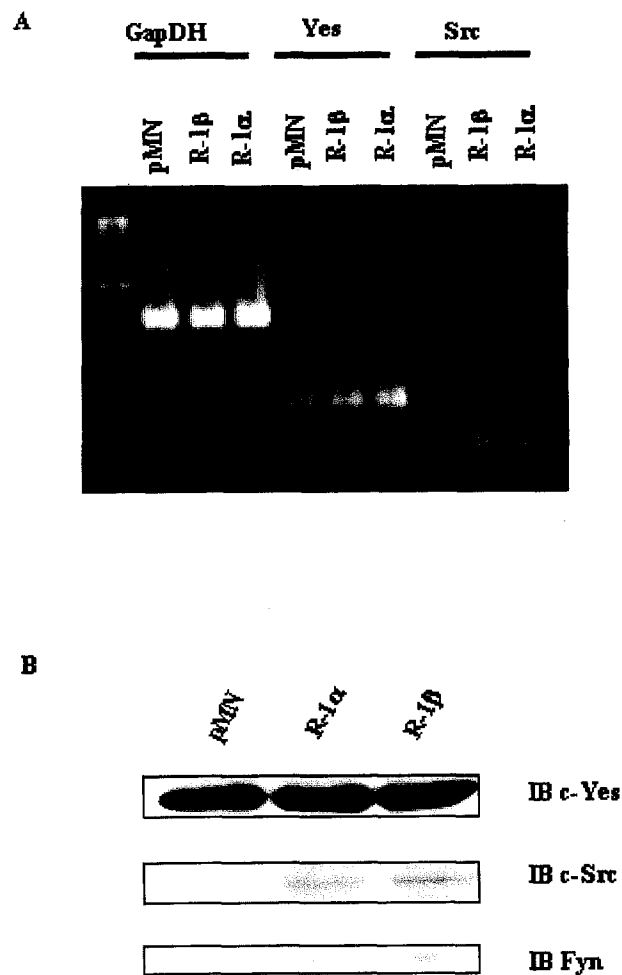


Fig. 1. RT-PCR and Western analysis of RVEC. (A) Expression of total RNA for c-Yes and c-Src from pMN, R-1 α , and R-1 β cells was examined by RT-PCR using SFK-specific primers. (B) Expression of total SFK levels in total cellular lysates from pMN, R-1 α , and R-1 β cells was examined by Western analysis using antibodies specific for c-Yes, c-Src, and Fyn.

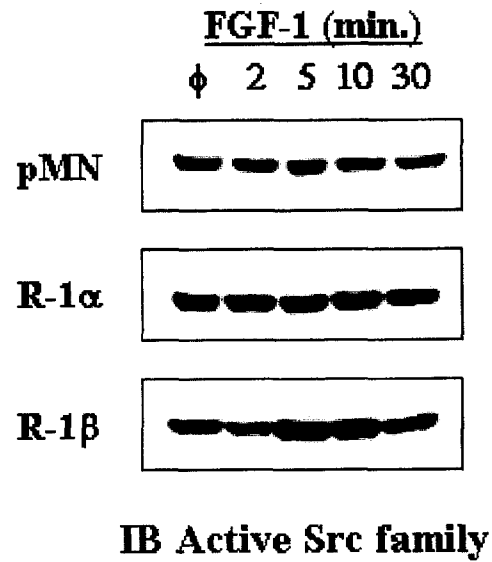


Fig. 2. Kinetics of c-Yes activation. RVEC cells were treated with FGF-1 (50 ng/ml) complexed with heparin (50 U/ml) for indicated times. Total cellular proteins were Western analyzed using a polyclonal antibody recognizing active SFK.

ng/ml)/heparin (50 U/ml) complex (10 min) and total cellular extracts were assessed with phosphospecific antibodies recognizing the catalytic kinase domain (Fig. 3A) or regulatory tail domain (Fig. 3B). R-1 β cells demonstrated an increase in positive immunoreactivity for c-Yes phosphorylated in the kinase domain. Immunoreactivity for c-Yes in R-1 β was significantly different compared to pMN ($p < 0.002$). Immunoreactivity in R-1 α was not significantly different than in pMN. Changes in tyrosine phosphorylation of the regulatory domain were not significant between pMN and R-1 α or R-1 β .

The association between c-Yes and FGFR-1 isoforms was assessed by co-immunoprecipitation studies (Fig. 4). Following stimulation (10 min) with FGF-1 (50 ng/ml)/heparin (50 U/ml) complex, only FGFR-1 β was found to associate with c-Yes. This experiment could be performed by immunoprecipitation with either FGFR-1 antibody (Fig. 4A) or the Src family antibody (Fig. 4B). Productive signal transduction from ligand-activated FGFR-1 β through c-Yes was examined. Increased association between c-Yes and the actin binding protein cortactin was observed following stimulation (10 min) with FGF-1 (50 ng/ml) and heparin (50 U/ml) (Fig. 5A). In addition, cortactin tyrosine phosphorylation was increased in ligand-activated R-1 β (Fig. 5A).

R-1 β cells treated daily with FGF-1 (50 ng/ml)/heparin (50 U/ml) complex demonstrated cord-like structural arrays when grown at high density in vitro (Fig. 6A). This morphological change was not observed in pMN or R-1 α . In addition, FGF-1 (50 ng/ml)/heparin (50 U/ml) treatment (2 h) of R-1 β resulted in cord formation in Matrigel (Fig. 6B). To assess structural changes in vivo, pMN, R-1 α , and R-1 β cells were suspended in Matrigel and implanted subcutaneously in Balb/c nude mice. In vivo,

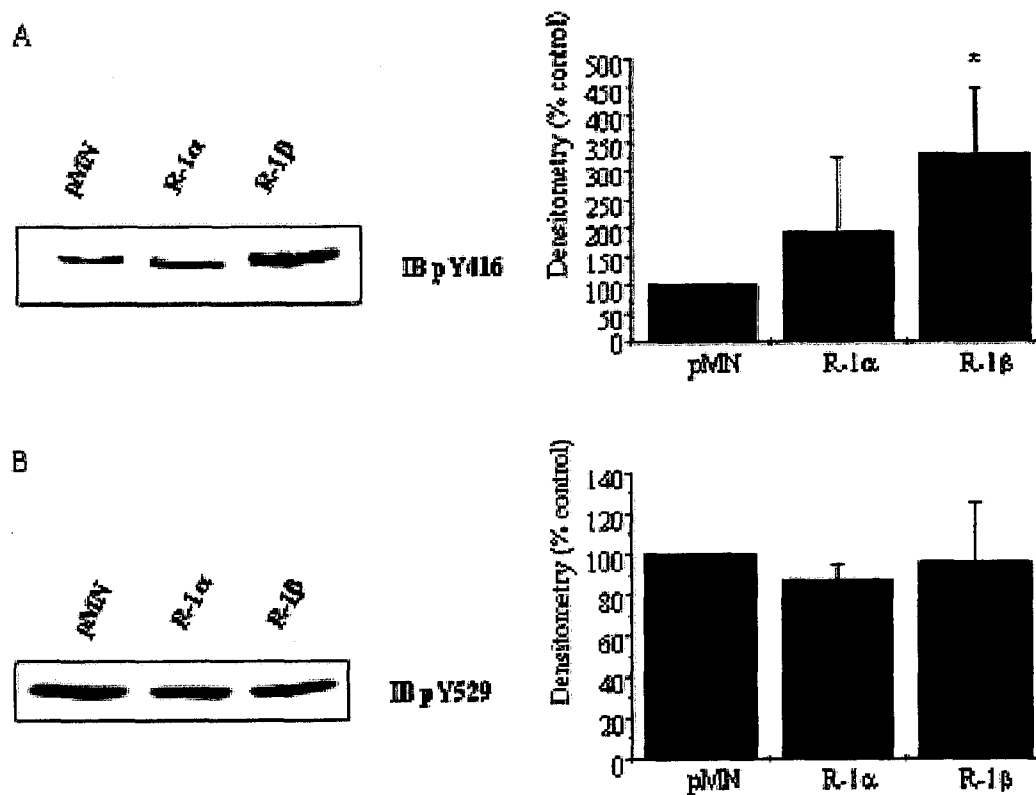


Fig. 3. Phosphorylation of c-Yes tyrosines. pMN, R-1 α , and R-1 β cells were treated with FGF-1 (50 ng/ml) complexed with heparin (50 U/ml) for 10 min. Total cellular proteins were Western analyzed with a polyclonal antibody recognizing (A) pY within the kinase domain (pY416) or (B) pY within the regulatory tail domain (pY529).

* Differential significance of $p < 0.05$ compared to pMN and R-1 α .

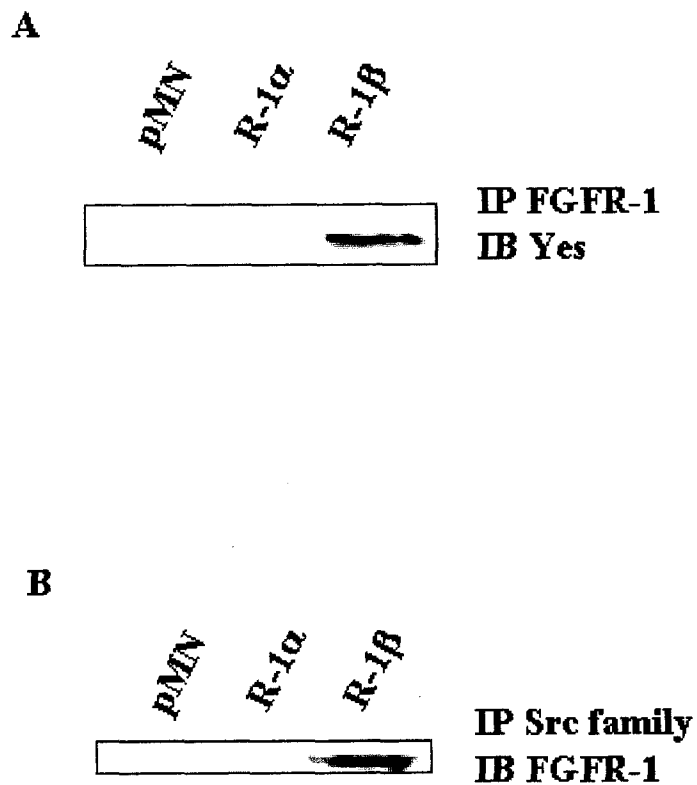


Fig. 4. Association between FGFR-1 isoforms and c-Yes. pMN, R-1 α , and R-1 β cells were treated with FGF-1 (50 ng/ml) complexed with heparin (50 U/ml) for 10 min. (A) Total cellular proteins were immunoprecipitated with anti-FGFR-1 polyclonal antibody and Western analyzed with monoclonal antibody recognizing c-Yes. (B) Total cellular protein were immunoprecipitated with anti-SFK polyclonal antibody and Western analyzed with polyclonal antibody recognizing FGFR-1.

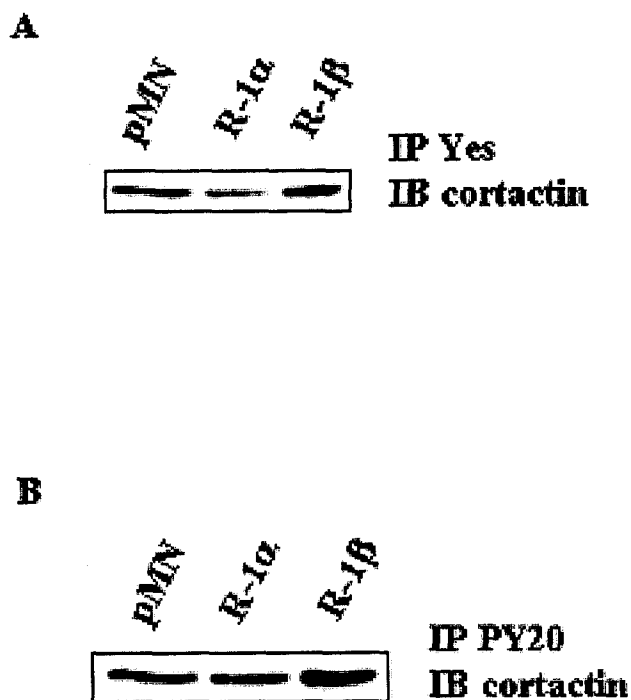


Fig. 5. c-Yes association and activation of cortactin. pMN, R-1 α , and R-1 β cells were treated with FGF-1 (50 ng/ml) complexed with heparin (50 U/ml) for 10 min. Total cellular proteins were immunoprecipitated with (A) monoclonal antibody recognizing c-Yes or (B) monoclonal antibody recognizing phosphotyrosine and Western analyzed with monoclonal antibody recognizing cortactin.

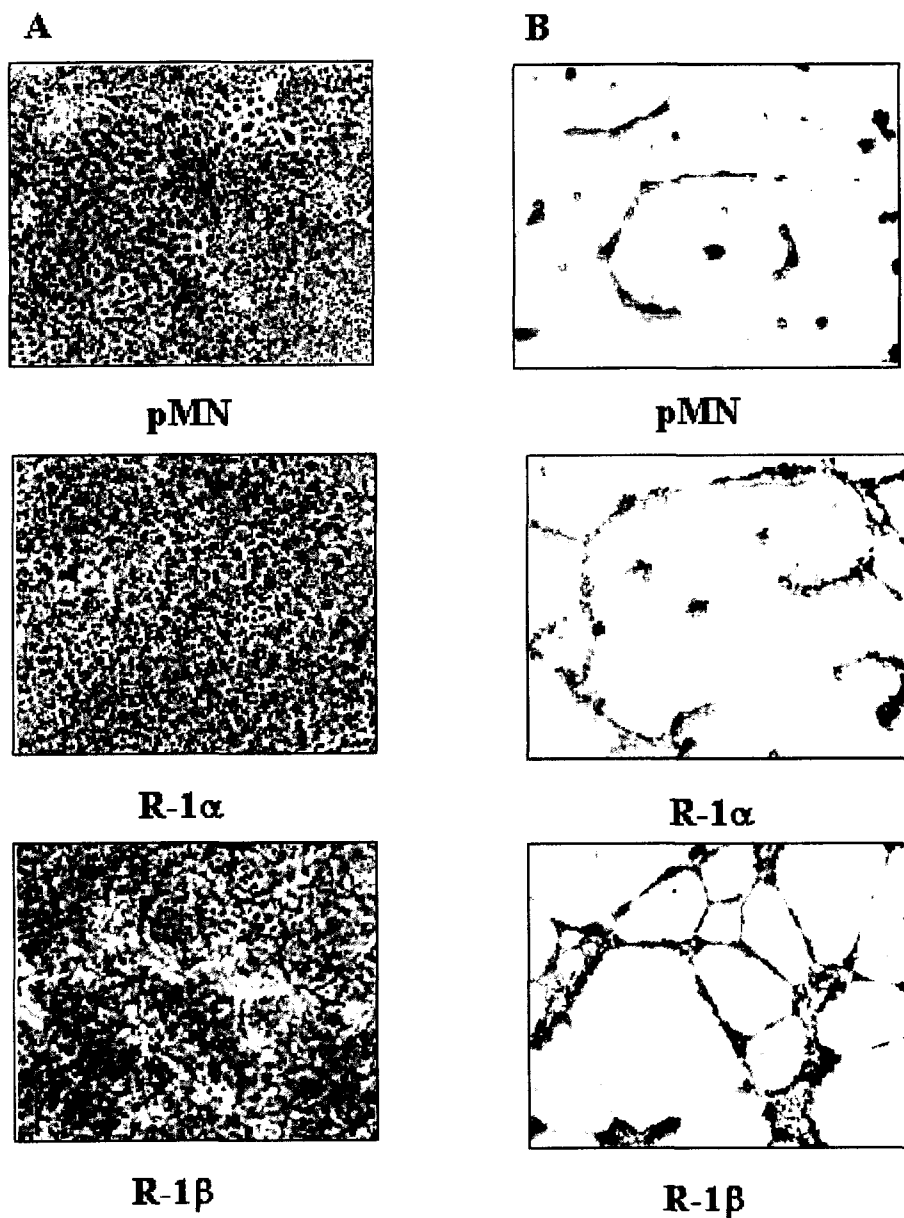


Fig. 6. Differential cord formation in vitro. (A) pMN, R-1 α , and R-1 β cells were grown to high density in normal culture media supplemented with FGF-1 (50 ng/ml) complexed with (50 U/ml) and examined for cord-arrays. (B) pMN, R-1 α , and R-1 β cells were cultured in reduced serum media, treated with FGF-1 (50 ng/ml) complexed with (50 U/ml) (2 h) and plated onto Matrigel. Cord formation was visualized after 24 h.

continuous ligand stimulation of R-1 β resulted in angiogenic cord-like structures in the Matrigel implant that were not observed in pMN or R-1 α (Fig. 7).

To examine if cord formation was dependent on c-Yes activity in FGFR-1 β , R-1 β cells were pretreated with the Src family inhibitor PP2 (30 min) prior to FGF-1 (50 ng/ml)/heparin (50 U/ml) treatment (2 h). Cells were plated onto Matrigel and cord formation was examined after 24 h. Cord formation was significantly increased in R-1 β ($p < 0.003$) compared to pMN (data not shown). A significant decrease ($p < 0.002$) was observed in R-1 β pretreated with PP2 compared to the R-1 β receiving vehicle only (Fig. 8). In cells pretreated with PP2, no significant difference in cord-formation was observed in pMN or R-1 α compared to the same cell line treated with vehicle only.

DISCUSSION

FGF activation of FGFR-1 stimulates diverse cellular processes, including mitogenesis, migration, and differentiation [27]. These are essential processes during angiogenesis, where endothelial cells must become activated, migrate to sites requiring neovascularization, and form differentiated tubule structures [28]. Studies by Takenake et al. (1997) suggest that the major FGFR-1 isoform involved in angiogenesis and wound healing is FGFR-1 β [9], an isoform that differs from the full-length FGFR-1 α solely by the absence of the first Ig-like loop in the extracellular domain [6]. These findings are consistent with the observation that FGFR-1 β is the predominant FGFR-1 isoform in pancreatic adenocarcinoma [10] and malignant astrocytoma [11], suggesting that activation of FGFR-1 β specific pathways is involved in cell activation and transformation.

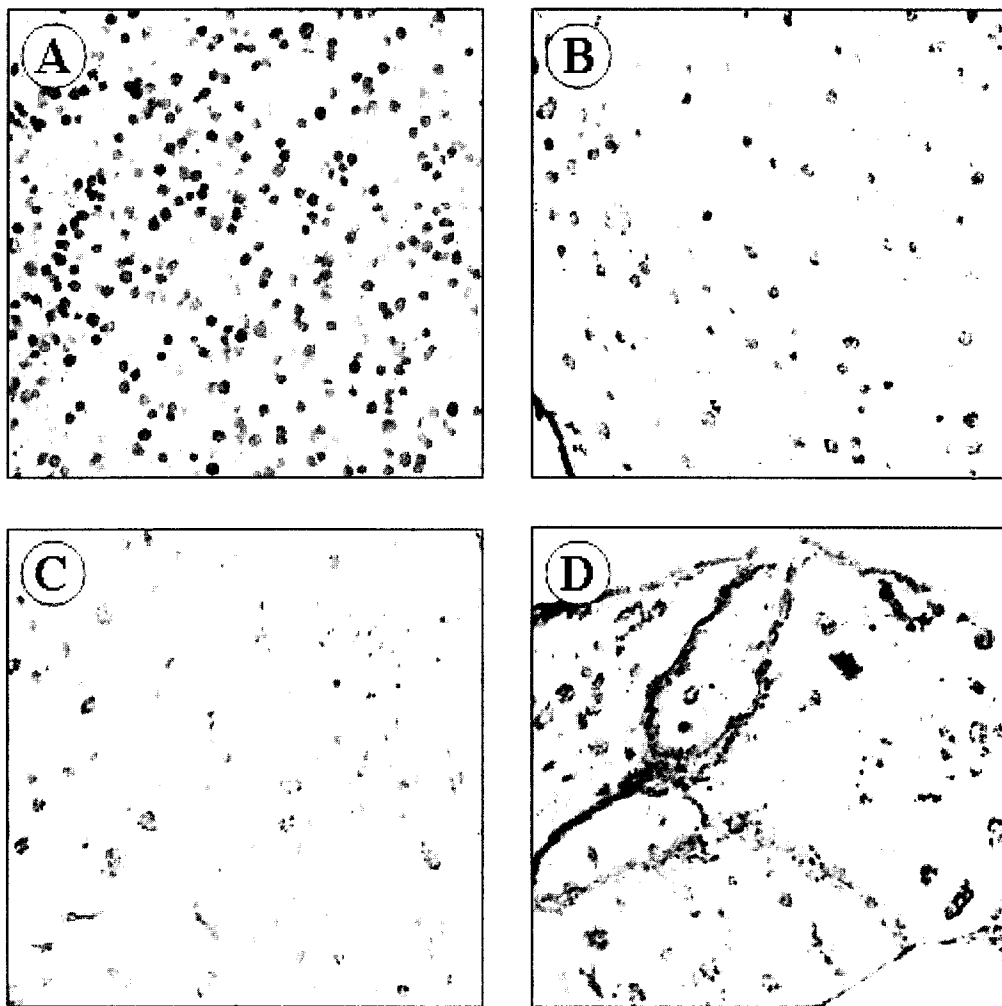


Fig. 7. Differential cord formation in vivo. pMN, R-1 α , or R-1 β cells (20×10^6) were suspended in Matrigel, implanted subcutaneously into Balb/c nude mice, harvested after 10 days, and visualized by staining (β -Gal). (A) Representative Matrigel plug containing RVEC prior to implantation. Ex vivo implants containing (B) pMN cells, (C) R-1 α cells, and (D) R-1 β cells.

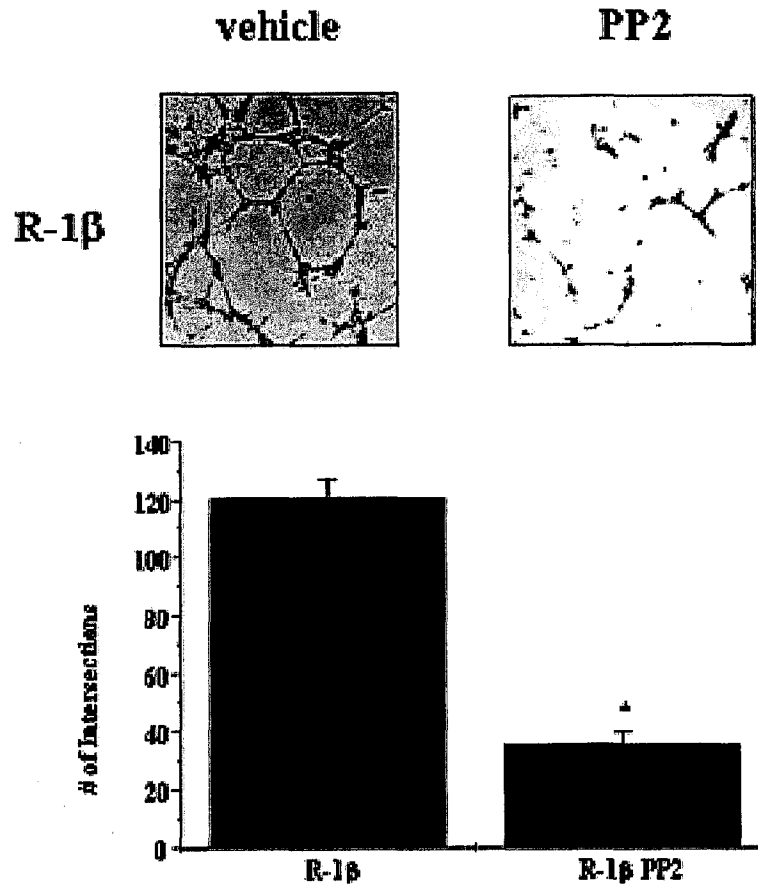


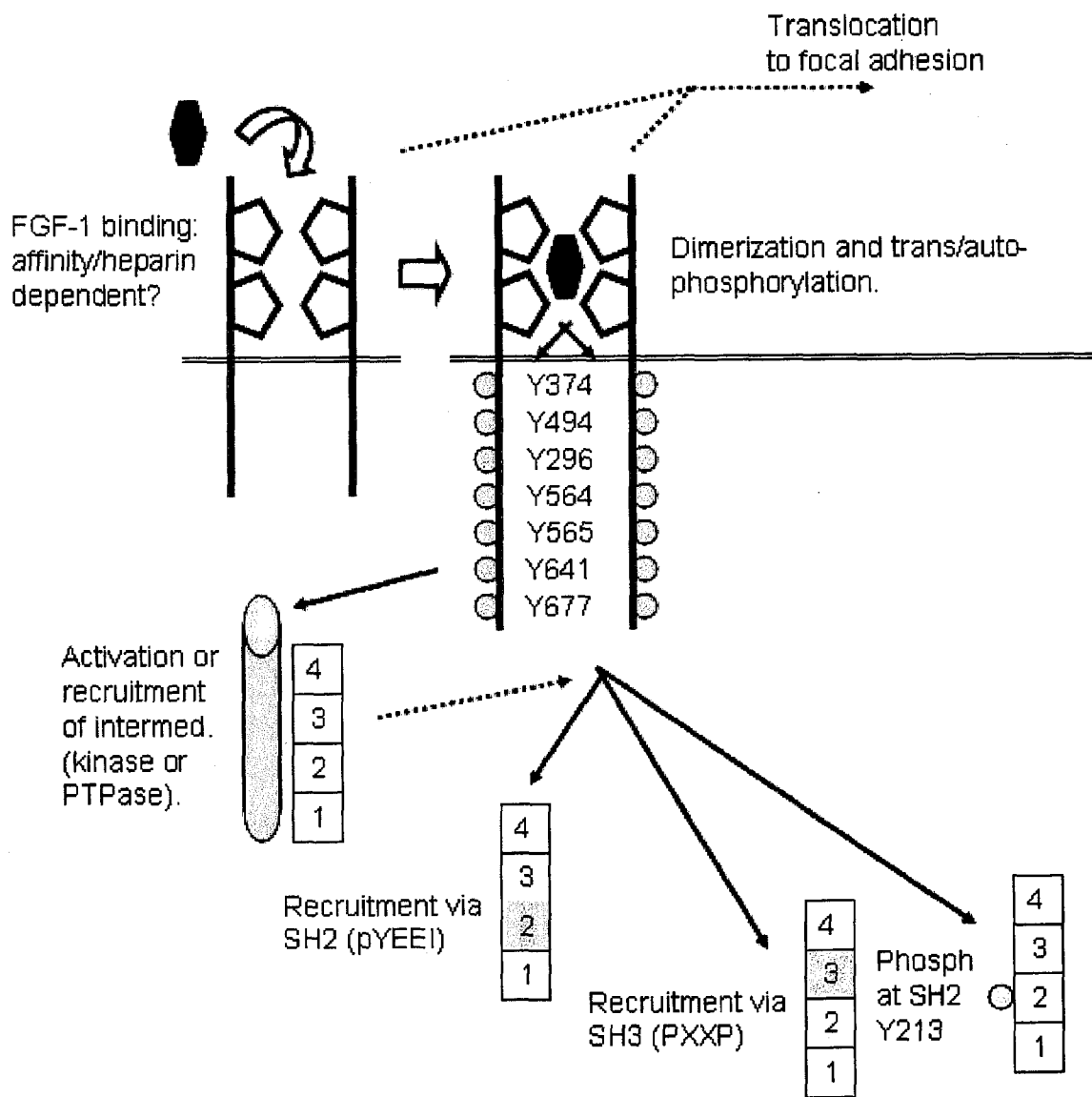
Fig. 8. c-Yes dependent cord-formation in vitro. R-1b cells were pretreated with 20 mM PP2 or vehicle (DMSO) (30 min) followed by treatment with FGF-1 (50 ng/ml) complexed with heparin (50 U/ml) (2 h). Cells were plated on Matrigel and assessed for cord formation after 24 h. * Differential significance of $p < 0.05$ compared to R-1 β .

SFK, which play important roles in angiogenesis and tumorigenesis, have been reported to be substrates of ligand-activated FGFR-1, but the precise interaction is unclear. Zhan et al. (1994) reported an increase in Src activity and association with FGFR-1 following FGF-1 stimulation, while Landgren et al. (1995) found no association between FGF-2 stimulated FGFR-1 and saw decreased Src activity in FGF-2 treated cells [16,17]. SFK are important signaling components involved in cytoskeletal remodeling [29], mitogenesis [30], and survival [31]; therefore, clarifying the interaction between FGFR-1 isoforms and SFK may provide insight into the regulation of angiogenesis and tumorigenesis.

We have recently characterized a FGFR-negative resistance vessel endothelial cell (RVEC) and RVEC transfected with FGFR-1 α (R-1 α), FGFR-1 β (R-1 β), or control vector (pMN) [18]. RVEC cells allow dissection of specific signaling pathways induced by FGF-1-activated FGFR-1 α or FGFR-1 β and avoid the complications found in other cultured cells, including the presence of multiple FGFR family members, multiple isoforms of FGFR, and multiple FGF ligands. Using RVEC, we present evidence that FGFR-1 β , but not FGFR-1 α , signals the SFK c-Yes. FGF-1-activated FGFR-1 β demonstrated increased association with the SFK c-Yes, increased c-Yes tyrosine phosphorylation within the tyrosine kinase domain, and increased c-Yes signaling to the F-actin binding protein cortactin. Tyrosine phosphorylation of cortactin inhibits its ability to cross-link F-actin [32] and results in disorganization of the actin cytoskeleton, decreased contact inhibition, and alterations in cell morphology [33]. Consistent with this signaling pathway is our observations that cells expressing FGFR-1 β formed vascular cords *in vivo* and c-Yes- dependent cords *in vitro*.

Important studies for the future will determine how FGFR-1 β and FGFR-1 α interact with specific substrates. Compartmentalization of FGFR-1 isoforms may allow access to different substrates. Plopper et al. (1995) identified both FGFR-1 and c-Src as proteins that localize at focal adhesion complexes [34]. If localization of FGFR-1 was restricted to the β isoform, this could result in specific signaling to SFK, as observed in the RVEC model. Different expression of HSPG/HLGAG at different cell sites may also contribute to FGFR-1 isoform specific signaling. Lundin et al. (2000) demonstrated that HSPG sulfation patterns, which differ between tissues, can affect FGFR-1 signaling and FGFR-1 induced angiogenesis [35]. Ligand-binding to FGFR-1 isoforms may also initiate auto-phosphorylation at different intracellular tyrosine residues. FGFR-1 has seven tyrosines (Y463, Y583, Y585, Y653, Y654, and Y730 in FGFR-1 α) that may be phosphorylated in vitro [5]. Differential auto-phosphorylation between FGF-1-activated FGFR-1 α and FGFR-1 β may result in recruitment of different substrates.

Of particular importance will be determining how c-Yes associates with FGFR-1 β (Ill. 1). While our results indicate that c-Yes directly associates with FGFR-1 β , this interaction may be facilitated by an intermediate binding protein. Alternatively, auto-phosphorylation of activated FGFR-1 could recruit c-Yes via its SH2 domain. c-Src associates with the PDGFR in a manner dependent on the c-Src SH2 domain and two neighboring PDGFR tyrosines within the juxtamembrane domain [36]. FGFR-1 has similarly located tyrosines: a juxtamembrane tyrosine (Y463 in FGFR-1 α or Y374 in FGFR-1 β) and two neighboring tyrosines (Y583 and Y585 in FGFR-1 α or Y494 and Y496 in FGFR-1 β) that may be potential sites of tyrosine phosphorylation and SFK recruitment in FGFR-1 β . SFK may also associate with FGFR-1 β through an SH3



III. 1. Potential interactions between FGF-1-activated FGFR-1 β and SFK.

domain interaction; the FGFR-1 β sequence has at least four intracellular spans of residues with the PXXP motif, the minimum binding requirement for an SH3 interaction [37].

The findings presented in this study indicate that FGF-1-activated RVEC expressing FGFR-1 β develop angiogenic structures *in vitro* and *in vivo*. Important future studies will examine what factors control alternative splicing of FGFR-1 mRNA to the FGFR-1 β isoform. Results from G. Cote's laboratory have identified a nucleotide exon required for translating FGFR-1 α [38], a downstream exon required for translating FGFR-1 β [39], and polypyrimidine tract-binding protein as a regulatory protein for splicing to the β isoform during development of malignant glioma [40]. Determining the factors regulating the expression of FGFR-1 α and FGFR-1 β has important implications for diseases with excessive angiogenesis, such as cancer, diabetic retinopathy, and arthritis [41], and for diseases with inadequate angiogenesis, such as myocardial ischemia and vascular insufficiency [42].

REFERENCES

- [1] M. Ford-Perriss, H. Abud, M. Murphy, *Clin. Exp. Pharm. Physiol.* 28 (2001) 493-503.
- [2] C.J. Powers, S.W. McLeskey, A. Wellstein, *Endocr.-Relat. Cancer* 7 (2000) 165-197.
- [3] P. Gerwins, E. Skoldenberg, L. Claesson-Welsh, *Crit. Rev. Oncol. Hematol.* 34 (2000) 185-194.
- [4] P. Klint, S. Kanda, Y. Kloog, L. Claesson-Welsh, *Oncogene* 18 (1999) 3354-3364.
- [5] M. Mohammadi, I. Dikic, A. Sorokin, W.H. Burgess, M. Jaye, J. Schlessinger, *Mol. Cell. Biol.* 16 (1996) 977-989.

- [6] J. Xu, M. Nakahara, J.W. Crabb, E. Shi, Y. Matuo, M. Fraser, M. Kan, J. Hou, W.L. McKeehan, *J. Biol. Chem.* 267 (1992) 17792-17803.
- [7] F. Wang, M. Kan, G. Yan, J. Xu, W.L. McKeehan, *J. Biol. Chem.* 270 (1995) 10231-10235.
- [8] I.A. Prudovsky, N. Savion, T.M. LaVallee, T. Maciag, *J. Biol. Chem.* 271 (1996) 14198-14205.
- [9] H. Takenaka, S. Kishimoto, I. Tooyama, H. Kimura, H. Yasuno, *J. Invest. Dermatol.* 109 (1997) 108-112.
- [10] M.S. Kobrin, Y. Yamanaka, H. Friess, M.E. Lopez, M. Korc, *Cancer Res.* 53 (1993) 4741-4744.
- [11] F. Yamaguchi, H. Saya, J.M. Bruner, R.S. Morrison, *Proc. Natl. Acad. Sci. USA* 91 (1994) 484-488.
- [12] T. Shono, Y. Mochizuki, H. Kanetake, S. Kanda, *Exp. Cell Res.* 268 (2001) 169-178.
- [13] B.P. Eliceiri, R. Paul, P.L. Schwartzberg, J.D. Hood, J. Leng, D.A. Cheresh, *Mol. Cell* 4 (1999) 915-924.
- [14] M. Marx, S.L. Warren, J.A. Madri, *Exp. Mol. Pathol.* 70 (2001) 201-213.
- [15] M.P. Lutz, I.B.S. Eber, B.B.M. Flossmann-Kast, R. Vogelmann, H. Luhrs, H. Friess, M.W. Buchker, G. Adler, *Biochem. Biophys. Res. Comm.* 243 (1998) 503-508.
- [16] X. Zhan, C. Plourde, X. Hu, R. Friesel, T. Maciag, *J. Biol. Chem.* 269 (1994) 20221-20224.
- [17] E. Landgren, P. Blume-Jensen, S.A. Courtneidge, L. Claesson-Welsh, *Oncogene* 10 (1995) 2027-2035.
- [18] J. Jiao, J.S. Greendorfer, P. Zhang, K.R. Zinn, C.A. Diglio, J.A. Thompson, *Arch. Biochem. Biophys.* 410 (2003) 187-200.
- [19] C. A. Diglio, W. Liu, P. Grammas, F. Giacomelli, J. Wiender, *Tissue Cell* 25 (1993) 833-846.
- [20] D. Martin-Zanca, R. Oskam, G. Mitra, T. Copeland, M. Barbacid, *Mol. Cell Biol.* 9 (1989) 24-33.

- [21] S. R. Opalenik, J. T. Shin, J. N. Wehby, V. K. Mahesh, J. A. Thompson, *J. Biol. Chem.* 270 (1995) 17457-17467.
- [22] W. Zhao, S. Cavallaro, P. Gusev, D. L. Alkon, *PNAS* 97 (2000) 8098-8103.
- [23] G. Li, Y. F. Chen, S. S. Kelpke, S. Oparil, J. A. Thompson, *Circulation* 101 (2000) 2949-2955.
- [24] G. Bernardini, G. Spinetti, D. Ribatti, G. Camarda, L. Morbidelli, M. Ziche, A. Santoni, M. C. Capogrossi, M. Napolitano, *Blood* 15 (2000) 4039-4045.
- [25] D. Markowitz, S. Goff, A. Bank, *J. Virol.* 62 (1988) 1120-1124.
- [26] D. Ribatti, A. Vacca, *Int. J. Biol. Markers* 14 (1999) 207-213.
- [27] D.E. Johnson, L.T. Williams, *Adv. Cancer Res.* 60 (1993) 1-41.
- [28] A.W. Griffioen, G. Molema, *Pharmacol. Rev.* 52 (2000) 237-268.
- [29] D. Small, D. Kovalenko, D. Kacer, L. Liaw, M. Landriscina, C. Di Serio, I. Prudovsky, T. Maciag, *J. Biol. Chem.* 276 (2001) 32022-32030.
- [30] C.L. Abram, S.A. Courtneidge, *Exp. Cell Res.* 254 (2000) 1-13.
- [31] A.G. Tatosyan, O.A. Mizenina, *Biochemistry (Moscow)* 65 (2000) 49-58.
- [32] C. Huang, Y. Ni, T. Wang, Y. Gao, C.C. Haudenschild, X. Zhan, *J. Biol. Chem.* 272 (1997) 13911-13915.
- [33] S. Nada, M. Okada, S. Aizawa, H. Nakagawa, *Oncogene* 9 (1994) 3571-3578.
- [34] G.E. Plopper, H.P. McNamee, L.E. Dike, K. Bojanowski, D.E. Ingber, *Mol. Biol. Cell* 6 (1995) 1349-1365.
- [35] L. Lundin, H. Larsson, J. Kreuger, S. Kanda, U. Lindahl, M. Salmivirta, L. Claesson-Welsh, *J. Biol. Chem.* 275 (2000) 24653-24660.
- [36] K.A. DeMali, S.L. Godwin, S.P. Soltoff, A. Kazlauskas, *Exp. Cell Res.* 253 (1999) 271-279.
- [37] A.B. Sparks, J.E. Rider, N.G. Hoffman, D.M. Fowlkes, L.A. Quilliam, B.K. Kay, *Proc. Natl. Acad. Sci. USA* 93 (1996) 1540-1544.
- [38] W. Jin, E.S. Huang, W. Bi, G.J. Cote, *J. Biol. Chem.* 273 (1998) 16170-16176.
- [39] W. Jin, W. Bi, E.S. Huang, G.J. Cote, *Cancer Res.* 59 (1999) 316-319.

- [40] W. Jin, I.E. McCutcheon, G.N. Fuller, E.S. Huang, G.J. Cote, *Cancer Res.* 60 (2000) 1221-1224.
- [41] T.D. Fan, R. Jaggar, R. Bicknell, *TiPS* 16 (1995) 57-66.
- [42] R.J. Tomanek, G.C. Schatteman, *Anat. Rec. (New Anat.)* 261 (2000) 126-135.

TYROSINE NITRATION OF c-SRC TYROSINE KINASE
IN HUMAN PANCREATIC DUCTAL ADENOCARCINOMA

by

LEE ANN MACMILLAN-CROW, JESSICA S. GREENDORFER,
SELWYN M. VICKERS, AND JOHN A. THOMPSON

Archives of Biochemistry and Biophysics 377:350-356

Copyright

2000

by

Academic Press

Used by permission

Format adapted for dissertation

ABSTRACT

During pancreatic tumorigenesis, the equilibrium between cell survival and cell death is altered, allowing aggressive neoplasia and resistance to radiation and chemotherapy. Local oxidative stress is one mechanism regulating programmed cell death and growth and may contribute to both tumor progression and suppression. Our recent in situ immunohistochemical studies demonstrated that levels of total nitrotyrosine, a footprint of the reactive nitrogen species peroxynitrite, are elevated in human pancreatic ductal adenocarcinomas. In this study, quantitative HPLC-EC techniques demonstrated a 21- to 97-fold increase in the overall levels of nitrotyrosine of human pancreatic tumor extracts compared to normal pancreatic extracts. Western blot analysis of human pancreatic tumor extracts showed that tyrosine nitration was restricted to a few specific proteins. Immunoprecipitation coupled with Western analysis identified c-Src tyrosine kinase as a target of both tyrosine nitration and tyrosine phosphorylation. Peroxynitrite treatment of human pancreatic carcinoma cells in vitro resulted in increased tyrosine nitration and tyrosine phosphorylation of c-Src kinase, increased (>2-fold) c-Src kinase activity, and increased association between c-Src kinase and its downstream substrate cortactin. Collectively, these observations suggest that peroxynitrite-mediated tyrosine nitration and tyrosine phosphorylation of c-Src kinase may lead to enhanced tyrosine kinase signaling observed during pancreatic ductal adenocarcinoma growth and metastasis.

INTRODUCTION

Pancreatic ductal adenocarcinoma remains one of the most lethal forms of cancer. This stems in part from the inadequacy to minimize tumor growth and metastasis with therapeutic strategies such as radiation or chemotherapy, as well as an inability to excise an advanced pancreatic tumor [1]. At the time of diagnosis only 8% of tumors are deemed candidates for surgical resection, leaving more than 92% of pancreatic tumors untreatable. The biochemical/molecular basis for these dismal statistics of pancreatic cancer is unknown. Clearly, multiple mechanisms are involved with tumor growth, progression, and metastasis.

The nonreceptor SRC family of tyrosine kinases has been shown to be overexpressed and upregulated in both human pancreatic carcinoma tissue and human pancreatic tumor cell lines [2]. Interestingly, these authors found that the levels of c-Src tyrosine kinase (c-Src) protein did not correlate with the increase in kinase activity observed, suggesting that posttranslational modification of the protein may be involved with the increased activity. This potential would be consistent with the suggestion that phosphatases, cytokines, growth factors, and high-affinity receptor tyrosine kinases which can activate c-Src may be involved in the onset and progression of pancreatic adenocarcinoma [3-9].

Numerous investigators have hypothesized that oxidants, such as nitric oxide (NO), hydrogen peroxide (H₂O₂), and peroxynitrite (ONOO⁻), produced from the diffusion limited reaction between NO and superoxide (O₂⁻) [10], might be involved in tumorigenesis [11-13]. ONOO⁻ nitrates protein tyrosine residues, a modification we and others have shown previously to adversely affect protein function [14-19]. Previous

immunohistological studies from this laboratory demonstrated that enhanced expression of fibroblast growth factor (FGF) ligands and receptors was associated with an increased appearance of the inducible isoform of nitric oxide synthase (NOS-2) and protein tyrosine nitration during pancreatic tumorigenesis, thereby predicting a role for oxidant stress in pancreatic cancer [13]. We extended this issue further and designed the current study to identify a specific protein nitration target relevant to tumorigenesis. These experimental results provide a first indication that in human pancreatic ductal adenocarcinoma tissue, c-Src is both tyrosine nitrated and phosphorylated. In addition, in vitro treatment of human pancreatic ductal adenocarcinoma cells with ONOO^- increased c-Src activity. Collectively, these results suggest that ONOO^- -mediated modification of c-Src may play a pivotal role in the enhanced cellular growth during human pancreatic ductal adenocarcinoma.

MATERIALS AND METHODS

Tissue specimens

Pancreatic tissue from three patients who underwent resection due to pancreatic ductal adenocarcinoma was examined in this study. These tissues were found to have a Grade III malignancy. A heart-beating organ donor, whose pancreas was determined unsuitable for transplantation, was utilized as a control.

Tissue culture

A human pancreatic ductal adenocarcinoma cell line (HPAC) was obtained from the American Type Culture Collection (ATCC No. CRL-2119). The cell line was cultured in Dulbecco's modified Eagle's medium (DMEM) supplemented with 2 mM glutamine, 100 units/ml penicillin, 100 mg/ml streptomycin (all from Sigma), and 10% heat-inactivated fetal bovine serum (FBS) (Hyclone). Cells were grown in a humidified atmosphere of 95% air and 5% CO₂ at 37°C and subcultured at about 80% confluency using trypsin-EDTA.

For protein analysis, cells were placed on ice, washed with cold phosphate buffered saline (PBS) containing 1 mM phenylmethylsulfonyl fluoride (PMSF), and lysed with lysis buffer (50 mM HEPES, pH 7.4, 150 mM NaCl, 1% Triton X-100, 0.1% SDS, 1% sodium deoxycholate, 1 mM EGTA, 1 mM sodium orthovanadate, 1mM PMSF, 10 µg/ml leupeptin, and 10 µg/ml aprotinin). Lysates were clarified by centrifugation at 10,000 rpm (10 min; 4°C), and the protein concentration of the supernatant was determined by Bradford analysis (Pierce).

Pancreatic extract preparation

Extracts were made from fresh tissue by homogenizing (0.1 g/ml) using a Polytron homogenizer in buffer containing 50 mM potassium phosphate, pH 7.4, 150 mM NaCl, and 1 mM PMSF. Solubilized extracts were sonicated (two 10-s bursts at 30% power) and centrifuged at 10,000 rpm (10 min, 4°C) to remove tissue debris. Protein concentrations were determined by the Bradford Assay (Pierce).

Immunoprecipitation

Extracted proteins (1-2 mg) were incubated (4°C, 18 h) with either 7 µg of monoclonal anti-nitrotyrosine antibody (generous gift from Dr. Joe Beckman, Upstate Biotechnology Inc., UBI), 10 µg of polyclonal anti-SRC2 antibody (Santa Cruz), or 7 µg of monoclonal anti-phosphotyrosine (PY20) antibody (Transduction Laboratories). Immune complexes were precipitated with protein-A/G Sepharose (UBI), washed, and fractionated by 10% SDS/PAGE as described [14,20].

Western blot Analysis

Western blot analysis was performed as described [14,20]. For nitrotyrosine Western analysis we used the monoclonal anti-nitrotyrosine (1:500). Blocking experiments for nitrotyrosine immunoreactivity were performed by pre-incubating (25°C, 30 min) the nitrotyrosine antibody with 10 mM 3-nitrotyrosine (Sigma) prior to incubation with membrane. Western analyses for c-Src, phosphotyrosine, and cortactin were performed using polyclonal anti-SRC2 antibody (1:2000), monoclonal anti-phosphotyrosine antibody (1:1000), or monoclonal anti-cortactin antibody (1:3000; UBI). Probed membranes were washed three times and immunoreactive proteins detected using horseradish peroxidase conjugated secondary antibodies and enhanced chemiluminescence.

c-Src kinase activity assay

C-Src, immunoprecipitated from cellular extracts (2 mg) was assayed for kinase activity essentially as described [2]. Briefly, immunoprecipitates were incubated in ice-cold kinase buffer (50 mM Hepes, pH 7.2, 150 mM NaCl, 10 mM MgCl₂). Phosphorylation was initiated by adding 5 μM (γ-³²P)-ATP (10 μCi per reaction) in 25 μl reaction buffer containing 1 μg acid-denatured rabbit muscle enolase for 15 min at 37°C. The reaction was stopped by incubation (95°C, 5 min) in SDS-sample loading buffer. Proteins were resolved by 10% SDS-PAGE, and labeled proteins were detected by autoradiography. Quantitative analysis was performed by phosphoimaging (PhosphorImager; Molecular Dynamics).

ONOO⁻ treatment of cells

ONOO⁻ was synthesized from sodium nitrite and acidified H₂O₂ and quantified as described previously [21]. HPAC cells were treated with ONOO⁻ (1 mM) by washing subconfluent (80%) cells with PBS and incubating with 3 ml PBS containing an additional 50 mM potassium phosphate buffer, pH 7.4. ONOO⁻ was added (5 min, 23°C) to adhered HPAC cells with rapid mixing. Working solutions of ONOO⁻ were prepared by diluting stocks in water just prior to use. Untreated cells served as negative controls.

HPLC-EC determination of protein-bound nitrotyrosine

Pancreatic extracts were ultrafiltered (Millipore 5 kD MWCO centrifugal ultrafilters) and the retentates were ethanol precipitated. Protein precipitates were resuspended in 100 μl water and protein concentrations were determined using the

Bradford Assay (Pierce). Proteins (100 μ g) were transferred to hydrolysis tubes and hydrolyzed for 20 h at 105°C under an inert atmosphere containing high purity 6 N HCl and 1% phenol. Dried, hydrolyzed samples were resuspended in 100 μ l of polished buffer A (50 mM sodium acetate, pH 4.8) and centrifuged at 12,000g for 10 min to pellet any particulates. Clarified samples (50 μ l) were injected onto a TOSOHAAS ODS 80-TM (5 μ m, 4.6 X 250 mm) and eluted at 0.75 ml/min with 95% buffer A and 5% methanol. Peaks were monitored electrochemically using a 12-channel ESA Couloarray detector with the following potentials: channels 1-12 were set to +225, 295, 365, 435, 505, 575, 645, 715, 805, 850, 875, and 925 mV, respectively. Nitrotyrosine, chlorotyrosine, and tyrosine were quantified relative to known standards and nitrotyrosine content was expressed as a percentage of total protein-bound tyrosine [22].

RESULTS

Increased Nitrotyrosine Immunoreactivity during Human Pancreatic Ductal Adenocarcinoma

We have recently demonstrated an increase of tyrosine nitration during human pancreatic ductal adenocarcinoma using nitrotyrosine immunohistochemistry [13]. In order to identify specific nitration targets in human pancreatic ductal adenocarcinoma, nitrotyrosine immunoprecipitation of pancreatic extracts followed by nitrotyrosine Western analysis was performed (Fig. 1A). Specificity was confirmed by blocking strategies using excess nitrotyrosine (Fig. 1B). The immunoreactive proteins remaining in Fig. 1B represent the nitrotyrosine monoclonal antibody (heavy and light chains, ~55 and 25 kDa, respectively) used in the immunoprecipitation, since the identical antibody was used for Western analysis. These results suggested that a few specific proteins

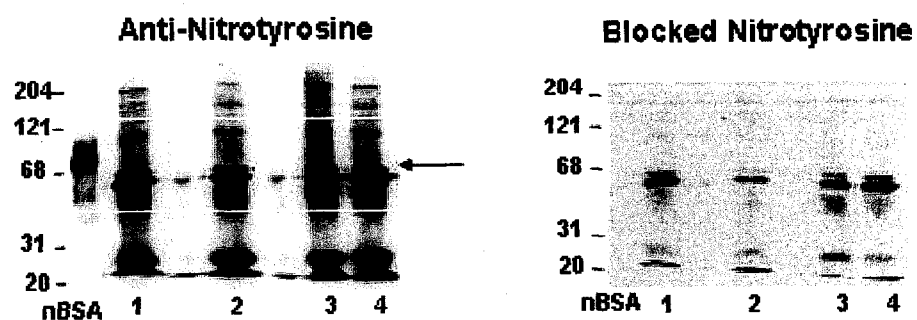


Fig. 1. Western analysis of tyrosine nitration in human pancreatic tissue. (A) Protein extracts (1.5 mg) isolated from normal pancreas (lane 1) and three separate pancreatic ductal adenocarcinomas (lanes 2-4) were subjected to nitrotyrosine immunoprecipitation followed by nitrotyrosine Western blot analysis using a monoclonal anti-nitrotyrosine antibody. (B) The identical blot stripped of primary antibody and reprobbed with antibody pretreated with 10 mM 3-nitrotyrosine. Tyrosine-nitrated BSA (N-BSA) served as a positive control. The results are representative of three different experiments. The arrow represents the migration of c-Src.

appeared to be tyrosine nitrated in three different pancreatic adenocarcinoma tissues (Fig. 1A, lanes 2-4) and one normal pancreatic tissue (lane 1). To overcome limitations imposed by comparing overall levels of chemiluminescence obtained during Western analysis, a more quantitative method was employed to determine protein-bound nitrotyrosine levels between samples (Table 1).

Table 1
HPLC-EC Quantitative Measures of Tyrosine Modifications
in Human Pancreatic Tissue

Tissue sample	Tyrosine (μM)	Nitrotyrosine (μM)	Chlorotyrosine (μM)	Ratio ntyr/tyr (percent) ^a
Normal	81.88	0.042	0	0.05
Tumor 1	52.60	0.567	0	1.07
Tumor 2	11.03	0.565	0	4.87
Tumor 3	73.65	1.052	0	1.41

^a Calculated by dividing total nitrotyrosine content by total tyrosine content (tyrosine + nitrotyrosine) and multiplying by 100.

Compared to normal pancreatic tissue, HPLC-EC quantitative measures revealed significant increases in protein-bound nitrotyrosine in tumor extracts. When standardized to total tyrosine content, human pancreatic tumor extracts demonstrated a significant increase (>21- to 97-fold) in overall levels of nitrotyrosine. Interestingly, levels of chlorotyrosine were nondetectable. Chlorotyrosine has been implicated as another marker of oxidant stress, specifically being produced by myeloperoxidase, an enzyme associated with activated neutrophils [23].

Tyrosine Nitration and Phosphorylation of c-Src Associated with Human Pancreatic Cancer.

c-Src was identified as one of these endogenous nitration targets in human pancreatic ductal adenocarcinoma by immunoprecipitating total nitrated proteins (NT IP) followed by Western analysis using the polyclonal anti-SRC2 antibody (SRC) (Fig. 2A). Tyrosine nitrated c-Src was observed only in human pancreatic ductal adenocarcinoma (CA), but not in a human chronic pancreatitis (CH), or the control human pancreatic tissue (N). Likewise, tyrosine phosphorylation of c-Src was observed only in the human pancreatic ductal adenocarcinoma sample, as shown by immunoprecipitating total tyrosine phosphorylated proteins (PY IP), followed by SRC Western analysis (Fig. 2B).

Increased Tyrosine Nitration and Phosphorylation Following ONOO⁻ Treatment of Pancreatic Cancer Cells.

In order to better understand the possible role that ONOO⁻ has on tyrosine kinase signaling by c-Src, a human pancreatic ductal adenocarcinoma cell line (HPAC) was utilized. ONOO⁻ treatment (1 mM) of adhered HPACs resulted in a dramatic increase in both tyrosine nitration and phosphorylation (Figs. 3A and 3B).

In addition, when compared to untreated cells, exposure of HPACs to ONOO⁻ resulted in increased nitration and phosphorylation of tyrosine residues in c-Src as demonstrated by nitrotyrosine (Fig. 4A) and phosphotyrosine (Fig. 4B) Western analysis following SRC immunoprecipitation using the polyclonal anti-SRC2 antibody (SRC IP). The arrow shows the migration of nitrated/phosphorylated c-Src. Moreover, this effect was probably not due to an increase in c-Src protein levels since SRC Western analysis using the polyclonal anti-SRC2 antibody demonstrated that c-Src protein levels were not

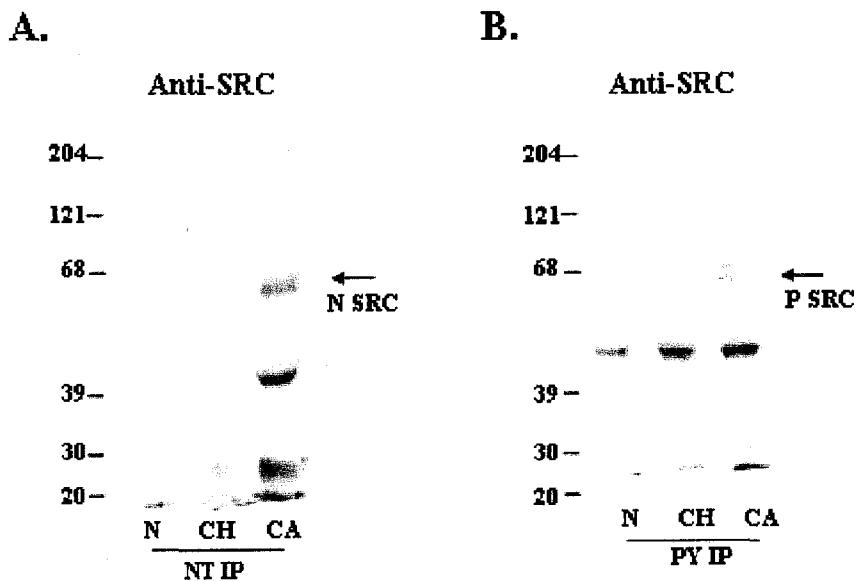


Fig. 2. Western analysis of modified tyrosine residues in c-Src associated with human pancreatic tissue. Protein extracts (1.5 mg) isolated from normal pancreas (N), chronic pancreatitis (CH), or pancreatic ductal adenocarcinoma (CA) tissue were immunoprecipitated with either the anti-nitrotyrosine antibody (A) (NT IP) or anti-phosphotyrosine antibody (B) (PY IP) and Western analyzed with the polyclonal SRC2 antibody. Arrows represent migration of tyrosine-nitrated c-Src (N SRC) or tyrosine-phosphorylated c-Src (P SRC). The results are representative of three different experiments.

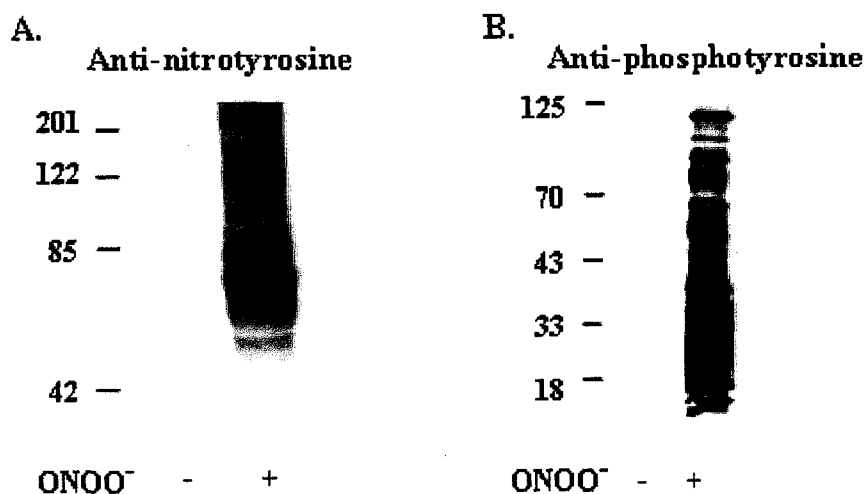


Fig. 3. Western analysis of tyrosine modifications in ONOO⁻-treated human pancreatic adenocarcinoma cells. Protein extracts (100 μ g/lane) were isolated from HPACs following treatment (5 min) in the absence (-) or presence (+) of 1 mM ONOO⁻ on the plate, prior to fractionation by 10% SDS-PAGE. Western analysis was performed using antibodies against either nitrotyrosine (A) or phosphotyrosine (B). These results are representative of five different experiments.

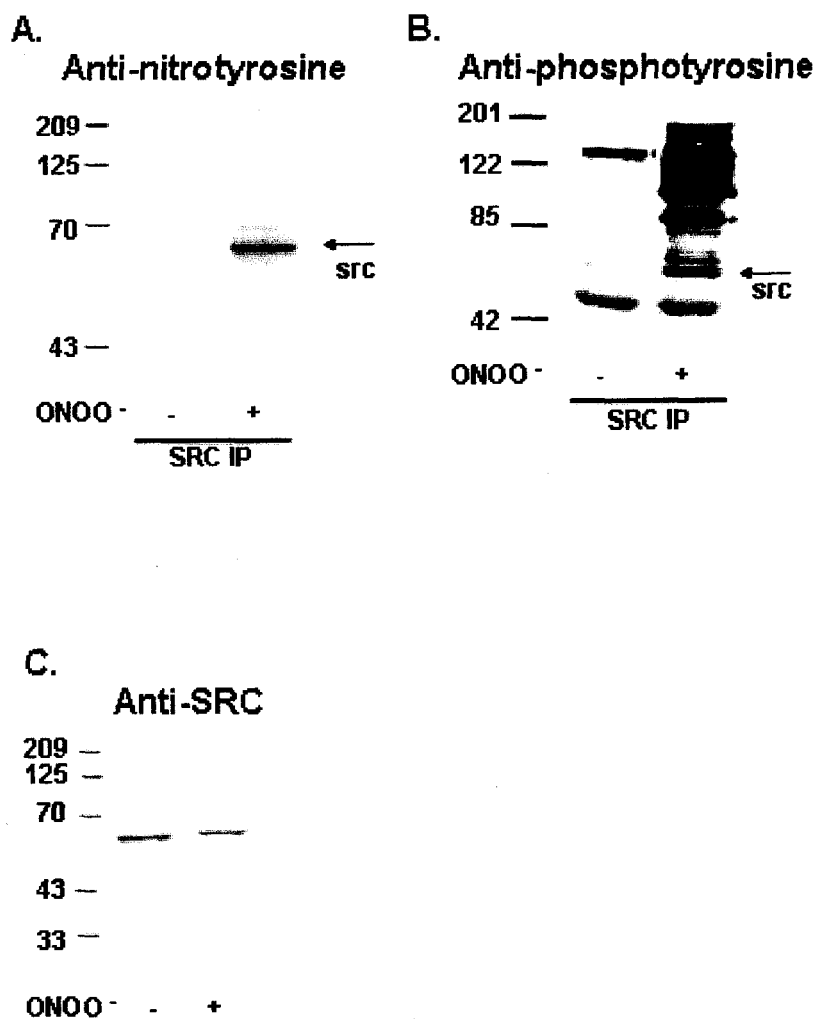


Fig. 4. Western analysis of tyrosine modifications of c-Src following ONOO⁻ treatment of human pancreatic adenocarcinoma cells. (A and B) Protein extracts (1.5 mg) were isolated from HPACs following treatment (5 min) in the absence (-) or presence (+) of 1 mM ONOO⁻, immunoprecipitated with the polyclonal SRC2 antibody (SRC IP), fractionated by 10% SDS-PAGE, and Western analyzed using antibodies against either nitrotyrosine (A) or phosphotyrosine (B). Arrows represent migration of c-Src. (C) Total cellular extracts (50 μ g) from untreated (-) and ONOO⁻-treated (+) HPACs were Western analyzed with the polyclonal SRC2 antibody. These results are representative of three different experiments.

altered following ONOO⁻ treatment (Fig. 4C). Since the polyclonal anti-SRC2 antibody is thought to recognize only the dephosphorylated, active conformation under native conditions [33], it is reasonable to anticipate that ONOO⁻ treatment of HPACs increase kinase activity by a mechanism involving both nitration and phosphorylation of critical tyrosine residues. The multiple phosphotyrosine immunoreactive bands co-immunoprecipitating with c-Src following ONOO⁻ treatment are probably c-Src docking proteins or substrates (Fig. 4B), consistent with increased activity of c-Src.

ONOO⁻-Mediated Effects on c-Src Kinase Activity.

The effect of ONOO⁻ treatment on c-Src activity in HPACs was determined using a c-Src in vitro kinase assay. Compared to untreated cells, treatment of adherent HPACs with ONOO⁻ (1 mM) resulted in an upregulation of c-Src activity as demonstrated by increased phosphorylation of the exogenous c-Src substrate enolase as well as increased autophosphorylation (Fig. 5A). Phosphoimaging quantification revealed a 2.24-fold increase in enolase phosphorylation following ONOO⁻ treatment (62.5 versus 139.6 arbitrary units for untreated and ONOO⁻-treated HPAC cells, respectively) and a 2.45 fold increase in c-Src autophosphorylation following ONOO⁻ treatment (67.8 versus 166.4 arbitrary units) (Fig. 5B).

Additional evidence supporting increased c-Src activity following ONOO⁻ treatment was shown by increased association of c-Src with one of its substrates, cortactin. Compared to untreated cells, HPACs treated with ONOO⁻ demonstrated increased levels of cortactin coprecipitating with c-Src, as well as increased tyrosine phosphorylation of this c-Src substrate. Adherent HPAC cells were treated with ONOO⁻

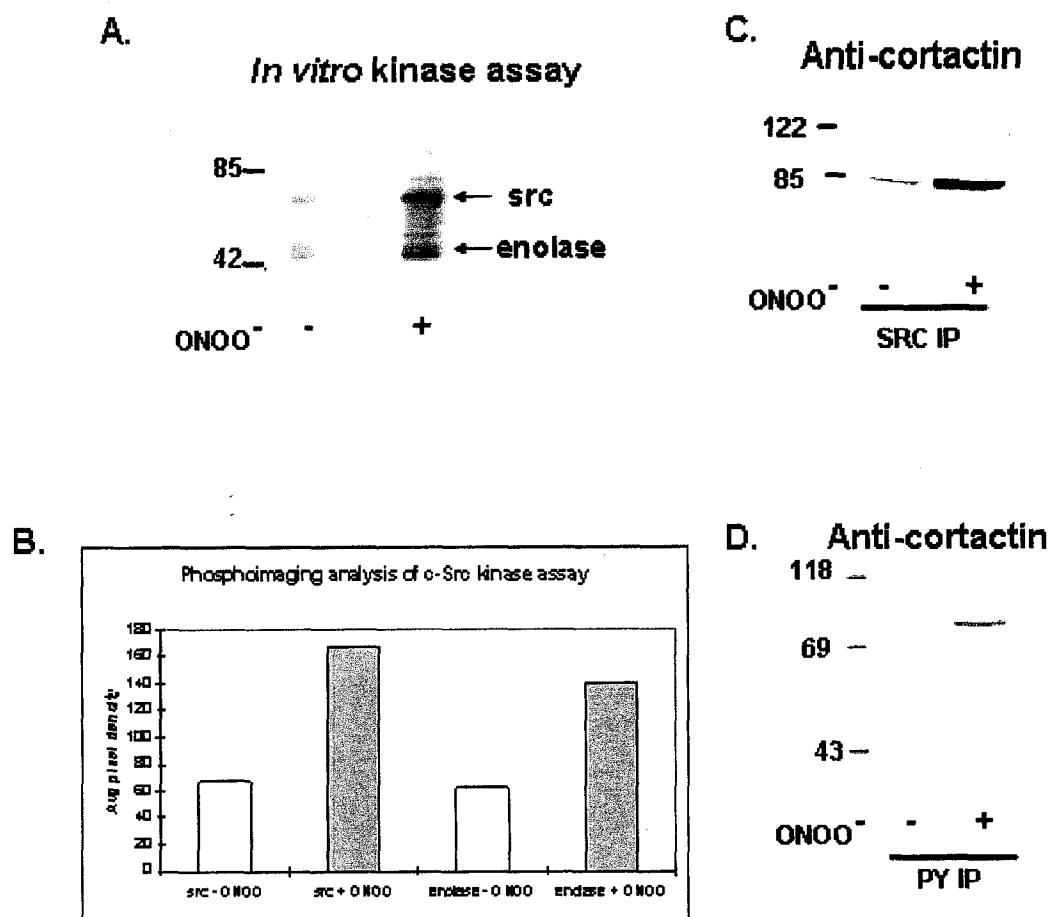


Fig. 5. Analysis of c-Src activity in human pancreatic adenocarcinoma cells following ONOO⁻ treatment. (A and B) Protein extracts (2.0 mg) were isolated from HPACs following treatment (5 min) in the absence (-) or presence (+) of 1 mM ONOO⁻, immunoprecipitated with the polyclonal SRC2 antibody, and subjected to the in vitro kinase assay (Materials and Methods). Proteins were resolved by 10% SDS-PAGE, and radioactively labeled (³²P) proteins were detected by autoradiography (A) and quantitatively analyzed by phosphoimaging (B). The positions of phosphorylated enolase and phosphorylated c-Src are noted with the arrows. (C and D) Protein extracts (1.5 mg) were isolated from HPACs following treatment (5 min) in the absence (-) or presence (+) of 1 mM ONOO⁻, immunoprecipitated with antibodies against either c-Src (C) (SRC IP) or phosphotyrosine (D) (PY IP), and Western analyzed with antibodies against the c-Src substrate, cortactin. Similar results were obtained three times.

(1 mM) followed by a SRC immunoprecipitation (SRC IP) and Western analysis using the monoclonal anti-cortactin antibody (Fig. 5C). Likewise, increased cortactin phosphorylation following ONOO⁻ treatment was demonstrated by immunoprecipitation of tyrosine phosphorylated proteins (PY IP) and cortactin Western analysis using the monoclonal anti-cortactin antibody (Fig. 5D). The low, but detectable levels of active c-Src present in the untreated HPACs is consistent with previous reports showing increased c-Src activity in other human pancreatic carcinoma cell lines [2].

DISCUSSION

Several observations in this study provide insight to a potential mechanism regulating activation of c-Src in human pancreatic ductal adenocarcinoma beyond that previously reported [2]. Both immunologic and quantitative biochemical techniques established that protein tyrosine nitration occurs during human pancreatic tumorigenesis. More specifically, c-Src extracted from human pancreatic tumor tissue was demonstrated to contain both tyrosine nitration and tyrosine phosphorylation. In addition, treatment of HPACs with ONOO⁻-induced activation of c-Src, an observation accompanied by increased tyrosine nitration and tyrosine phosphorylation of c-Src as well as association with cortactin. Collectively these results are consistent with increased c-Src activity observed in pancreatic cancer [2] and suggest a transforming role for ONOO⁻ during pancreatic tumor growth and metastasis.

The catalytic activity of Src family of kinases is repressed by the c-terminal Src kinase (Csk), which phosphorylates the carboxyl terminal tyrosine (Y530) of c-Src kinase [24, 25]. This phosphorylated tyrosine presumably interacts with the SH2 and SH3

domain of c-Src, keeping c-Src in a folded, “inactive” conformation (Fig. 6). There are at least five reported mechanisms that can lead to the unfolding and activation of c-Src. One involves dephosphorylation of Y530, thereby displacing this carboxy-terminal regulatory domain [26]. The precise tyrosine phosphatase responsible for this is unknown, but recent data suggest that the SHP-1 phosphatase could be a likely candidate [4]. Other mechanisms promoting conformational changes and activation of c-Src include: (i) competition for the c-Src SH2 domain by a tyrosine phosphorylated substrate; (ii) competition for the c-Src SH3 domain by a proline-rich substrate; (iii) competition for phosphorylated Y530 of c-Src by a substrate containing a SH2 domain; (iv) or tyrosine phosphorylation of the SH2 domain of c-Src itself [5,9,27,28].

At present, the specific tyrosine residue(s) that are nitrated in c-Src remain unknown; however, we show here, consistent with recent reports by Lutz et al., that c-Src activity is elevated in pancreatic cancer [2]. We hypothesize that nitration of critical tyrosine residues in c-Src might lead to an altered regulation of the kinase thereby increasing c-Src activity (Fig. 6). Previous studies have demonstrated that nitration of a tyrosine residue may prevent further phosphorylation of that residue [29-31]. Alternatively, nitration of tyrosine residues is very similar to phosphorylation of tyrosine residues with respect to the addition of a negative charge and similar electron density (NO_2 and PO_4) to the protein.

Consequently, nitration of critical tyrosine residues within c-Src could essentially mimic tyrosine phosphorylation, resulting in activation of the kinase and recruitment of downstream substrates. Early preliminary results suggest that tyrosines within the c-src SH3 domain of c-Src may be targets for nitration. Immunoprecipitation of c-Src from

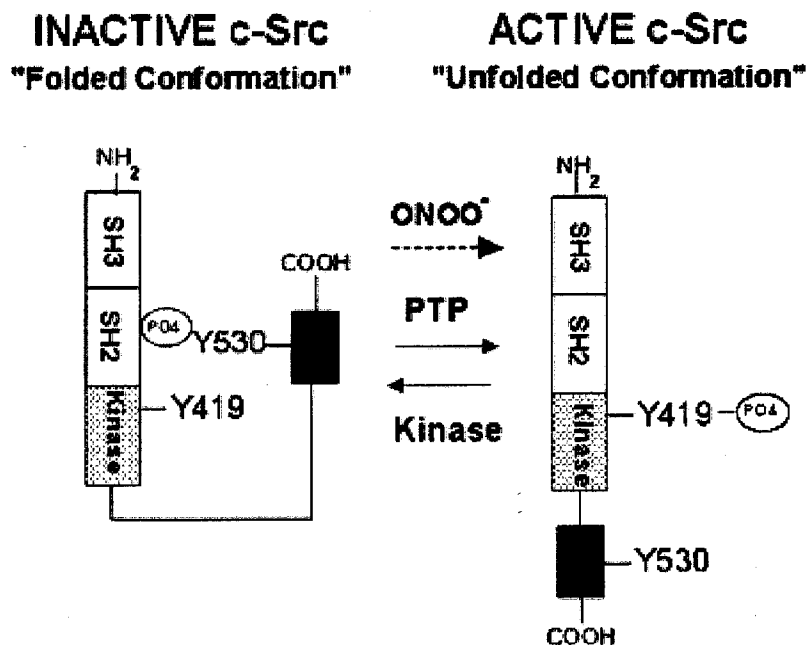


Fig. 6. Schematic showing c-Src kinase (human) activation pathway. Dephosphorylation of the carboxy-terminal tyrosine residue (Y530) by a protein tyrosine phosphatase (PTP) results in a conformational change to the "unfolded" active c-Src. Tyrosine phosphorylation of Y530 by a kinase leads to the "folded" inactive conformation of c-Src, presumably through the interaction with the c-Src SH2 domain. The dotted arrow indicates the possibility that ONOO⁻ treatment could also lead to activation of c-Src through an unknown mechanism. Tyrosine 419 (Y419) represents the major autophosphorylation site.

either human pancreatic cancer tissue or ONOO⁻-treated HPAC cells with the monoclonal anti-Src antibody (clone 327), whose recognition epitope lies within the Src SH3 domain, fails to precipitate tyrosine nitrated c-Src, but efficiently precipitates non-nitrated c-Src (unpublished observations). Because of the complexity of pathways resulting in activation of c-Src (as described above) the potential effects of tyrosine nitration on c-Src activity are equally complex.

Several recent reports have depicted how ONOO⁻ can alter signal transduction processes. For example, ONOO⁻ treatment of a neuroblastoma cell line (SH-SY5Y) resulted in inhibition of phosphoinositide signaling and transiently increased tyrosine phosphorylation of the p120 c-Src substrate, while decreasing the phosphorylation of paxillin and focal adhesion kinase [32]. Using the same cell line Saeki et al. showed that 3-morpholinosydnonimine (SIN-1, a ONOO⁻ generator) induced tyrosine nitration of another c-Src substrate, p130^{cas}, which prevented its ability to be phosphorylated [31]. Likewise, ONOO⁻ treatment of rat liver epithelial cells resulted in differential activation of mitogen activated protein kinases [33]. A recent report by Di Stasi et al. demonstrated that ONOO⁻ treatment of bovine synaptic proteins increased c-Src tyrosine phosphorylation and activity [34], a result similar to our present findings. Even though tyrosine nitration may inhibit phosphorylation of that tyrosine, it remains possible that a protein containing multiple tyrosine residues (e.g., c-Src) could also contain both tyrosine-phosphorylated and tyrosine-nitrated residues.

Results presented here show that the c-Src is both tyrosine-nitrated and -phosphorylated during human pancreatic ductal adenocarcinoma. ONOO⁻-mediated tyrosine modifications resulting in increased c-Src activity may lead to rapid and

uncontrolled cell growth/transformation, a process that may be similar to the constitutively active mutant of c-Src where the regulatory tyrosine residue (Y530) has been mutated to phenylalanine [35-37]. Therefore, we suggest that tyrosine nitration may be an important modification in the regulation of c-Src and may play a significant role in the enhanced cellular growth observed in pancreatic cancer.

ACKNOWLEDGMENTS

This work was supported by a Scientist Development Grant from the American Heart Association (LAMC), a grant from the Robert Wood Johnston Association (SMV), and grants from the National Institutes of Health (HL45990 and DK51629, JAT). We would like to thank Dr. John Crow and Mr. Evan McWhorter for the work involving the HPLC-EC measurements of nitrotyrosine, and Dr. Joe Beckman (UAB) for the monoclonal anti-nitrotyrosine antibody.

REFERENCES

- [1] V.N. Verovski, D.L. Van den Berge, G.A. Soete, B.L. Bols, G.A. Storme, *Br. J. Cancer* 74 (1996) 1734-1742.
- [2] M.P. Lutz, I.B.S. Esser, B.B.M. Flossmannkast, R. Vogelmann, H. Luhrs, H. Friess, M.W. Buchler, G. Adler, *Biochem. Biophys. Res. Commun.* 243 (1998) 503-508.
- [3] J. Su, M. Muranjan, J. Sap, *Curr. Biol.* 9 (1999) 505-511.
- [4] A.K. Somani, J.S. Bignon, G.B. Mills, K.A. Siminovitch, D.R. Branch, *J. Biol. Chem.* 272 (1997) 21113-21119.
- [5] S.M. Thomas, J.S. Brugge, *Annu. Rev. Cell. Dev. Biol.* 13 (1997) 513-609.
- [6] X. Zhan, C. Plourde, X. Hu, R. Friesel, T. Maciag, *J. Biol. Chem.* 269 (1994) 20221-20224.

- [7] V.G. Brunton, B.W. Ozanne, C. Paraskeva, M.C. Frame, *Oncogene* 14 (1997) 283-293.
- [8] M.A. Broome, T. Hunter, *J. Biol. Chem.* 271 (1996) 16798-16806.
- [9] D.R. Stover, P. Furet, N.B. Lydon, *J. Biol. Chem.* 271 (1996) 12481-12487.
- [10] R.E. Huie, S. Padmaja, *Free Radical Res. Comm.* 18 (1993) 195-199.
- [11] S. Ambs, W.G. Merriam, W.P. Bennett, E. Felley-Bosco, M.O. Ogunfusika, S.M. Oser, S. Klein, P.G. Shields, T.R. Billiar, C.C. Harris, *Cancer Res.* 58 (1998) 334-341.
- [12] M. Kojima, T. Morisaki, Y. Tsukahara, A. Uchiyama, Y. Matsunari, R. Mibu, M.J. Tanaka, *J. Surg. Oncol.* 70 (1999) 222-229.
- [13] S.M. Vickers, L.A. MacMillan-Crow, M. Green, C. Ellis, J.A. Thompson, *Arch. Surg.* 134 (1999) 245-251.
- [14] L.A. MacMillan-Crow, J.P. Crow, J.D. Kerby, J.S. Beckman, J.A. Thompson, *Proc. Natl. Acad. Sci. USA* 93 (1996) 11853-11858.
- [15] J.P. Crow, Y.Z. Ye, M. Strong, M. Kirk, S. Barnes, J.S. Beckman, *J. Neurochem.* 69 (1997) 1945-1953.
- [16] R.I. Viner, D.A. Ferrington, T.D. Williams, D.J. Bigelow, C. Schoneich, *Biochem. J.* 340 (1999) 657-669.
- [17] M. Zou, C. Martin, V. Ullrich, *Biol. Chem.* 378 (1997) 707-713.
- [18] D. Trotti, D. Rossi, O. Gjesdal, L.M. Levy, G. Racagni, N.C. Danbolt, A. Volterra, *J. Biol. Chem.* 271 (1996) 5976-5979.
- [19] J. Ara, S. Przedborski, A.B. Naini, V. Jackson-Lewis, R.R. Trifiletti, J. Horwita, H. Ischiropoulos, *Proc. Natl. Acad. Sci. USA* 95 (1998) 7659-7663.
- [20] L.A. MacMillan-Crow, J.P. Crow, J.A. Thompson, *Biochemistry* 37 (1998) 1613-1622.
- [21] J.P. Crow, J.S. Beckman, J.M. McCord, *Biochemistry* 34 (1995) 3544-3552.
- [22] J.P. Crow, *Methods Enzymol.* 301 (1999) 151-160.
- [23] J.P. Eiserich, C.E. Cross, A.D. Jones, B. Halliwell, A. van der Vliet, *J. Biol. Chem.* 271 (1996) 19199-19208.

- [24] H. Sabe, A. Hata, M. Okada, H. Nakagawa, H. Hanafusa, *Proc. Natl. Acad. Sci. USA* 91 (1994) 3984-3988.
- [25] S.M. Murphy, M. Bergman, D.O. Morgan, *Mol. Cell. Biol.* 13 (1993) 5290-5300.
- [26] B.S. Cobb, J.T. Parsons, *Oncogene* 8 (1993) 2897-2903.
- [27] J.W. Thomas, B. Ellis, R. J. Boerner, W.B. Knight, G.C. White 2., M. D. Schaller, *J. Biol. Chem.* 273 (1998) 577-583.
- [28] X. Liu, T. Pawson, *Rec. Prog. Horm. Res.* 49 (1994) 149-160.
- [29] S.K. Kong, M.B. Yim, E.R. Stadtman, P.B. Chock, *Proc. Natl. Acad. Sci. USA* 93 (1996) 3377-3382.
- [30] A.J. Gow, D. Duran, S. Malcolm, H. Ischiropoulos, *FEBS Lett* 385 (1996) 63-66.
- [31] M. Saeki, S. Maeda, *Neurosci. Res.* 33 (1999) 325-328.
- [32] X. Li, P. De Sarno, L. Song, J.S. Beckman, R.S. Jope, *Biochem. J.* 331 (1998) 599-606.
- [33] S.M. Schieke, K. Briviba, L.O. Klotz, H. Sies, *FEBS Lett* 448 (1999) 301-303.
- [34] A.M. Di Stasi, C. Mallozzi, G. Macchia, T.C. Petrucci, M. Minetti, *J. Neurochem.* 73 (1999) 727-735.
- [35] R. Ferracini, J. Brugge, *Oncogene Res.* 5 (1990) 205-219.
- [36] C.A. Cartwright, W. Eckhart, S. Simon, P.L. Kaplan, *Cell* 49 (1987) 83-91.
- [37] R.R. Roussel, S.R. Brodeur, D. Shalloway, A.P. Laudano, *Proc. Natl. Acad. Sci. USA* 88 (1991) 10696-10700.

CONCLUSIONS

Determining the signal transduction pathways initiating mitogenesis, migration, and cell survival are critical for understanding the regulation of tumorigenesis, inflammation, and angiogenesis during the progression of pancreatic adenocarcinoma. The studies presented in this dissertation were designed to test the hypothesis that FGFR-1 α and FGFR-1 β differentially signal SFK following stimulation with FGF-1. This hypothesis was based on the following observations: (i) *in vitro*, cells expressing FGFR-1 isoforms in ratios favoring the expression of FGFR-1 α or FGFR-1 β demonstrate enhancement or protection, respectively, towards cytotoxicity induced by reactive nitrogen and oxygen species; (ii) both ligand-activated FGFR-1 and reactive nitrogen species activate Src family kinases; (iii) the signaling interaction between SFK and FGFR-1 or reactive nitrogen species was incompletely understood; (iv) pancreatic adenocarcinomas express FGFR-1 β as the major FGFR-1 isoform; (v) pancreatic adenocarcinomas overexpress FGF-1, suggesting continuous signaling *in vivo*; (vi) pancreatic adenocarcinomas demonstrate increased SFK activity; and (vii) pancreatic adenocarcinoma tissue contains nitrotyrosine, a marker of reactive nitrogen species.

The first step was to establish and characterize a cell line in which signaling induced by FGFR-1 α or FGFR-1 β could be specifically dissected. As a collaboration with Jing Jiao in the Department of Biochemistry and Molecular Genetics at the University of Alabama at Birmingham, FGFR-negative resistance vessel endothelial cells (RVEC) were transfected with cDNAs encoding control vector (pMN), FGFR-1 α (R-

1 α), or FGFR-1 β (R-1 β) and assessed for FGFR-1 expression (RT-PCR and Western analysis), FGF-1 ligand binding (Scatchard analysis), and FGFR-1 isoform functionality (growth behavior).

To determine if FGFR-1 isoform-specific signaling would modulate cytotoxicity induced by reactive nitrogen species, pMN, R-1 α , and R-1 β cells were treated with ONOO⁻, a reactive nitrogen species used as an experimental reagent for these studies. ONOO⁻ induced a delayed cell death that was more characteristic of apoptosis than necrosis [138]. ONOO⁻-induced cytotoxicity was enhanced in cells expressing activated FGFR-1 α and decreased in cells expressing activated FGFR-1 β . This protective effect was dependent in part on SFK, linking SFK to the FGFR-1 β pathway. These observations are consistent with the observation that pancreatic adenocarcinomas, which are resistant to cytotoxic insult, predominantly express FGFR-1 β [21].

To correlate these endothelial cell studies more directly with pancreatic cancer, ARIP cells expressing altered ratios of FGFR-1 isoforms were developed during a collaboration with Dr. Selwyn Vickers, Department of Surgery, the University of Alabama at Birmingham. ARIP cells are derived from a Wistar rat pancreatic tumor in athymic mice [159]. These cells predominantly express FGFR-1 β (J. A. Thompson, personal communication), but do not form tumors unless they receive a continuous delivery of FGF-1 [105]. ARIP cells were stably transfected with FGFR-1 α , FGFR-1 β , or control vector. Continuous delivery of FGF-1 to ARIP expressing FGFR-1 β resulted in tumor formation in athymic mouse xenografts; however, ARIP expressing FGFR-1 α did not form tumors [160]. In addition, FGF-1-activated ARIP cells expressing FGFR-1 α were susceptible to ONOO⁻-induced cell death (Fig. 1). Clinically, pancreatic

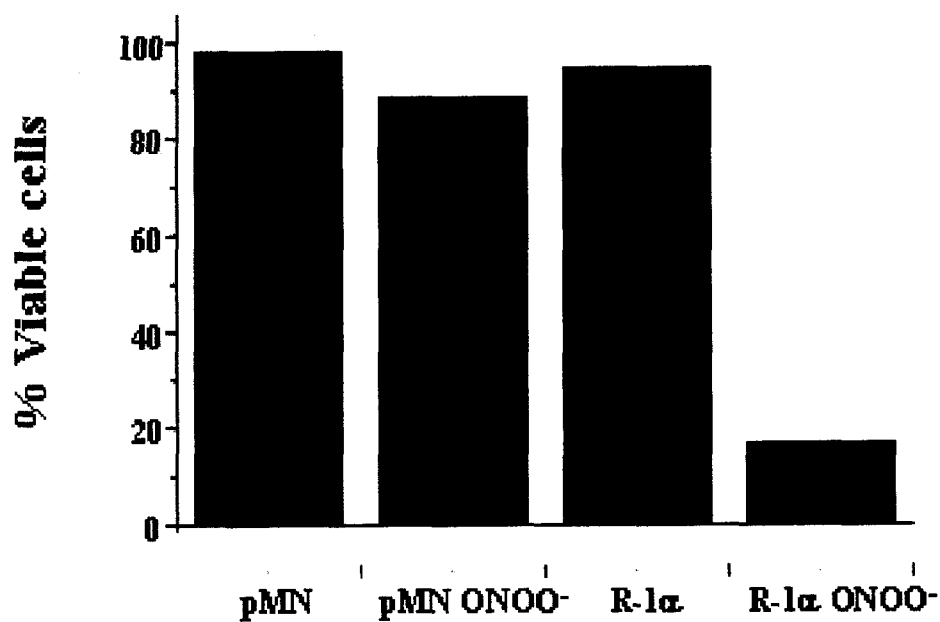


Fig. 1. Viability of ONOO⁻-treated ARIP cells. ARIP cells, which predominantly express FGFR-1 β , were transfected with control vector (pMN) or vector encoding FGFR-1 α (R-1 α). Cells were given continuous delivery of FGF-1 and examined for viability (24 h) following ONOO⁻ (150 μ M).

adenocarcinomas are extremely resistant to therapeutic radiation [3]. External beam radiation, which results in the generation of reactive nitrogen species and tyrosine nitration [161], is cytotoxic to FGF-1-activated ARIP cells expressing FGFR-1 α , while FGF-1-activated ARIP cells expressing FGFR-1 β are protected (Fig. 2). These preliminary findings suggest that altering the ratio of FGFR-1 in pancreatic cells can affect growth and survival. FGFR-1 α and FGFR-1 β differ solely in the extracellular domain, an area that may be accessible for drug therapies targeting the β isoform.

To further explore the specific interaction between FGFR-1 β and SFK, the RVEC cells were used. Despite sharing identical intracellular domains, FGFR-1 α and FGFR-1 β differentially signaled the SFK c-Yes in FGF-1-treated RVEC. FGF-1-activated FGFR-1 β demonstrated increased association with the SFK c-Yes, increased c-Yes tyrosine phosphorylation within the tyrosine kinase domain, and increased c-Yes signaling to the cytoskeletal protein cortactin. Cells expressing FGFR-1 β also formed vascular cords in vivo and c-Yes dependent cords in vitro. The finding that FGFR-1 β -specific signaling to SFK alters cytoskeletal structure may have important consequences for understanding both vascular remodeling and the ability of a tumor cell expressing FGFR-1 β to migrate and metastasize. Important future studies will further define the signaling pathway between FGFR-1 β and SFK and will explore the downstream pathways initiated by FGFR-1 α (III. 1).

Studies presented in this dissertation tested the hypothesis that ligand-activated FGFR-1 α and FGFR-1 β differentially signal SFK. The last chapter explores the role of inflammatory reactive nitrogen species in modulating signaling to SFK in pancreatic

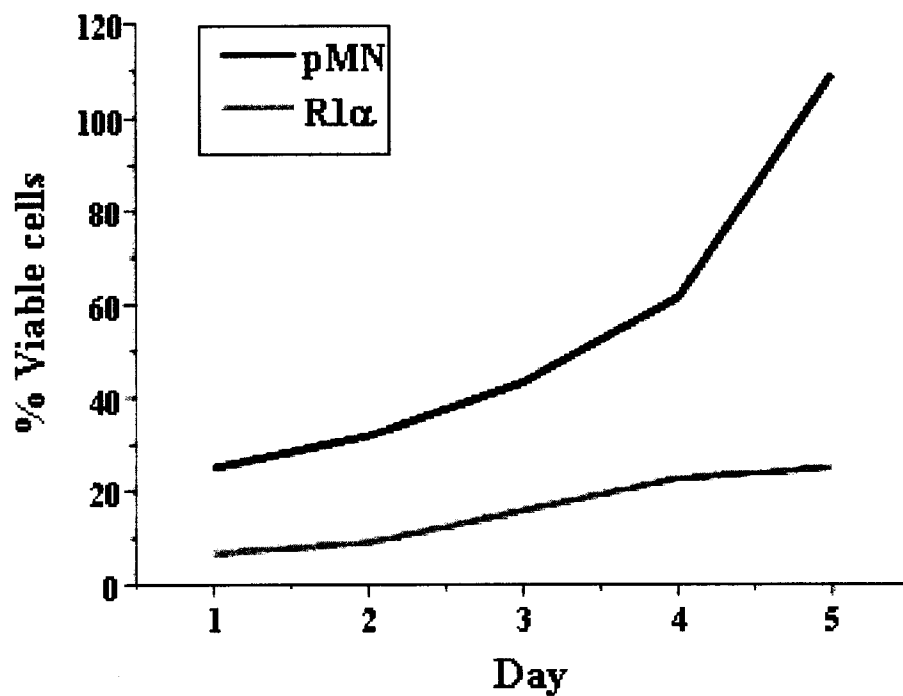
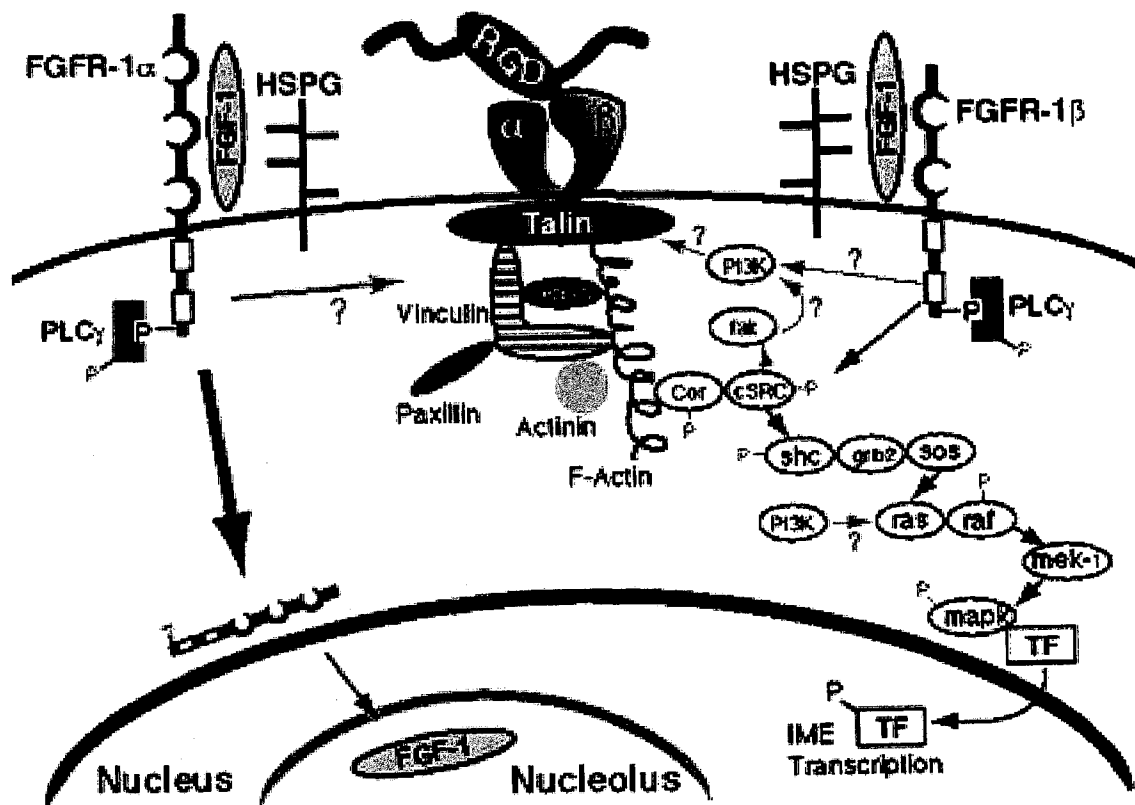
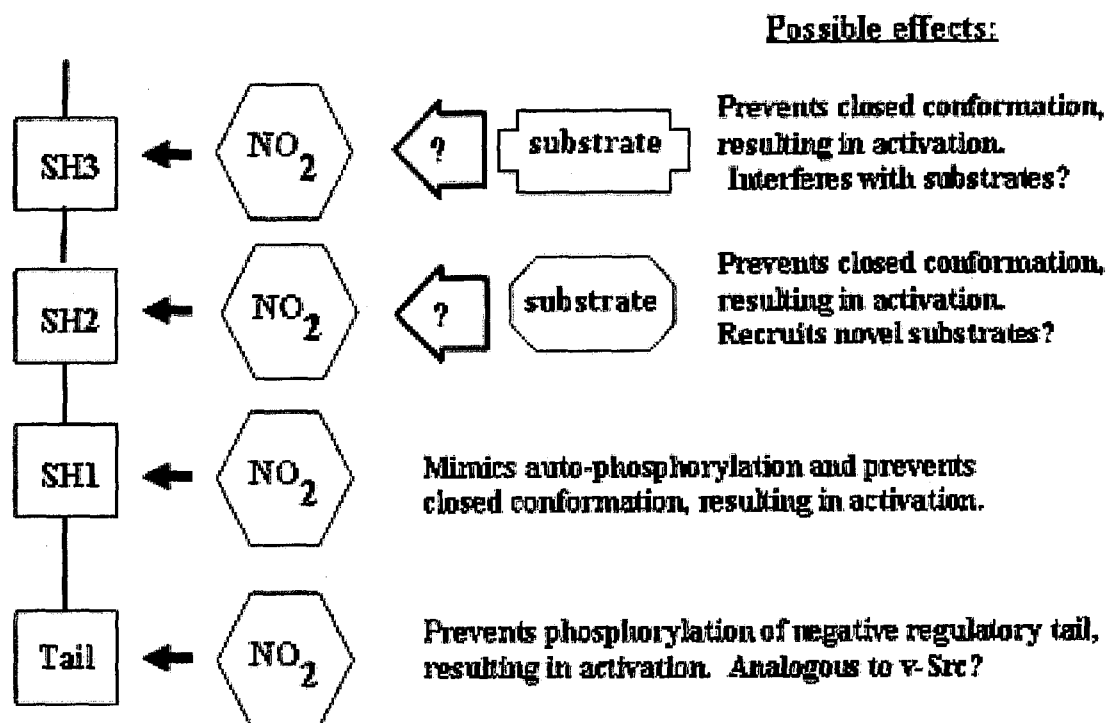


Fig. 2. Viability of irradiated ARIP. ARIP cells, which predominantly express FGFR-1 β , were transfected with control vector (pMN) or vector encoding FGFR-1 α (R-1 α). Cells were given continuous delivery of FGF-1 and examined for viability (24 h) following external beam radiation (8 Gray).



III. 1. Possible signaling pathways induced by FGFR-1 α or FGFR-1 β following FGF-1 stimulation.

adenocarcinomas, which predominantly express FGFR-1 β and are resistant to cytotoxicity induced by reactive nitrogen species. These studies were a continued collaboration with Dr. Vickers. Pancreatic adenocarcinomas were found to contain nitrotyrosine, a marker of reactive nitrogen species. c-Src was identified as a specific target for tyrosine nitration in human pancreatic adenocarcinoma tissue. Pancreatic adenocarcinoma cells treated with the reactive nitrogen species ONOO⁻ in vitro demonstrated tyrosine nitrated c-Src, increased c-Src tyrosine phosphorylation, increased c-Src activity, and increased c-Src signaling. c-Src is regulated by tyrosine modifications, therefore the stable addition of a NO₂ group to the phenolic ring of tyrosine has the potential to dramatically affect c-Src (Ill. 2). Tyrosine nitration has been shown to block subsequent phosphorylation at that residue [115], therefore nitration of pro-activating tyrosines could have an attenuating effect. However, results presented here imply that ONOO⁻ treatment of pancreatic adenocarcinoma cells activates c-Src kinase. If Y530 were a target for nitration and if phosphorylation at this regulatory site were blocked, c-Src could be constitutively activated. Obviously, the constitutive activation of a proto-oncogenic protein would promote cell transformation and tumorigenesis. Alternatively, by providing an area of similar electron density, tyrosine nitration could mimic a phosphotyrosine. Nitration of Y419, therefore, could have an activating effect. Tyrosine nitration within the SH2 or SH3 protein-binding domains could serve as a novel protein recognition motif for recruitment of substrates or could block substrate access to the modified domain, promoting interactions with the unaffected domain. In addition, tyrosine nitration within the SH2 or SH3 domains could electrostatically repel the regulatory tail, resulting in activation.



III. 2. Potential effects of tyrosine nitration within SFK domains.

Determining c-Src tyrosines targeted for nitration will be an important future study. Preliminary results suggest that ONOO⁻ treatment of pancreatic adenocarcinoma cells resulted in a loss of c-Src recognition by an anti-Src monoclonal antibody (clone 327). This strongly implicates the c-Src SH3 domain, the site of the antibody epitope, as a potential target for ONOO⁻-induced tyrosine modifications. The human c-Src SH3 domain contains 4 tyrosines (Y93, Y95, Y134, Y139) [162]. Interestingly, a second anti-Src monoclonal antibody (GD11) with a SH3 epitope also fails to recognize c-Src in ONOO⁻-treated HPAC cells. This antibody epitope spans v-Src residues 92-128 [163] and suggests that c-Src Y93 and/or Y95 are the most likely nitration targets. The hypothesized effects of nitration within this domain are activation of c-Src, interference with the c-Src SH3 domain, and increased binding of substrates to the c-Src SH2 domain. Increased association with phosphotyrosyl substrates was observed following ONOO⁻ treatment, suggesting enhanced c-Src interactions at the SH2 domain.

c-Src can exist in a number of phosphorylation states due to the different modes of activation; therefore, key tyrosines may or may not be available as targets for reactive nitrogen species. Signaling to SFK was examined in FGFR-negative RVEC and RVEC stably transfected with FGFR-1 α or FGFR-1 β . Following FGF-1/heparin treatment (10 min), the SFK c-Yes demonstrated increased tyrosine phosphorylation within the kinase domain in RVEC expressing FGFR-1 β , the major FGFR-1 isoform in pancreatic adenocarcinoma. Phosphorylation of this residue would most likely exclude it from nitration by reactive nitrogen species. The RVEC model is ideal for future studies to specifically dissect SFK signaling and examine the effects of tyrosine modifications induced by reactive nitrogen species on inactive and FGFR-1 β -activated SFK.

Studies presented in this dissertation investigated: (i) the role of FGFR-1 β -specific signaling to SFK in modulating cytotoxicity induced by reactive nitrogen species, including the reactive nitrogen species ONOO⁻, (ii) the signaling interaction between SFK and activated FGFR-1 α or FGFR-1 β , and (iii) the result of signaling by FGFR-1 β and reactive nitrogen species in modulating SFK tyrosine modifications and activity in pancreatic adenocarcinoma tissue (Ill. 3). In summary, these studies have provided insight into signal transduction cascades induced by FGFR-1 β that are critical to regulating tumorigenesis, inflammation, and angiogenesis.

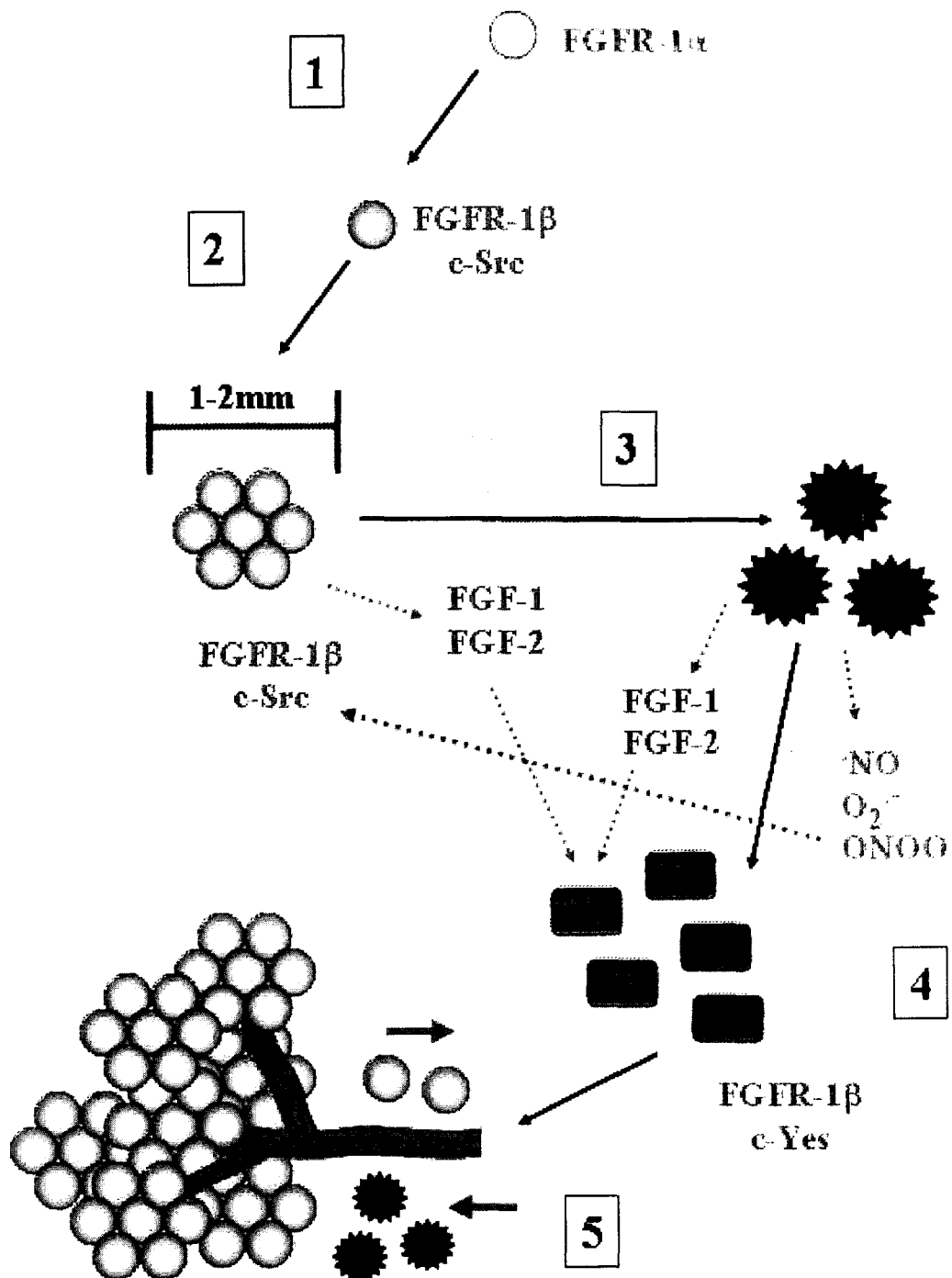


Fig. 5. Possible roles of FGFR-1 β and SFK during pancreatic tumorigenesis, inflammation, and angiogenesis. (1) Transformed pancreatic ductal epithelial cells undergo alternative splicing from FGFR-1 α to FGFR-1 β . (2) Growing tumor reaches 1-2 mm and becomes hypoxic. (3) Hypoxia recruits inflammatory cells that release FGF ligands and reactive nitrogen and oxygen species that can activate SFK. (4) FGF ligands recruit endothelial cells that signal SFK through FGFR-1 β and induce angiogenesis. (5) Angiogenesis supports tumor, allows further inflammatory infiltration, and allows metastasis of cancer cells.

LIST OF GENERAL REFERENCES

- [1] G.H. Sakorafas, A.G. Tsiotou, G.G. Tsiotos, *Cancer Treat. Rev.* 26 (2000) 29-52.
- [2] H.G. Hotz, O.J. Hines, T. Foitzik, H.A. Reber, *Int. J. Colorectal Dis.* 15 (2000) 136-143.
- [3] T.J. Howard, *Curr. Probl. Cancer* 20 (1996) 283-328.
- [4] R.M. Case, B.E. Argent, in: V.L.W. Go (Ed.), *The Exocrine Pancreas*, Raven Press, New York, 1986, pp. 213-244.
- [5] H.F. Kern, in: V.L.W. Go (Ed.), *The Exocrine Pancreas*, Raven Press, New York, 1986, pp. 9-20.
- [6] H. Rinderknecht, in: V.L.W. Go (Ed.), *The Exocrine Pancreas*, Raven Press, New York, 1986, pp.163-184.
- [7] M. Egerbacher, P. Bock, *Microscopy Research and Technique* 37 (1997) 407-417.
- [8] Q. Shi, K. Xie, *Int. J. Oncol.* 17 (2000) 217-225.
- [9] A.W. Griffioen, G. Molema, *Pharmacol. Rev.* 52 (2000) 237-268.
- [10] M. Crowther, N.J. Brown, E.T. Bishop, C.E. Lewis, *J. of Leukocyte Biol.* 70 (2001) 478-490.
- [11] J.R. Jackson, M.P. Seed, C.H. Kircher, D.A. Willoughby, J.D. Winkler, *FASEB J.* 11 (1997) 457-465.
- [12] G.W. Sullivan, I.J. Sarembock, J. Linden, *J. Leukocyte Biol.* 67 (2000)-591-602.
- [13] K.J. O'Byrne, A.G. Dalglish, *Br. J. Cancer* 85 (2001) 473-483.
- [14] V.M. Byrd, D.W. Ballard, G.G. Miller, J.W. Thomas, *J. Immunol.* 162 (1999) 5853-5859.
- [15] J.D. Kerby, D.J. Verran, K.L. Luo, Q. Ding, Y. Tagouri, G.A. Herrera, A.G. Diethelm, J.A. Thompson, *Transplantation* 62 (1996) 190-200.

- [16] J.D. Kerby, D.J. Verran, K.L. Luo, Q. Ding, Y. Tagouri, G.A. Herrera, A.G. Diethelm, J.A. Thompson, *Transplantation* 62 (1996) 467-475.
- [17] S.E. Hughes, *Cardiovasc. Res.* 32 (1996) 557-569.
- [18] L.A. Chandler, B.A. Sosnowski, L. Greenlees, S.L. Aukerman, A. Baird, G.F. Pierce, *Int. J. Cancer* 81 (1999) 451-458.
- [19] F. Ozawa, H. Friess, A. Tempia-Caliera, J. Kleeff, M.W. Buchler, *Teratog. Carcinog. Mutagen.* 21 (2001) 27-44.
- [20] M.P. Lutz, I.B.S. Eber, B.B.M. Flossmann-Kast, R. Vogelmann, H. Luhrs, H. Friess, M.W. Buchker, G. Adler, *Biochem. Biophys. Res. Comm.* 243 (1998) 503-508.
- [21] M.S. Kobrin, Y. Yamanaka, H. Friess, M.E. Lopez, M. Korc, *Cancer Res.* 53 (1993) 4741-4744.
- [22] M. Ford-Perriss, H. Abud, M. Murphy, *Clin. Exp. Pharm. Physiol.* 28 (2001) 493-503.
- [23] C.J. Powers, S.W. McLeskey, A. Wellstein, *Endocr. Relat. Cancer* 7 (2000) 165-197.
- [24] M.S.F. Clarke, R.W. Caldwell, H. Chiao, K. Miyake, P.L. McNeil, *Circ. Res.* 76 (1995) 927-934.
- [25] A. Jackson, S. Friedman, X. Zhan, K.A. Engleka, R. Forough, T. Maciag, *Proc. Natl. Acad. Sci. USA* 89 (1992) 10691-10695.
- [26] S.R. Opalenik, Q. Ding, S.R. Mallery, J.A. Thompson, *Arch. Biochem. Biophys.* 351 (1998) 17-26.
- [27] C. Mouta Carreira, M. Landriscina, S. Bellum, I. Prudovsky, T. Maciag, *Growth Factors* 18 (2001) 277-285.
- [28] J.T. Shin, S.R. Opalenik, J.N. Wehby, V.K. Mahesh, A. Jackson, F. Tarantini, T. Maciag, J.A. Thompson, *Biochim. Biophys. Acta* 1312 (1996) 27-38.
- [29] C. Mouta Carreira, T.M. LaVallee, F. Tarantini, A. Jackson, J.T. Lathrop, B. Hampton, W.H. Burgess, T. Maciag, *J. Biol. Chem.* 273 (1998) 22224-22231.
- [30] T.M. LaVallee, I.A. Prudovsky, G.A. McMahon, X. Hu, T. Maciag, *J. Cell Biol.* 141 (1998) 1647-1658.
- [31] S. Klein, M. Roghani, D.B. Rifkin, *EXS* 79 (1997) 159-92.

- [32] T. Spivak-Kroizman, M.A. Lemmon, I. Dikic, J.E. Ladbury, D. Pinchasi, J. Huang, M. Jaye, G. Crumley, J. Schlessinger, I. Lax, *Cell* 79 (1994) 1015-1024.
- [33] Y. Luo, J.L. Gabriel, F. Wang, X. Zhan, T. Maciag, M. Jan, W.L. McKeehan, J. Biol. Chem. 271 (1996) 26876-26883.
- [34] D.M. Ornitz, J. Xu, J.S. Colvin, D.G. McEwen, C.A. MacArthur, F. Coulier, G. Gao, M. Goldfarb, *J. Biol. Chem.* 271 (1996) 15292-15297.
- [35] G. Szebenyi, J.F. Fallon, *Int. Rev. Cytology* 185 (1999) 45-106.
- [36] D.E. Johnson, L.T. Williams, *Adv. Cancer Res.* 60 (1993) 1-41.
- [37] J.X. Yan, N.H. Packer, A.A. Gooley, K.L. Williams, *J. Chromatography A* 808 (1998) 23-41.
- [38] P. Klint, L. Claesson-Welsh, *Front. Biosci.* 4 (1999) d165-177.
- [39] P.A. Maher, *J. Cell Biol.* 134 (1996) 529-536.
- [40] I.A. Prudovsky, N. Savion, T.M. LaVallee, T. Maciag, *J. Biol. Chem.* 271 (1996) 14198-14205.
- [41] H. Beer, L. Vindevoghel, M.J. Gait, J. Revest, D.R. Duan, I. Mason, C. Dickson, S. Werner, *J. Biol. Chem.* 275 (2000) 16091-16097.
- [42] M. Mohammadi, I. Dikic, A. Sorokin, W.H. Burgess, M. Jaye, J. Schlessinger, *Mol. Cell. Biol.* 16 (1996) 977-989.
- [43] J. Xu, M. Nakahara, J.W. Crabb, E. Shi, Y. Matuo, M. Fraser, M. Kan, J. Hou, W.L. McKeehan, *J. Biol. Chem.* 267 (1992) 17792-17803.
- [44] M. Kornmann, M.E. Lopez, H.G. Beger, M. Korc, *Int. J. Pancreatol.* 29 (2001) 85-92.
- [45] F. Wang, M. Kan, G. Yan, J. Xu, W.L. McKeehan, *J. Biol. Chem.* 270 (1995) 10231-10235.
- [46] E. Shi, M. Kan, J. Xu, F. Wang, J. Hou, W.L. McKeehan, *Mol. Cell. Biol.* 13 (1993) 3907-3918.
- [47] G.E. Plopper, H.P. McNamee, L.E. Dike, K. Bojanowski, D.E. Ingber, *Mol. Biol. Cell* 6 (1995) 1349-1365.
- [48] X. Zhan, X. Hu, R. Friesel, T. Maciag, *J. Biol. Chem.* 268 (1993) 9611-9620.

- [49] E. Shaoul, R. Reich-Slotky, B. Berman, D. Ron, *Oncogene* 10 (1995) 1553-1561.
- [50] H. Larsson, P. Klint, E. Landgren, L. Claesson-Welsh, *J. Biol. Chem.* 274 (1999) 25726-25734.
- [51] X. Zhan, X. Hu, B. Hampton, W.H. Burgess, R. Friedel, T. Maciag, *J. Biol. Chem.* 268 (1993) 24427-24431.
- [52] J.F. Reilly, G. Mickey, P.A. Maher, *J. Biol. Chem.* 275 (2000) 7771-7778.
- [53] H. Xu, K.W. Lee, M. Goldfarb, *J. Biol. Chem.* 273 (1998) 17987-17990.
- [54] A. Yayon, Y. Ma, M. Safran, M. Klagsbrun, R. Halaban, *Oncogene* 14 (1997) 2999-3009.
- [55] P. Klint, S. Kanda, Y. Kloog, L. Claesson-Welsh, *Oncogene* 18 (1999) 3354-3364.
- [56] N.E. Kremer, G. D'Arcangelo, S.M. Thomas, M. DeMarco, J.S. Brugge, S. Halegoua, *J. Cell Biol.* 115 (1991) 809-819.
- [57] X. Zhan, C. Plourde, X. Hu, R. Friesel, T. Maciag, *J. Biol. Chem.* 269 (1994) 20221-20224.
- [58] E. Landgren, P. Blume-Jensen, S.A. Courtneidge, L. Claesson-Welsh, *Oncogene* 10 (1995) 2027-2035.
- [59] K.A. DeMali, S.L. Godwin, S.P. Soltoff, A. Kazlauskas, *Exp. Cell Res.* 253 (1999) 271-279.
- [60] R.J. Jones, V.G. Brunton, M.C. Frame, *Eur. J. Cancer* 36 (2000) 1595-1606.
- [61] Z. Korade-Mirnic, S.J. Corey, *J. Leukoc. Biol.* 68 (2000) 603-613.
- [62] C.L. Abram, S.A. Courtneidge, *Exp. Cell Res.* 254 (2000) 1-13.
- [63] A.G. Tatosyan, O.A. Mizenina, *Biochemistry (Moscow)* 65 (2000) 49-58.
- [64] C.A. Lowell, P. Soriano, *Genes Dev.* 10 (1996) 1845-1857.
- [65] P.L. Stein, H. Vogel, P. Soriano, *Genes Dev.* 8 (1994) 1999-2007.
- [66] D. Coppola, *Cancer Control* 7 (2000) 421-427.
- [67] N.M. Han, S.A. Curley, G.E. Gallick, *Clin. Canc. Res.* 2 (1996) 1397-1404.

- [68] F. Loganzo, Jr, J.S. Dosik, Y. Zhao, M.J. Vidal, D.M. Nanus, M. Sudol, A.P. Albino, *Oncogene* 8 (1993) 2637-2644.
- [69] M. Pu, A.A. Akhand, M. Kato, M. Hamaguchi, T. Koike, H. Iwata, H. Sabe, H. Suzuki, I. Nakashima, *Oncogene* 13 (1996) 2615-2622.
- [70] J.D. Bjorge, T.J. O'Connor, D.J. Fujita, *Biochem. Cell Biol.* 74 (1996) 477-484.
- [71] W. Xu, S.C. Harrison, M.J. Eck, *Nature* 385 (1997) 595-602.
- [72] T.E. Kmiecik, D. Shalloway, *Cell* 49 (1987) 65-73.
- [73] H. Okamura, M.D. Resh, *Oncogene* 9 (1994) 2293-2303.
- [74] A. Somani, J.S. Bignon, G.B. Mills, K.A. Siminovitch, D.R. Branch, *J. Biol. Chem.* 272 (1997) 21113-21119.
- [75] X. Zheng, R.J. Resnick, D. Shalloway, *EMBO J.* 19 (2000) 964-978.
- [76] M. Sudol, *Oncogene* 17 (1998) 1469-1474.
- [77] R.J. Sicilia, M.L. Hibbs, P.A. Bello, J.D. Bjorge, D.J. Fujita, I.J. Stanley, A.R. Dunn, H. Cheng, *J. Biol. Chem.* 273 (1998) 16756-16763.
- [78] A.B. Sparks, J.E. Rider, N.G. Hoffman, D.M. Fowlkes, L.A. Quilliam, B.K. Kay, *Proc. Natl. Acad. Sci. USA* 93 (1996) 1540-1544.
- [79] M.T. Brown, J.A. Cooper, *Biochim. Biophys. Acta* 1287 (1996) 121-149.
- [80] H. Okamura, M.D. Resh, *J. Biol. Chem.* 270 (1995) 26613-26618.
- [81] Z. Shen, A. Batzer, J.A. Koehler, P. Polakis, J. Schlessinger, N.B. Lydon, M.F. Moran, *Oncogene* 18 (1999) 4647-4653.
- [82] Z. Weng, J.A. Taylor, C.E. Turner, J.S. Brugge, C. Seidel-Dugan, *J. Biol. Chem.* 268 (1993) 14956-14963.
- [83] M. Sudol, *Oncogene* 9 (1994) 2145-2152.
- [84] J.W. Thomas, B. Ellis, R.J. Boerner, W.B. Knight, G.C. White II, M.D. Schaller, *J. Biol. Chem.* 273 (1998) 577-583.
- [85] D.C. Flynn, T.H. Leu, A.B. Reynolds, J.T. Parsons, *Mol. Cell. Biol.* 13 (1993) 7892-7900.
- [86] E.C. Lerner, T.E. Smithgall, *Nat. Struct. Biol.* 9 (2002) 365-369.

- [87] D.R. Stover, P. Furet, N.B. Lydon, *J. Biol. Chem.* 271 (1996) 12481-12487.
- [88] M.A. Broome, T. Hunter, *Oncogene* 14 (1997) 17-34.
- [89] S.J. Taylor, D. Shalloway, *Bioessays* 18 (1996) 9-11.
- [90] G. Sun, A.K. Sharma, R.J.A. Budde, *Oncogene* 17 (1998) 1587-1595.
- [91] K.B. Kaplan, K.B. Bibbins, J.R. Swedlow, M. Arnaud, D.O. Morgan, H.E. Varmus, *EMBO J.* 13 (1994) 4745-4756.
- [92] T. Volberg, L. Romer, E. Zamir, B. Geiger, *J. Cell Sci.* 114 (2001) 2279-2289.
- [93] Y. Zhao, H. Uyttendaele, J.G. Krueger, M. Sudol, H. Hanafusa, *Mol. Cell. Biol.* 13 (1993) 7507-7514.
- [94] M. Ariki, O. Tanabe, H. Usui, H. Hayashi, R. Inoue, Y. Nishito, H. Kagamiyama, M. Takeda, *J. Biochem.* 121 (1997) 104-111.
- [95] M. Susa, N. Luong-Nguyen, J. Crespo, R. Maier, M. Missbach, G. McMaster, *Protein Expr. Purif.* 19 (2000) 99-106.
- [96] H. Tang, Z.J. Zhao, E.J. Landon, T. Inagami, *J. Biol. Chem.* 275 (2000) 8389-8396.
- [97] Y. Chen, Q. Lu, D.A. Goodenough, B. Jeansonne, *Mol. Biol. Cell* 13 (2002) 1227-1237.
- [98] J.M. Summy, A.C. Guappone, M. Sudol, D.C. Flynn, *Oncogene* 19 (2000) 155-160.
- [99] F. Yamaguchi, H. Saya, J.M. Bruner, R.S. Morrison, *Proc. Natl. Acad. Sci. USA* 91 (1994) 484-488.
- [100] M. Kornmann, H.G. Beger, M. Korc, *Pancreas* 17 (1998) 169-175.
- [101] T. Ohta, M. Yamamoto, M. Numata, S. Iseki, Y. Tsukioka, T. Miyashita, M. Kayahara, T. Nagakawa, I. Miyazaki, K. Nishikawa, Y. Yoshitake, *Br. J. Cancer* 72 (1995) 824-831.
- [102] Y. Yamanaka, H. Friess, M. Buchler, H.G. Beger, E. Uchida, M. Onda, M.S. Kobrin, M. Korc, *Cancer Res.* 53 (1993) 5289-5296.
- [103] M. Kornmann, T. Ishiwata, H.G. Beger, M. Korc, *Oncogene* 15 (1997) 1417-1424.
- [104] M. Wagner, M.E. Lopez, M. Cahn, M. Korc, *Gastroenterology* 114 (1998) 798-807.

- [105] S.M. Vickers, L.A. MacMillan-Crow, Z. Huang, J.A. Thompson, *Free Rad. Biol. & Med.* 30 (2001) 957-966.
- [106] R.B. Irby, T.J. Yeatman, *Oncogene* 19 (2000) 5636-5642.
- [107] F. Meric, W. Lee, A. Sahin, H. Zhang, H. Kung, M. Hung, *Clin. Cancer Res.* 8 (2002) 361-367.
- [108] Y. Daigo, Y. Furukawa, T. Kawasoe, H. Ishiguro, M. Fujita, S. Sugai, S. Nakamori, G. Liefers, R.A.E.M. Tollenaar, C.J.H. van de Velde, Y. Nakamura, *Cancer Res.* 59 (1999) 4222-4224.
- [109] V. Darley-Usmar, H. Wiseman, B. Halliwell, *FEBS Letters* 369 (1995) 131-135.
- [110] A.G. Estevez, J. Jordan, *Ann. NY Acad. Sci.* 962 (2002) 207-211.
- [111] S.M. Vickers, L.A. MacMillan-Crow, M. Green, C. Ellis, J.A. Thompson, *Archives of Surgery* 134 (1999) 245-251.
- [112] H. Ischiropoulos, A.B. al-Mehdi, *FEBS Letters* 364 (1995) 279-282.
- [113] R. Radi, G. Peluffo, M.N. Alvarez, M. Naviliat, A. Cayota, *Free Rad. Biol. & Med.* 30 (2001) 463-488.
- [114] K.A. Hanafy, J.S. Krumenacker, F. Murad, *Med. Sci. Monit.* 7 (2001) 801-819.
- [115] B.L. Martin, D. Wu, S. Jakes, D.J. Graves, *J. Biol. Chem.* 265 (1990) 7108-7111.
- [116] A.J. Gow, D. Duran, S. Malcolm, H. Ischiropoulos, *FEBS Letters* 385 (1996) 63-66.
- [117] S. Kong, M.B. Yim, E.R. Stadtman, P.B. Chock, *Proc. Natl. Acad. Sci. USA* 93 (1996) 3377-3382.
- [118] J.P. Eiserich, R.P. Patel, V.B. O'Donnell, *Mol. Aspects Med.* 19 (1998) 221-357.
- [119] M.M. Tarpey, I. Fridovich, *Circ. Res.* 89 (2001) 224-236.
- [120] C. Mallozi, A.M.M. Di Stasi, M. Minetti, *FEBS Letters* 503 (2001) 189-195.
- [121] R.S. Jope, L. Zhang, L. Song, *Arch. Biochem. Biophys.* 376 (2000) 365-370.
- [122] L. Klotz, S.M. Schieke, H. Sies, N.J. Holbrook, *Biochem. J.* 352 (2000) 219-225.
- [123] K. Takakura, J.S. Beckman, L.A. MacMillan-Crow, J.P. Crow, *Arch. Biochem. Biophys.* 369 (1999) 197-207.

- [124] X. Li, P. De Sarno, L. Song, J.S. Beckman, R.S. Jope, *Biochem. J.* 331 (1998) 599-606.
- [125] S.Y. Low, M. Sabetkar, K.R. Bruckdorfer, K.M. Naseem, *FEBS Letters* 511 (2002) 59-64.
- [126] J.P. Crow, H. Ischiropoulos, *Methods in Enzymology* 269 (1996) 185-194.
- [127] Y. Kamisaki, K. Wada, K. Bian, B. Balabinli, K. Davis, E. Martin, F. Behbod, Y. Lee, F. Murad, *Proc. Natl. Acad. Sci. USA* 95 (1998) 11584-11589.
- [128] J.M. Souza, I. Choi, Q. Chen, M. Weisse, E. Daikhin, M. Yudkoff, M. Obin, J. Ara, J. Horwitz, H. Ischiropoulos, *Arch. Biochem. Biophys.* 380 (2000) 360-366.
- [129] C. Mallozzi, A.M.M. Di Stasi, M. Minetti, *FEBS Letters* 456 (1999) 201-206.
- [130] A.M.M. Di Stasi, C. Mallozzi, G. Macchia, T.C. Petrucci, M. Minetti, *J. Neurochem.* 73 (1999) 727-735.
- [131] C. Mallozzi, A.M.M. Di Stasi, M. Minetti, *Free Rad. Biol. & Med.* 30 (2001) 1108-1117.
- [132] A.A. Akhand, M. Pu, T. Senga, M. Kato, H. Suzuki, T. Miyata, M. Hamaguchi, I. Nakashima, *J. Biol. Chem.* 274 (1999) 25821-25826.
- [133] Y. Devary, R.A. Gottlieb, T. Smeal, M. Karin, *Cell* 71 (1992) 1081-1091.
- [134] E. Bonfoco, D. Krainc, M. Ankarcona, P. Nicotera, S.A. Lipton, *Proc. Natl. Acad. Sci. USA* 92 (1995) 7162-7166.
- [135] A.G. Estevez, R. Radi, L. Barbeito, J.T. Shin, J.A. Thompson, J.S. Beckman, *J. Neurochemistry* 65 (1995) 1543-1550.
- [136] S. Zhuang, G. Simon, *Am. J. Physiol. Cell Physiol.* 279 (2000) C341-C351.
- [137] M. Granerus, W. Engstrom, *Cell Prolif.* 29 (1996) 309-314.
- [138] S.H. Kaufmann, M.O. Hengartner, *Trends Cell Biol.* 11 (2001) 526-534.
- [139] A.G. Estevez, N. Spear, S.M. Manuel, R. Radi, C.E. Henderson, L. Barbeito, J.S. Beckman, *J. Neuroscience* 18 (1998) 923-931.
- [140] J.T. Shin, L. Barbeito, L.A. MacMillan-Crow, J.S. Beckman, J.A. Thompson, *Arch. Biochem. Biophys.* 335 (1996) 32-41.

- [141] S.S. Kelpke, D. Reiff, C.W. Prince, J.A. Thompson, *J. Bone Miner. Res.* 16 (2001) 1917-1925.
- [142] N. Spear, A.G. Estevez, G.V.W. Johnson, D.E. Bredesen, J.A. Thompson, J.S. Beckman, *Arch. Biochem. Biophys.* 356 (1998) 41-45.
- [143] D. Hanahan, J. Folkman, *Cell* 86 (1996) 353-364.
- [144] P.J. Polverini, *Crit. Rev. Oral Biol. Med.* 6 (1995) 230-247.
- [145] S. Kanda, E. Landgren, M. Ljungstrom, L. Claesson-Welsh, *Cell Growth Differ.* 7 (1996) 383-395.
- [146] B. Rousseau, D. Dubayle, F. Sennlaub, J.C. Jeanny, P. Costet, A. Bikfalvi, S. Javerzat, *Exp. Eye Res.* 71 (2000) 395-404.
- [147] S.H. Lee, D.J. Schloss, J.L. Swain, *J. Biol. Chem.* 275 (2000) 33679-33687.
- [148] P. Auguste, D.B. Gursel, S. Lemièrre, D. Reimers, P. Cuevas, F. Carceller, J.P. Di Santo, A. Bikfalvi, *Cancer Res.* 61 (2001) 1717-1726.
- [149] P. Gerwins, E. Skoldenberg, L. Claesson-Welsh, *Crit. Rev. Oncol. Hematol.* 34 (2000) 185-194.
- [150] K. Yamazaki, T. Nagao, T. Yamaguchi, H. Saisho, Y. Kondo, *Virchows Arch.* 431 (1997) 95-101.
- [151] J. Jouanneau, J. Plouet, G. Moens, J.P. Thiery, *Oncogene* 14 (1997) 671-676.
- [152] Y. Wang, D. Becker, *Nat. Med.* 3 (1997) 887-893.
- [153] A. Compagni, P. Wilgenbus, M. Impagnatiello, M. Cotten, G. Christofori, *Cancer Res.* 60 (2000) 7163-7169.
- [154] M.J. Cross, L. Claesson-Welsh, *Trends Pharmacol. Sci.* 22 (2001) 201-207.
- [155] T. Shono, Y. Mochizuki, H. Kanetake, S. Kanda, *Exp. Cell Res.* 268 (2001) 169-178.
- [156] B.P. Eliceiri, R. Paul, P.L. Schwartzberg, J.D. Hood, J. Leng, D.A. Cheresh, *Mol Cell* 4 (1999) 915-924.
- [157] M. Marx, S.L. Warren, J.A. Madri, *Exp. Mol. Pathol.* 70 (2001) 201-213.
- [158] D. Small, D. Kovalenko, D. Kacer, L. Liaw, M. Landriscina, C. Di Serio, I. Prudovsky, T. Maciag, *J. Biol. Chem.* 276 (2001) 32022-32030.

- [159] N.W. Jessop, R.J. Hay, *In Vitro* 16 (1980) 212.
- [160] S.M. Vickers, Z. Huang, L.A. MacMillan-Crow, J.S. Greendorfer, J.A. Thompson, *J. Gastrointest. Surg.* 6 (2002) 546-553.
- [161] J.K. Leach, S.M. Black, R.K. Schmidt-Ullrich, R.B. Mikkelsen, *J. Biol. Chem.* 277 (2002) 15400-15406.
- [162] A. Tanaka, C.P. Gibbs, R.R. Arthur, S.K. Anderson, B.K. Kung, D.J. Fujita, *Mol. & Cell Biol.* 7 (1987) 1978-1983.
- [163] S.J. Parsons, D.J. McCarley, V.W. Raymond, J.T. Parsons, *J. Virol.* 59 (1986) 755-758.

**GRADUATE SCHOOL
UNIVERSITY OF ALABAMA AT BIRMINGHAM
DISSERTATION APPROVAL FORM
DOCTOR OF PHILOSOPHY**

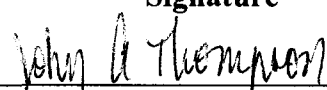
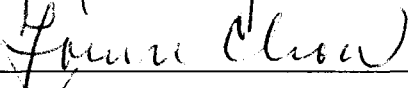
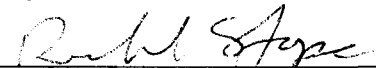
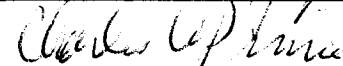
Name of Candidate Jessica Samit Greendorfer

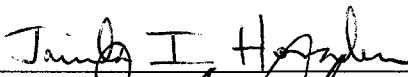
Graduate Program Biochemistry

Title of Dissertation Differential Signaling to Src Family Kinases by Specific Isoforms
of Fibroblasts Growth Factor Receptor-1

I certify that I have read this document and examined the student regarding its content. In my opinion, this dissertation conforms to acceptable standards of scholarly presentation and is adequate in scope and quality, and the attainments of this student are such that she may be recommended for the degree of Doctor of Philosophy.

Dissertation Committee:

Name	Signature
<u>John A. Thompson</u> , Chair	<u></u>
<u>Louise T. Chow</u>	<u></u>
<u>Gerald M. Fuller</u>	<u></u>
<u>Richard S. Jope</u>	<u></u>
<u>Charles W. Prince</u>	<u></u>

Director of Graduate Program 

Dean, UAB Graduate School 

Date _____